GLUTAMATERGIC SYNAPSE FORMATION IN DEVELOPING ZEBRAFISH EMBRYOS

by

JAVIER FIERRO, JR.

A DISSERTATION

Presented to the Department of Chemistry and Biochemistry
and the Graduate School of the University of Oregon
in partial fulfillment of the requirements
for the degree of
Doctor of Philosophy

December 2014

DISSERTATION APPROVAL PAGE

Student: Javier Fierro, Jr.

Title: Glutamatergic Synapse Formation in Developing Zebrafish Embryos

This dissertation has been accepted and approved in partial fulfillment of the requirements for the Doctor of Philosophy degree in the Department of Chemistry and Biochemistry by:

J. Andrew Berglund	Chairperson
Philip Washbourne	Advisor
Kenneth Prehoda	Core Member
Judith Eisen	Core Member
Tory Herman	Institutional Representative

and

J. Andrew Berglund	Dean of the Graduate School

Original approval signatures are on file with the University of Oregon Graduate School.

Degree awarded December 2014

DISSERTATION ABSTRACT

Javier Fierro, Jr.

Doctor of Philosophy

Department of Chemistry and Biochemistry

December 2014

Title: Glutamatergic Synapse Formation in Developing Zebrafish Embryos

In order for a human being to process complex thought, cells within the brain must communicate with each other in a very precise manner. The mechanisms which underlie the development of these connections, however, are poorly understood and thus require a thorough investigation. In this dissertation, we attempt to identify components involved in stabilizing synaptic contacts and the mechanisms by which synaptic proteins are trafficked to newly forming contact sites. Interestingly, we also identify a gene involved in the formation of the myotome.

To identify proteins involved in stabilizing synaptic contacts, we characterized the function of 4.1B in developing zebrafish embryos. 4.1B is a scaffolding molecule involved in stabilizing protein complexes at sites of cell adhesion. We identified two *4.1B* genes in the zebrafish genome, *4.1B-a* and *4.1B-b*, which are differentially expressed and have evolved divergent functions. *4.1B-a* is expressed within the central nervous system, specifically within primary motor neurons. Knockdown studies show a reduction in the number of synapses and altered kinetics of touch evoked-responses, suggesting a role in synaptic stabilization. In contrast, *4.1B-b* is primarily expressed in muscle cells. Knockdown of 4.1B-b results in severe muscle fiber disorganization as well as altered locomotor behaviors. Together, these data suggest the basic functions of 4.1B are

evolutionarily conserved, with new roles described in the development of synapses and muscle fibers.

To determine the mechanisms that underlie protein recruitment to newly forming synapses, we examined the recruitment of three distinct transport packets in the zebrafish spinal cord. During presynaptic assembly, we found synaptic vesicle protein transport vesicles preceded piccolo-containing active zone precursor transport vesicles, which in turn preceded synapsin transport vesicles. We identified the last transport packet as a unique and independent mechanism for the recruitment of synapsin, a protein involved in regulating the reserve pool of synaptic vesicles. Importantly, we found cyclin-dependent kinase 5 regulated the late recruitment of synapsin transport packets to synapses, thus identifying kinases as a key signaling molecule in the formation of synaptic contacts. Together, this work provides new insight into the mechanisms that underlie synaptogenesis.

This dissertation includes both previously published and unpublished co-authored material.

CURRICULUM VITAE

NAME OF AUTHOR: Javier Fierro, Jr.

GRADUATE AND UNDERGRADUATE SCHOOLS ATTENDED:

University of Oregon, Eugene
New Mexico State University, Las Cruces

DEGREES AWARDED:

Doctor of Philosophy, Chemistry, 2014, University of Oregon
Bachelor of Science, Biochemistry, 2008, New Mexico State University

AREAS OF SPECIAL INTEREST:

Developmental Neurobiology
Neuroscience

PROFESSIONAL EXPERIENCE:

Graduate Teaching Fellow, University of Oregon, 2012 – 2014
Graduate Teaching Fellow, University of Oregon, 2008 – 2009
Undergraduate Summer Research Fellow, Fred Hutchinson Cancer Research Center, 2007
Facilitator for Supplemental Instruction Program, New Mexico State University, 2006 – 2008
Research Assistant, New Mexico State University, 2006-2008

GRANTS, AWARDS, AND HONORS:

Biology Teaching Recognition Award, University of Oregon, 2014
Fred Hutchinson Cancer Research Center Internship Program Scholarship, Fred Hutchinson Cancer Research Center, 2014
NIH Molecular Biology Training Grant Appointee, University of Oregon, 2009 – 2012
Betty H. and Robert E. Neligan Scholarship, New Mexico State University, 2007
Fred Hutchinson Cancer Research Center Internship, Fred Hutchinson Cancer Research Center, 2007

PUBLICATIONS:

Blanco-Sanchez, Bernardo, Clement, Aurelie, **Fierro Jr., Javier**, Washbourne, Philip, Westerfield, Monte. 2014. Complexes of Usher Proteins Preassemble at the Endoplasmic Reticulum and are Required for Trafficking and ER Homeostasis. *Dis Model Mech* 5: 547-559

Easley-Neal, Courtney, **Fierro Jr., Javier**, Buchanan, JoAnne, Washbourne, Philip. 2013. Late Recruitment of Synapsin to Nascent Synapses is Regulated by CDK5. *Cell Rep* 4:1199-1212.

ACKNOWLEDGMENTS

I would like to thank my advisor Dr. Philip Washbourne and his wife Dr. Alex Tallafuss for all of the training and continued support they provided. They laid the foundation that was necessary for me to achieve this scientific endeavor. I would also like to thank the members of the Washbourne lab, past and present, for their support, training, and friendship throughout my graduate career. I would like to give a heartfelt thanks to all my colleagues in the Institute of Neuroscience for always stopping what they were doing to answer any question I had. Every single one of them contributed to my development as a scientist as well as my development as a person. I would also like to thank Dr. Nathan Tublitz for inspiring me both as a professor and a neuroscientist. Through his teachings, he has truly made me appreciate the complexities of the brain and the power that it holds, and I cannot wait to share this knowledge with others. To Dr. Judith Eisen and Dr. Andy Berglund, thank you for always taking time out of your day to provide invaluable advice; I truly appreciate everything you did for me over my graduate career.

Finally, I would like to acknowledge the six most important people in my life. To my friends Andrew, Luke, and Alesia, I thank you for providing your friendship and challenging me in the great outdoors; the three of you truly became my family. To Steve Seredick, I could not have asked for a better mentor. Your brilliance and support inspired me to become a better scientist. To Dylan Haynes, I could not have done any of this without you. You challenged me in more ways than you will ever know, and I cannot thank you enough for that. Finally, to my mother, this thesis is for you.

I dedicate this dissertation to my mother whose sacrifices and hard work paved the way for my success. Thank you for everything you have done.

TABLE OF CONTENTS

LIST OF FIGURES

CHAPTER I

INTRODUCTION

Studying the Nervous System

The nervous system is a highly complex molecular computer capable of processing trillions of computations per second. The central nervous system alone, which consists of the brain and spinal cord, is composed of approximately 100 billion neurons that make over 100 trillion connections for higher cognitive functions such as learning and memory, language acquisition and processing, and consciousness itself. It is no wonder then that a mutation in any of the vast number of proteins that can be found within the central nervous system can lead to a number of neurological disorders, as well as varying degrees of severity for each disorder characterized. The story, of course, becomes much more complex when we realize the architecture of the nervous system is highly dynamic, changing constantly over the development of an organism as well as influenced by environmental factors which cannot be accounted for as of yet. So how then can we solve the increasing number of cases of dementia, autism, and schizophrenia when we are dealing with the most complex entity in the universe? The answer is, we can't. Our understanding of the nervous system is so minimal, we cannot even begin to describe the mechanisms which underlie how a neuron finds its target neuron, how synapses form and mature, or how any of this leads to a conscious being. At the moment, all we can do is access each individual problem in a minimalistic way, understanding that every problem is temporally, spatially, and context specific. Neuroscientists take on this daunting task with the hope that one day we can put the answers to these individual

problems together to achieve our common goal of understanding how we exist as a conscious being, and how we can treat neurological disorders to enhance our existence as a species on this planet. In this dissertation, we are concerned with the development of the nervous system, specifically how the point of communication between two neurons, called a synapse, develops.

Basic Neurobiology

A neuron is a specialized cell found within the central and peripheral nervous systems that are capable of sending electrical signals from one neuron to another. The purpose of this communication is to regulate all functions of the human body including, but not limited to, simple reflex arcs and higher cognitive thought. In general, the neuron is an asymmetric structure with projections extending from either end of the cell body which allow it to communicate with other cells. At one end of the neuron you will find the dendrites. The role of the dendrites is to receive information from other cells and transmit them to the cell body. These structures form a highly complex branching network which is capable of receiving information from a few hundred to hundreds of thousands of different sources. At the other end of the cell body is the axon. The role of the axon is to regenerate that signal and transmit it to the next cell (Kandel, 2012).

The point of communication between two cells is called a synapse. This is a specialized region within the nervous system where an axon from the presynaptic cell meets the dendrite of the postsynaptic cell. It is important to note that the two neurons do not connect to each other directly, but are rather separated by a space called the synaptic cleft. At the terminal of an axon there are voltage-gated calcium channels, synaptic

vesicles filled with neurotransmitters, hundreds of proteins important for neurotransmitter release (called the active zone), a reserve pool of synaptic vesicles, endoplasmic reticulum, and mitochondria (Chia, 2013). At the dendritic membrane there is a protenacious area called the postsynaptic density (PSD) that is estimated to contain over ten thousand proteins important for cognitive functions such as learning and memory. Within this region you will find cell adhesion molecules, scaffolding molecules, motor proteins, cytoskeletal proteins, kinases, phosphatases, GTPases, receptors, and ion channels. There are also mitochondria within the postsynaptic terminal which are necessary for the various energy dependent processes (Sheng, 2011).

When an electrical signal in the presynaptic cell reaches the axon terminal, voltage-gated calcium channels open up allowing calcium to flow into the cell. This calcium is recognized by calcium sensing molecules located on synaptic vesicles at the plasma membrane. When this binding occurs, it causes a conformational change in the active zone components which allow the synaptic vesicle to fuse with the membrane and release the neurotransmitter. When the neurotransmitter is released, it binds to receptors on the postsynaptic terminal. If the receptors are excitatory, they will initiate the electrical signal in the next cell once bound by neurotransmitter. If they are inhibitory receptors, they will prevent the cell from initiating the electrical signal, thus regulating signals transmitted within the nervous system. The time scale of all of these events is between 1 ms and 10 ms, and thus, a single synaptic connection is capable of transmitting one to hundreds of signals per second (Südof, 2013). These events are critical for the proper functioning of the nervous system, but the mechanisms that underlie how these connections form is poorly understood.

The Zebrafish as a Model Organism for Studying Nervous System Development

To begin our discussion of how the nervous system develops, we first must consider the model organism for which we want to conduct our experiments in. *Danio rerio*, the zebrafish, provides the best model to study developmental processes as it combines the best features of all model organisms. The zebrafish is a vertebrate which develops externally and allows for the manipulation of the organism at all ages of development. By 24 hours post fertilization (hpf), the characteristic features of an adult zebrafish can be seen including eyes, ears, functioning heart, forebrain, midbrain, hindbrain, and spinal cord. Conveniently, the zebrafish is transparent up to 26 – 28 hpf, making the visualization of these structural elements easy to identify (Lieschke, 2007), as well as allows for the visualization of synaptogenesis (Jontes, 2000). The generation time is similar to the mouse (10 – 12 weeks) but the mature zebrafish can produces hundreds of fish on a weekly basis, whereas an adult mouse can only produce a litter of 6 – 8 pups 5 – 10 times a year. Finally, for the purpose of our studies, at early developmental stages they display simple behaviors. In particular, at 19 hpf, zebrafish embryos exhibit spontaneous coils which allow us to study electrical synapses within the nervous system. By 24 hpf, zebrafish are able to respond to a mechanical stimulus when applied to the dorsal region of the spinal cord; this gives us the opportunity to study the formation of glutamatergic chemical synapses. These simple reflex arcs involve a limited number of neurons within the spinal cord (Pietri, 2009) and provide a great model organism for which to study synapse development as well as other developmental processes (reviewed in Lieschke, 2007).

The Zebrafish Spinal Cord

The zebrafish spinal cord is a great model system to use for the study of neurodevelopment as it has a small number of identified neurons. The trunk and tail of the zebrafish is segmentally arranged, with each segment containing a stereotyped number of cells. At early developmental stages, the zebrafish spinal cord has a limited number of spinal neurons that can be easily identified based off of cellular morphology and axon trajectory. Despite this relatively small number, there are still too many to discuss in any amount of detail. To limit our discussion of spinal neurons, I will only discuss those that are involved in the touch response neuronal circuit. This circuit is a simple reflex behavior observed between 21 – 30 hpf which allows the zebrafish to contract its tail in resonse to a stimulus.

The first cell in the touch response neuronal circuit in zebrafish is the Rohon-Beard sensory cell. These cells lie in a double row along the dorsolateral spinal cord and are not segmentally arranged. They send projections out through the skin to sense touch via mechanoreceptors, and they send their axons out, emanating from both the rostral and caudal end of the cell body. Rohon-beard cells begin sending their axons out at 17 hpf, in which they pioneer the dorsal longitudinal fasical, an important track that other neurons use to find their neuronal targets. By 24 hpf, Rohon-beard cells have extended their axons along the entire length of the spinal cord (Metcalf, 1990). Rohon-Beard cells were first discovered in *Xenopus laevis* (the African clawed frog) and were found to be involved in triggering swimming episodes (Clarke, 1984). Interestingly, Rohon-beard cells die between the first and third day of development and are replaced by dorsal root ganglion sensory neurons in the peripheral nervous system (Reyes, 2004). It is hypothesized that

these cells are important for mediating hatching behavior in the early embryo. Embryos are enclosed in a chorion which is a membranous sac consisting of two inner layers and one outer layer (Hagenmaier, 1973). In order for the embryo to get out of the chorion, the hatching glad within the ventral yolk sac must release an enzyme that will weaken the inner layers of the chorion (Kim, 2006). As the zebrafish continues to develop, the zebrafish will be able to sense the walls of the chorion through the dendrites of the Rohon-beard cells, and thus they begin to move in response to this stimulus which ruptures the outer layer (Reyes, 2004).

The next cell within the zebrafish touch response neuronal circuit is the Commissural Primary Ascending (CoPA) interneuron. The CoPA cell lies just ventral of the Rohon-beard sensory cell in the dorsal spinal cord and is not segmentally arranged (Kuwada, 1990). CoPAs begin extending their axon ventrally by 16 hpf before crossing the midline and extending dorsally and rostrally to meet up with the dorsal longitudinal fasical extending toward the telencephalon. At early developmental stages, CoPA cells do not have any dendritic processes, and thus all Rohon-beard cells synapse onto the cell body. The furthest most caudal cells can extend their axon the entire length of the spinal cord (Bernhardt, 1990; Hale, 2001) and it is believed the CoPA cell provides the contralateral switch which is necessary for executing the contralateral coil during touch evoked behaviors (Pietri, 2009). CoPA cells were originally first identified in *Xenopus laevis*, named dorsolateral commissural interneurons, and were found to be an excitatory neuron involved in local bending circuits by exciting motor neurons contralateral to the sensory stimulus (Roberts, 1990). This provided the first evidence that CoPA cells may be involved in exciting motor neurons for producing bends away from the stimulus. Since

then, it has been shown that CoPA cells are involved in the touch response neuronal circuit (Pietri, 2009) and that a single Rohon-beard cell can make contact with every CoPA cell in the spinal cord (Easly-Neal, 2013). There has also been evidence to suggest that muscle contraction on the ipsilateral side (same side as the stimulus) is inhibited at the level of the CoPA cell, thus synchronizing activity on the two sides of the embryo (Saint-Amant, 2001). The exact mechanism for how this occurs however has not been determined.

The next cell in the touch response neuronal circuit is unknown. The criteria for this cell includes being ventrally located in apposition to the CoPA cell axon. It must have a descending axon which must synapse onto primary and secondary motor neurons, and it may be electrically active at early developmental stages. The latter criterion is based on the idea that spontaneous coiling is mediated by pacemaker activity from an electrically active cell (Drapeau, 2001; Knogler, 2014; Pietri, 2009). The pacemaker activity can come from this unknown cell, or it may come from another cell within the spinal cord. The pacemaker cell within the spinal cord responsible for spontaneous coils also remains unknown.

The final set of neurons that are involved in the touch response neuronal circuit are the primary motor neurons. Primary motor neurons develop early and have a large cell body (Mendelson, 1986). There are four identified primary motor neurons at 24 hpf. The caudal primary motor neuron (CaP) begins to extend its axon at 17 hpf to form the ventral root and pioneer the ventral nerve necessary for later axons to navigate (Eisen, 1986; Pike, 1992; Wilson, 1990). The CaP motor neuron extends its axon ventrally along the medial myotome and is believed to be the first neuron to initiate spontaneous coiling

(Drapeau, 2002; Melancon, 1997). The middle primary motor neuron (MiP) extends its axon ventrally before pausing at the ventral root and changing directions to grow dorsally along the medial mytome to form the dorsal nerve (Eisen, 1986; Westerfield, 1986). The rostral primary motor neuron (RoP) extends its axon ventrally towards the ventral root and extends laterally within the region that will form the horizontal myoseptum (the area which separates the dorsal and ventral myotome). Finally, there is the variable motor neuron (VaP) which is present in only half of the segments and dies by 36 hpf. The axon grows ventrally and does not pass the horizontal myoseptum (Eisen, 1990). All cells grow toward the ventral root and pause before diverging and extending their axons to their specific myotomal targets for muscle contraction after all connections have been formed (Beattie, 2000). With an understanding of the cells that are involved in the touch-response neuronal circuit, we can now begin our discussion of synaptogenesis in the zebrafish spinal cord.

Synaptogenesis in the Zebrafish Spinal Cord

Synaptogenesis is the study of the development of a synapse, from the initial formation to the maturation of the synaptic contact. In general, a neuron will send out an axon into the environment in search of its synaptic partner. The growth cone, a hand like projection at the tip of the axon, will send out fillopodia into the environment (Dent, 2011). At the plasma membrane of these fillopidia are cell adhesion molecules which are necessary for the axon to find its synaptic target. These cell adhesion molecules will interact like a lock and key with cell adhesion molecules on the dendrites, thus providing the specificity needed for proper synapse formation (Washbourne, 2004). When these cell

adhesion molecules interact, a cascade of signaling events occurs which begins the recruitment of pre and postsynaptic components (McAllister, 2007). Only proteins discussed within chapters 2 and 3 will be discussed below.

On the presynaptic side, proteins are recruited in very distinct packets with very distinct time courses. In the zebrafish spinal cord, the first packet to arrive at the synapse are the synaptic vesicle protein transport vesicles (STV) which contain proteins such as VAMP2, synaptotagmin, and SV2 (Ahmari, 2000; Takamori, 2006). Synaptotagmins are calcium sensing proteins, and are important for sensing calcium in the presynaptic terminal for neurotransmitter release (Südof, 2013). SV2 (Synaptic vesicle protein 2) is required for normal transmission and is thought to play a role in regulating exocytosis of neurotransmitters. VAMP2 (Vesicle associated membrane protein 2) is one of the main components of the protein complex involved in synaptic vesicle docking and fusion to the plasma membrane (Vautrin, 2009). Together these proteins regulate important functions of the presynaptic terminal involved in the release of neurotransmitter, and are all associated with synaptic vesicles. The next transport packet to be recruited to the plasma membrane is the piccolo-containing active zone precursor transport vesicle (PTV), which contains the proteins Piccolo, Bassoon, and SNAP-25 (Shapira, 2003; Zhai 2001). Piccolo and Bassoon are both scaffolding molecules that are important for organizing other active zone components involved in regulating neurotransmitter release. SNAP-25 is a t-SNARE protein involved in vesicle docking and membrane fusion. Finally, the last transport packet to be recruited to the presynaptic terminal is the synapsin transport packet which its only known protein is synapsin. Synapsin is involved in regulating the reserve pool of synaptic vesicles, which contains the majority of synaptic vesicles that

can only be released under intense stimulation (Benfenati, 1989; Bonanomi, 2005; Kuromi, 1998). This transport packet is regulated by cyclin-dependent kinase-5 (Cdk-5), which has also been shown to regulate the reserve pool of synaptic vesicles (Kim, 2010). The details regarding the dynamics of these various synaptic transport packets as well as the role Cdk-5 plays in regulating synapsin recruitment will be discussed further in Chapter 3. Other proteins at the presynaptic terminal, which constitute several hundred proteins, have not been studied in zebrafish. Many of these proteins may be recruited within the three described transport systems, or they may be recruited as independent packets with their own time course that has not yet been discovered.

Thirty minutes after the arrival of the transport packets on the presynaptic side, protein recruitment on the postsynaptic side begins. Much of our knowledge on postsynaptic recruitment has been determined in rat cortical and hippocampal neurons (Friedman, 2000; Washbourne, 2002). Despite these studies, extremely little is known about the dynamics of protein recruitment for the ten thousand proteins that exist within the postsynaptic density. Two of the major receptors that are recruited to nascent sites are NMDA and AMPA receptors. These receptors play a vital role in glutamatergic synapse formation and are involved in learning and memory (Rudy, 2014). For the purpose of this dissertation, it is important to note that NMDA and AMPA receptors are recruited independently of each other, with NMDA receptors being recruited before AMPA receptors. This creates a silent synapse which is an immature synapse (Washbourne, 2002; 2004). Despite our lack of understanding of postsynaptic recruitment, many of the proteins that exist at the postsynaptic side in other model systems also exist within zebrafish. Both NMDA and AMPA receptors have been shown to be expressed within the

spinal cord (Cox, 2005; Hoppmann, 2008), and have a role in touch-evoked coiling (Pietri, 2009). The PSD-95 family of membrane-associated guanylate kinases (MAGUKs) have also been shown to be expressed within the spinal cord of zebrafish. Specifically, it was shown that zebrafish posses one copy of PSD-95, PSD-93, and two copies of Sap-97. These are thought to act as scaffolding molecules involved in stabilizing molecular complexes at the plasma membrane at excitatory synapses (Meyer, 2005). Finally, it is also important to call attention to gephryin, a major component of inhibitory synapses which mediates the recruitment and stabilization of glycine receptors and GABA receptors. The zebrafish has duplicated gephryin genes which are expressed within the spinal cord at 24 hpf and are involved in escape behaviors (Ogino, 2011). The duplicated genes arose when teleost fish branched off from other vertebrates. Many of the genes in zebrafish are duplicated, with some duplicates partitioning the function of their human homologue, while other duplicates have either gained new functions or lost some of their original functions (Postlethwait, 1998)

As new techniques and data come in, we continue to develop a better picture of the proteins involved in synaptogenesis in zebrafish. More work will be needed to fully characterize the expression and function of the thousands of remaining proteins, however, in order to gain a complete understanding of synapse formation.

Project Overview

As stated previously, the nervous system is quite complex. An understanding of the material presented above is necessary for understanding the questions we are addressing, as well understanding the conclusions we are drawing based on the results we obtained. In this dissertation, we examine the role of 4.1B, a scaffolding molecule that is

capable of forming large macromolecular complexes at the plasma membrane. We identify 4.1B as an important component of excitatory synapses and find that loss of 4.1B containing synapses leads to altered locomotor behaviors. We also address the dynamics of protein trafficking to the presynaptic terminal and identify a new transport packet that gets recruited to the presynapse with its own distinctive time course. These new transport packets, referred to as synapsin transport packets, are recruited to nascent synapses by Cdk-5, suggesting a new role for kinases during the development of the nervous system. We are only beginning to shed light on the mechanisms underlying synaptogenesis, and these studies help brings us that much closer to our understanding of the inner workings of the brain.

This dissertation includes previously published and unpublished co-authored material. Chapter II contains material that will be published with co-authors Dylan Haynes, Kathryn Glaspey, and Philip Washbourne. Chapter III contains material that was previously published in *Cell Reports* in 2013 wit co-authors Courtney Easly-Neal, JoAnn Bucanan, and Philip Washbourne.

CHAPTER II

DUPLICATED *4.1B* GENES IN ZEBRAFISH EVOLVED DIVERGENT FUNCTIONS FOR THE DEVELOPMENT OF GLUTAMATERGIC SYNAPSES AND THE MYOTOME

The work described in this chapter was co-authored by myself, Dylan Haynes, Kathryn Glaspey, and Philip Washbourne. Kathryn Glaspey carried out the chromogenic *in situ* hybridizations. Dylan Haynes performed the initial experiments with 4.1B-a and helped with data analysis. Philip Washbourne helped in the design of the project as well as with the editing of the manuscript. I performed the majority of the experiments and wrote the manuscript.

Introduction

During the development of an organism, proper formation of cell adhesion contacts are necessary for forming synaptic contacts within the central nervous system, as well as attaching muscle fibers to the extracellular matrix in the musculoskeletal system. Mutations in cell adhesion molecules (Bleecker, 1994; Zhiling, 2008), scaffolding molecules (Boeckers, 2002; Constantin, 2014), and receptors (Campbell, 2006; Hodges, 1997) have been implicated in devastating disorders such as autism and Duchenne muscular dystrophy, but the mechanisms that underlie how these proteins are recruited and stabilized at cell adhesion sites is poorly understood. To gain insight into how these macromolecular complexes may form, we investigated the role of 4.1B during embryonic zebrafish development.

4.1B is a scaffolding molecule that belongs to the 4.1 family of proteins. The four proteins that make up this family were originally named based on their expression patterns and they include 4.1R (red blood cell), 4.1N (neuronal), 4.1G (general), and 4.1B (brain), with corresponding gene names *epb41*, *epb41l1*, *epb41l2*, and *epb41l3* respectively. It has since been shown that all four of these genes are ubiquitously expressed and knockdown of any one of these show a wide range of phenotypes. These studies have suggested that the overall function of the 4.1 family of proteins is to stabilize transmembrane signaling complexes at the plasma membrane in a distinct temporal and spatially determined pattern (reviewed in Baines, 2013).

At its N-terminus, all 4.1 proteins contain a FERM (4.1, ezrin, radixin, moesin) domain that is capable of interacting with the plasma membrane, cell adhesion molecules, ion channels, and other transmembrane domain containing proteins (reviewed in Baines, 2013). Adjacent to the FERM domain is the FERM adjacent (FA) region that regulates the activity of the FERM domain (Baines, 2006). At their C-terminus, there is a unique C-terminal domain (CTD) that defines the 4.1 proteins (Scott, 2001). The function of the CTD is not well understood, but the CTD of 4.1N and 4.1G has been shown to interact with the GluR1 and GluR3 subunits of the α-amino-3-hydroxy-5-methylisoxazole-4-propionic acid (AMPA) receptor (Coleman, 2003; Shen, 2000). It has also been shown that 4.1B can directly interact with αvβ8 integrin through the CTD; this is important for CNS function (McCarty, 2005). Finally, in between the FA and CTD domains is the spectrin actin binding domain (SAB) that stabilizes protein complexes at the F-actin-spectrin cytoskeleton (Gimm, 2002). Various studies have suggested the major function of the 4.1 proteins is to tether macromolecular complexes to the actin-spectrin

cytoskeleton (Delhommeau, 2005; Discher, 1995; Gimm, 2002; Shen, 2000) however, invertebrates do not possess an SAB domain in their 4.1 homologues (Baines, 2010). Loss of coracle, the 4.1 homologue in the fruit fly, is recessive embryonic lethal (Fehon, 1994). This result suggests the early function of this protein is involved in regulating multiple membrane proteins through the FERM and CTD domains, independent of SAB function. It has also been shown that 4.1N has lost the SAB activity throughout evolution (Gimm, 2002). This provides further evidence that the inclusion of the SAB domain was a gain of function during evolution, and thus may not be necessary for 4.1B function.

4.1B has long been known to interact with synaptic cell adhesion molecule 1 (SynCAM1), a cell adhesion molecule implicated in initiating synaptogenesis (Biederer, 2002; Yageta, 2002). The interaction occurs through lobe C of the FERM domain in 4.1B, to a cytoplasmic 4.1 binding motif on SynCAM1 (Yageta, 2002). These proteins are highly expressed within the brain (Fujita, 2005; Parra, 2000) and are enriched at postsynaptic densities (Scott, 2001). Both proteins play a critical role in the suppression of tumor formation and metastasis, and have been implicated in gliomagenesis (Gutmann, 2000; Nunes, 2005; Rajaram, 2005; Singh, 2002; Zhang, 2013). SynCAM1 has also been directly linked to autism spectrum disorders in profiled patients (Zhiling, 2008), while no such link has been established for 4.1B or other 4.1 proteins. Microarray studies in postmortem autistic brains, however, have shown an increase in 4.1N expression levels, suggesting a possible role for 4.1 proteins in the progression of autism (Purcell, 2001). To gain insight into the role of these two proteins during synaptogenesis, Hoy et al. (2009) recently showed SynCAM1 can recruit N-methyl-D-aspartate (NMDA) receptors to synaptic contact sites via 4.1B in nonneuronal cells. This correlated with an increase in

the frequency of NMDA receptor mediated activity and localization. They also showed that overexpression and knock-down of 4.1B in hippocampal neurons affected synaptogenesis and NMDA receptor mediated transmission, providing further evidence 4.1B can associate with NMDA receptors. Interestingly, SynCAM1 can recruit AMPA receptors via 4.1N, thus providing independent mechanisms for glutamate receptor recruitment during synaptogenesis (Hoy, 2009). These data complement data showing 4.1N regulates the surface expression of AMPA receptors in cultured cells (Chen, 2000).

The results from these *in vitro* cell culture experiments have been challenged, however, by results obtained from mice with severe knockdown of 4.1N and 4.1G (Wozny, 2009). These double knock-out mice show no alterations in synaptic structure or number, and are phenotypically normal. A reduction in the number of GluR1 and GluR2/3 subunits in synaptosome preparations was observed, but electrophysiological recordings from hippocampal neurons showed no differences in AMPA or NMDA receptor mediated transmission. Importantly, no deficits during short-term and long-term plasticity studies were observed, suggesting 4.1 proteins are not involved in proper neuronal transmission *in vivo* (Wozny, 2009). It is impossible to know the precise cause for the differences in these results, but it is possible that the *in vivo* studies are complicated by redundant or compensatory mechanisms masking phenotypes that resemble the data observed *in vitro*. It is also possible that studies done *in vitro* allow protein interactions to occur that are not physiologically relevant. There are many mechanisms that regulate the stabilization, recruitment and organization of proteins at the synapse of a living organism. For example, synaptic activity and neuronal depolarization within a circuit can lead to the induction of new gene synthesis, termed “the genomic

signaling hypothesis" (Rudy, 2014), thus providing a level of regulation that cannot be seen in cultured cells. This leaves us with significant questions about the involvement of 4.1B in the formation of glutamatergic synapses.

It is also important to note that *in situ* hybridization studies of 4.1B in mice have shown an isoform-specific variant expressed in muscle tissue that possesses a full SAB domain (Parra, 2000). The necessity of the full SAB domain versus the truncated form has not been studied, but evidence suggests both the full SAB and the truncated version are capable of binding to the actin-spectrin cytoskeleton in muscle (Delhommeau, 2005; Kontrogianni-Konstantopoulous, 2000). There has also been no study done that shows a direct link between 4.1B and muscle development, although studies have shown that 4.1R may regulate macromolecular complex formation at the sarcolemma (Delhommeau, 2005). Studies performed on human skeletal muscle tissue revealed an isoform-specific variant of 4.1R that contains a full SAB domain, similar to the 4.1B variant expressed in muscle (Delhommeau, 2005; Parra, 2000). Antibody staining shows 4.1R is localized to the sarcolemma and colocalizes with dystrophin, an important component of the dystrophin-glycoprotein complex that connects the cytoskeleton of the sarcolemma to the extracellular matrix (Campbell, 1989). Dystrophin is a key protein whose loss is directly linked to Duchenne muscular dystrophy (DMD). Analysis of skeletal muscle from patients who suffer from DMD reveal that 4.1R is completely lost, and correlates to the loss of dystrophin (Delhommeau, 2005). Thus, it is reasonable to hypothesize that 4.1R is involved in stabilizing the dystrophin-glycoprotein complex to the cytoskeleton and sarcolemma in muscle tissues. This study highlights the variability within 4.1 protein function as well as their importance in physiological diseases.

To shed more light on the role of 4.1B during development, we decided to characterize the function of 4.1B in zebrafish. Zebrafish are a great model organism to study 4.1B function because we can study the initial formation of synapses and muscle during the development of the embryo. Zebrafish also exhibit very simple behaviors at early developmental stages that can be attributed to a small number of identified spinal cord neurons that innervate the myotome. This provides the opportunity to directly compare our physiological data with our behavioral data to provide a more complete analysis of 4.1B function. We identified two 4.1B homologues in zebrafish which we named 4.1B-a and 4.1B-b. The genes that encode these proteins, *epb41l3a* and *epb41l3b,* are differentially expressed. *epb41l3a* is expressed within the central nervous system specifically within primary motor neurons. Using antisense morpholino technology (MO), we found that 4.1B-a knock-down caused a reduction in the number of synapses onto primary motor neurons which correlated with a decrease in kinetics of touch-evoked responses. Our studies suggest 4.1B-a is required for the formation of glutamatergic synapses that are necessary for proper circuit formation. Interestingly, *epb41l3b* is expressed within muscle cells. Knockdown of 4.1B-b results in severe muscle fiber disorganization as well as altered spontaneous and touch evoked responses. This suggests 4.1B-b is involved in stabilizing proteins at the sarcolemma of muscle cells, necessary for muscle fiber organization. Taken together, our data suggest that the basic functions of 4.1B are evolutionarily conserved in mediating macromolecular protein complex formation with new insights into synapse development and myotome organization.

Results

Characterization of Zebrafish epb41l3 Homologues

To search for zebrafish homologues of *epb41l3*, we searched the zebrafish genome database with mammalian 4.1B as a template. We identified two genes with similar identity, one on chromosome 24 and one on chromosome 2 which we designated *epb41l3a* and *epb41l3b* respectively. The corresponding protein names are 4.1B-a and 4.1B-b. To ensure the identified genes are co-orthologs of mammalian *epb41l3*, we performed an analysis of conserved synteny. We determined the putative *epb41l3* genes are related to mammalian *epb41l3* (Figure 1A) because the genes surrounding *epb41l3* on *Mus musculus* chromosome 17 are preserved with those genes present on *Danio rerio* chromosome 24 and chromosome 2. The genes *Lrrc30* and *Vapa*, appear to be the only other genes represented as duplicates in our analysis. Within this region of Chromosome 24 in *Danio rerio,* we observed only one chromosomal rearrangement between genes *zgc:66442* (orthologous to *Mus musculus Zfp161*) and *Vapa*. This suggests minimal rearrangement occurred on this chromosome throughout evolution. In contrast, chromosome 2 in *Danio rerio* has many rearrangements. Both *epb41l3* genes in *Danio rerio* are near the end of their respective chromosomes. It has been shown that chromosomal rearrangements are more likely to occur at chromosomal ends, and thus may explain why there is less conserved synteny for the *epb41l3b* gene (Bailey, 2006). No conserved syntenies were found between the zebrafish *epb41l3* genes and the other three mammalian *epb41l* genes, providing further evidence that the identified *epb41l3* genes are orthologous with mammalian *epb41l3*.

Pairwise alignments of the zebrafish 4.1B proteins with human 4.1B revealed both proteins contained a FERM domain, a FERM adjacent domain, and a CTD domain (Figure 1B). Only 4.1B-a possessed a predicted SAB domain, thus structurally, 4.1B-a is more conserved with human 4.1B. All vertebrate 4.1B proteins examined (data not shown) have retained an SAB domain, therefore our data suggest 4.1B-b has lost the SAB function during evolution. These results suggest the two zebrafish 4.1B proteins evolved divergent functions with a constraint to maintain the function of individual domains.

We next compared the genomic organization of human and zebrafish *epb41l3* genes to understand the structure and function of these evolutionarily distant species (Figure 1D). When focusing our attention only on the coding sequences of these genes, we found that the exons encoding the FERM and FERM-adjacent domains are nearly identical in size and are well conserved. For example, the FERM adjacent domain is translated from a single exon in all genes (Human *epb41l3*: exon 10; Zebrafish *epb41l3a*: exon 16; Zebrafish *epb41l3b*: exon 12). Pairwise alignments of these exons performed in Jalview revealed the FERM adjacent domain in *epb41l3a* is more conserved with human *epb41l3* compared to *epb41l3b* (71% vs 65% respectively). The overall percent identity of the FERM domain encoding exons are 62% between human 4.1B and zebrafish 4.1B-a and 66% between human 4.1B and zebrafish 4.1B-b. This is quite interesting as the amino acid sequence of the FERM domain is highly conserved between human 4.1B and zebrafish 4.1B-a (87%; Figure 1C). We found that many of the single nucleotide polymorphisms that exist between the two genes occurred at the third position within a given codon. Because the third position within a codon does not play a major role in dictating the amino acid incorporated into a protein, the high mutational rate observed at

the genetic level of the zebrafish *epb41l3* genes does not affect the overall amino acid sequence. We also identified an extra exon within the FERM domain of *epb41l3b* (exon 9) that accounts for an additional fourteen amino acids in the protein domain sequence. It will be interesting to determine if this additional exon provides the protein with a new function. The SAB is well conserved between human *epb41l3* and zebrafish *epb41l3a* (67%), but there are no exons within *epb41l3b* that resemble this domain, providing further evidence that 4.1B-b does not contain an SAB domain. The CTD domain is also well conserved both in structure and size. Interestingly, we found *epb41l3a* was missing the last exon (exon 28). The DNA that encodes this exon does exist within the chromosome, but there is a stop codon immediately after exon 27. To confirm whether *epb41l3a* mRNA contained exon 28, we designed a forward primer in exon 26 and reverse primers in exon 26, exon 27, and the putative exon 28. Using cDNA obtained by RT-PCR from 28 hpf embryos, we were able to amplify products from exon 26 and exon 27, but not from exon 28 (data not shown). This suggests that the truncated version of *epb41l3a* is exclusively expressed at 28 hpf.

We next conducted a phylogenetic analysis using Phylogeny.fr to confirm the relationship between various invertebrate and vertebrate 4.1B proteins (Dereeper, 2008; Figure 1E). We used predicted sequences of all 4.1 proteins in zebrafish and fugu, although these sequences have not been confirmed by syntenic analysis. Our analysis reveals that zebrafish 4.1B proteins are most closely related to all other vertebrate 4.1B proteins and not to any of the other 4.1 family members. This provides further evidence of the evolutionary conservation between these proteins. It is important to note that

zebrafish 4.1B-a is more closely related to fugu 4.1B-b in our phylogenetic analysis; we believe this is due to a problem with nomenclature.

epb41l3a and epb41l3b Are Differentially Expressed within the Developing Embryo

We next examined the temporal expression of the duplicated *epb41l3* genes to detect the presence of these genes during embryonic development (Figure 2A). RT-PCR analysis on cDNA prepared from various developmental stages suggests both genes are present at all ages of early development. There is very little expression of *epb41l3a* at 1.5 hpf, but this gradually increases as embryos develop. *epb41l3b* shows stronger expression at 1.5 hpf than *epb41l3a,* and also continues to increase gradually throughout development. We confirmed that the PCR products were specific to each gene by sequencing the products obtained at 1.5, 16, 24, and 72 hpf. Expression of these genes before the midblastula stage is an indicator of maternal mRNA expression and suggests they may have important roles during early development.

Figure 1 (next page): **Characterization of *epb41l3* Genes in Zebrafish.** (A) Syntentic analysis of duplicated zebrafish *epb41l3* genes. *epb41l3a* maps to Dre 24 whereas *epb41l3b* maps to Dre 2. Several genes surrounding both *epb41l3a* and *epb41l3b* are orthologous to genes surrounding mouse *epb41l3* on Mmu17. Red boxes and dashed lines indicate orthologous *epb41l3* genes. Distances between genes are not drawn to scale. (B) Schematic representation of 4.1B structure. All 4.1B proteins contain a four point one, ezrin, radixin, moesin domain (FERM - purple), a FERM adjacent domain (FA – pink), and a C-terminal domain (CTD - green). Only 4.1B-a contains a spectrin actin binding domain (SAB - blue) similar to human 4.1B. (C) Pairwise alignments of zebrafish 4.1B proteins and domains compared to human 4.1B represented as a percentage of amino acid identity. (D) Genomic analysis of *epb41l3* genes. Exons are drawn to scale; introns are not drawn to scale. Colored exons represent the genetic code for the various protein domains as in B. (E) Phylogenetic analysis of 4.1 proteins in various invertebrates and vertebrates. Amino acid sequences were trimmed to include unambiguously aligned regions and analyzed with Phylogeny.fr (Dereeper, 2008). Scale bar represents 0.5 substitutions per site.

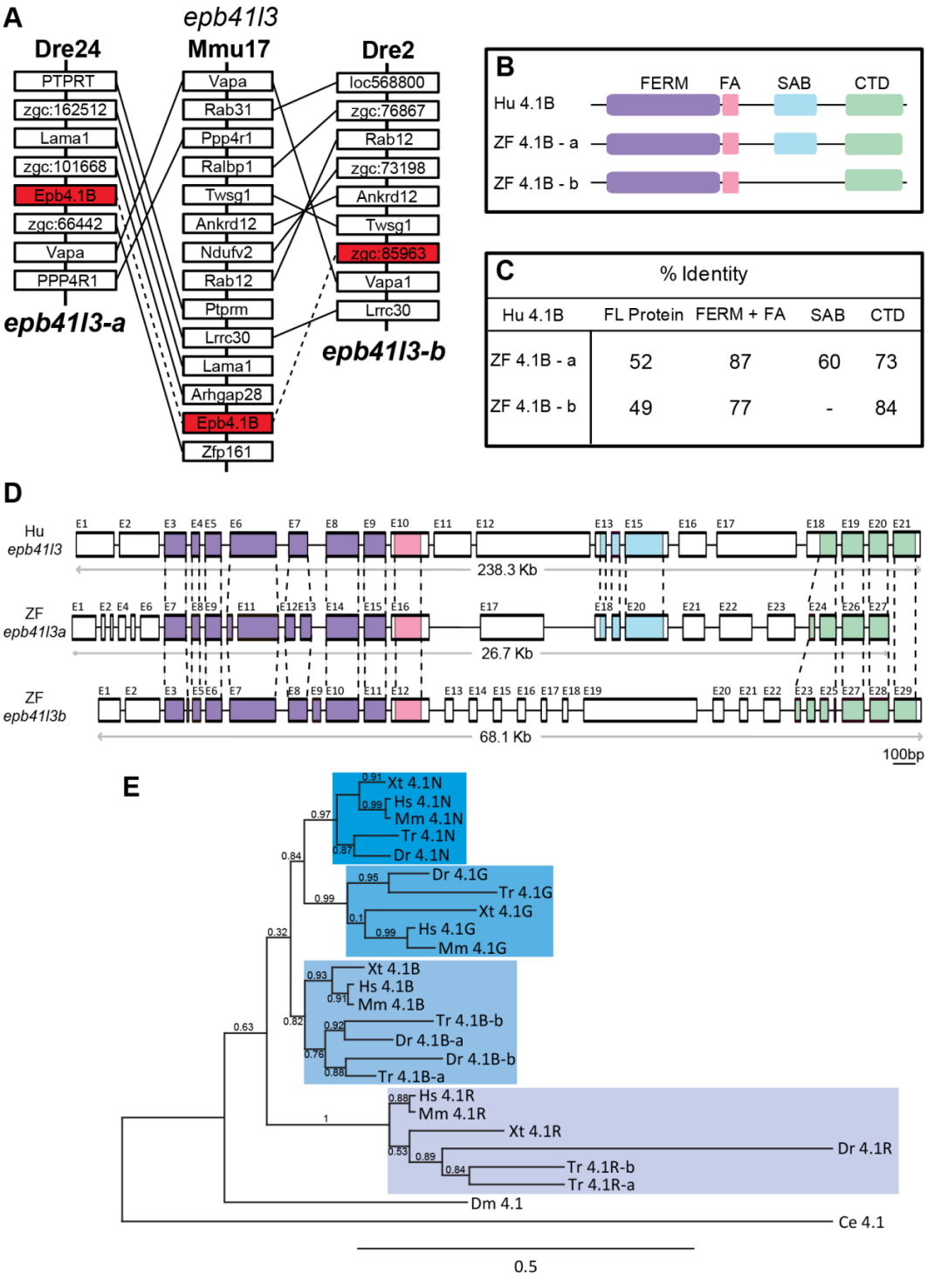
A
epb41l3
Dre24
Mmu17
Dre2
PTPRT
zgc:162512
Lama1
zgc:101668
Epb4.1B
zgc:66442
Vapa
PPP4R1
epb41l3-a
Vapa
Rab31
Ppp4r1
Ralbp1
Twsg1
Ankrd12
Ndufv2
Rab12
Ptprm
Lrrc30
Lama1
Arhgap28
Epb4.1B
Zfp161
loc568800
zgc:76867
Rab12
zgc:73198
Ankrd12
Twsg1
zgc:85963
Vapa1
Lrrc30
epb41l3-b
B
FERM
FA
SAB
CTD
Hu 4.1B
ZF 4.1B - a
ZF 4.1B - b
C
% Identity
Hu 4.1B
FL Protein
FERM + FA
SAB
CTD
ZF 4.1B - a
52
87
60
73
ZF 4.1B - b
49
77
-
84
D
Hu epb41l3
238.3 Kb
ZF epb41l3a
26.7 Kb
ZF epb41l3b
68.1 Kb
100bp
E
Xt 4.1N
Hs 4.1N
Mm 4.1N
Tr 4.1N
Dr 4.1N
Dr 4.1G
Tr 4.1G
Xt 4.1G
Hs 4.1G
Mm 4.1G
Xt 4.1B
Hs 4.1B
Mm 4.1B
Tr 4.1B-b
Dr 4.1B-a
Dr 4.1B-b
Tr 4.1B-a
Hs 4.1R
Mm 4.1R
Xt 4.1R
Dr 4.1R
Tr 4.1R-b
Tr 4.1R-a
Dm 4.1
Ce 4.1
0.5

To determine the spatial expression of *epb41l3* genes in the trunk of zebrafish embryos, we performed whole mount *in situ* hybridization at 19, 28, and 72 hpf (Figure 2B). These ages correspond to specific observable behaviors including spontaneous coiling, touch-evoked coiling, and free swimming respectively. We were interested in the trunk at these time points because spontaneous coils are mediated by electrical synapses, whereas touch-evoked behaviors are mediated by chemical synapses (Pietri, 2009; Saint-Amant, 1998; 2001). These behaviors are controlled by a subset of neurons within the spinal cord, and thus expression of either *epb41l3* gene in the spinal cord may indicate they are involved in synapse formation. Since there is high conservation between different *epb41* genes in zebrafish (62% conservation between *epb41l3a* and *epb41l3b*; data not shown) we designed antisense probes in regions unique to each gene and confirmed they could only recognize their respective genes using the BLAST tool from NCBI. We amplified the template from 24 hpf embryo cDNA and confirmed the identity of the probe by sequencing, thus providing further evidence that our probes specifically identify our genes of interest. Results from our *in situ* hybridization show *epb41l3a* is expressed within the spinal cord at 19 hpf and 28 hpf. Expression was strongest near the hindbrain and gradually decreased further caudally. *epb41l3a* is expressed in dorsal and ventral neurons with equal expression along the dorsoventral axis. No detectable expression could be seen within the spinal cord at 72 hpf. In contrast, *epb41l3b* showed expression within the myotome at all ages examined. There is strong expression in both the dorsal and ventral myotome, with expression remaining proportional to myotome size along the rostralcaudal axis. Because the expression was so strong within the myotome, it was difficult to determine if *epb41l3b* was expressed within the spinal cord.

To resolve whether or not *epb41l3b* was expressed within the spinal cord, we performed fluorescent *in situ* hybridization (FISH). We analyzed the expression patterns of both *epb41l3a* and *epb41l3b* in 28 hpf Mnx1:GFP embryos. Mnx1 is a transcription factor expressed within motor neurons and other ventral interneuons (Zelenchuk, 2011; Seredick, 2012). We chose to determine the expression patterns in motor neurons because our initial analysis revealed *epb41l3a* may be expressed within motor neurons. FISH experiments were carried out for each individual probe followed by immunohistochemistry (IHC) to label motor neurons with antibodies to GFP. Interestingly, we determined that the chicken anti-GFP antibody can faintly label the myotome following FISH, thus providing a method to analyze expression patterns of *epb41l3* genes in muscle. We saw expression of *epb41l3a* throughout the spinal cord, with specific expression of *epb41l3a* within primary motor neurons (Figure 2C). No detectable expression of *epb41l3a* was found within the myotome (Figure 2D). *epb41l3b* was not expressed within primary motor neurons or in any other neuronal population within the spinal cord (Figure 2C), but it was highly expressed within the myotome (Figure 2D). Consistent with sequence analysis, we conclude from these data that *epb41l3a* and *epb41l3b* are differentially expressed, providing strong evidence that these proteins have evolved divergent functions.

Knockdown of 4.1B-a Causes a Reduction in the Number of Synapses at Primary Motor Neurons

Since 4.1B-a is expressed within the spinal cord, we decided to perform knockdown studies in Mnx1:GFP zebrafish embryos using a MO. We assayed each

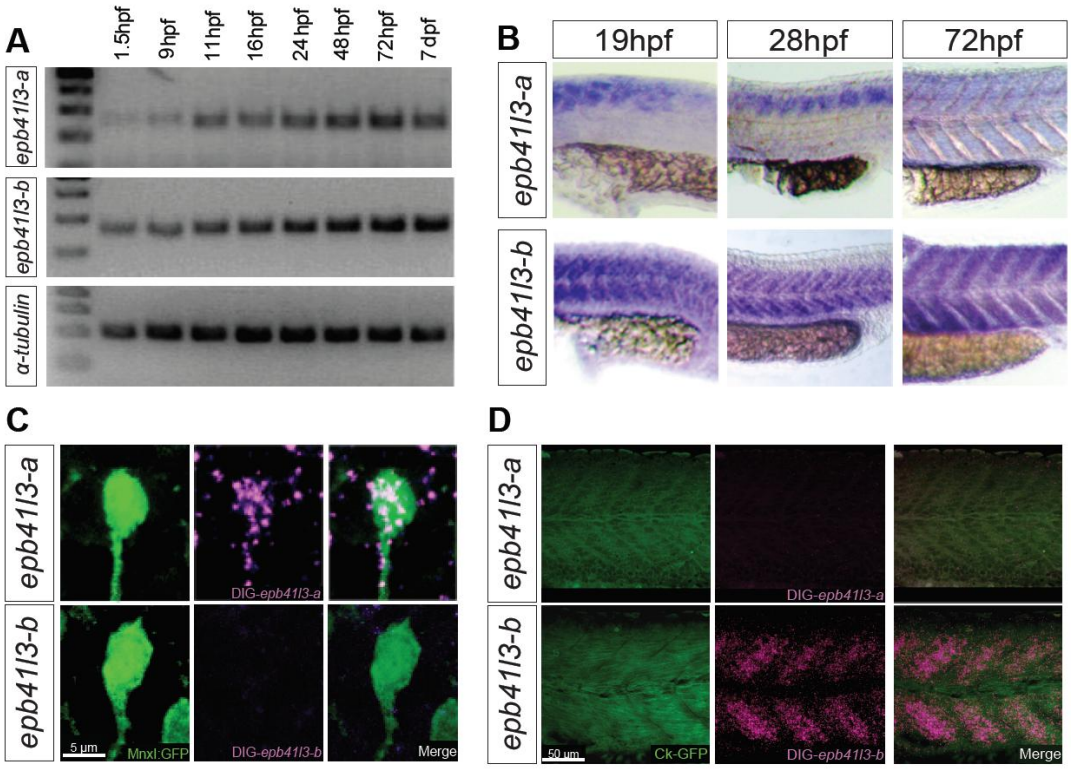

Figure 2: Duplicated *epb41l3* Genes in Zebrafish Are Differentially Expressed. (A) Analysis of *epb41l13* expression levels during development. From left to right, cDNA samples were prepared from AB/Tübingen at the 16-cell (1.5 hpf), 90% epiboly (9 hpf), 3-somite (11 hpf), 16, 24, 48, 72 hpf, and 7 dpf stages. Primers were designed to unique regions in each *epb41l3* gene as well as for the α-tubulin control. Samples isolated from 1.5, 16, 24, and 72 hpf were sequenced to confirm specificity. (B) Expression patterns of *epb41l3* in the trunk of the developing embryo. Expression patterns were revealed by whole mount *in situ* hybridization with probes unique to each individual gene. Images are displayed as lateral views at 19, 28, and 72hpf corresponding to various locomotor behaviors. Experiments were carried out in Mnx1:GFP embryos not expressing GFP. (C) Expression profiles of *epb41l3* in primary motor neurons and in (D) muscle revealed through fluorescent *in situ* hybridization at 26hpf. Experiments were carried out in Mnx1:GFP embryos expressing GFP. GFP labeling of primary motor neurons and muscle was performed after completion of the fluorescent in situ hybridization. (C) Scale bar, 5 µm. (D) Scale bar, 50 µm.

embryo between 26 – 28 hpf for differences in the localization of the presynaptic protein synapsin (synapsin 1/2 antibody) and the postsynaptic proteins PSD-93, PSD95, and Sap-97A (pan-MAGUK antibody; Meyer, 2004). Synapsin is an important component of synapses and regulates the reserve pool of synaptic vesicles (Bonanomi, 2005). It has been found that synapsin localizes to greater than 99% of synapses in mouse cortex (Micheva, 2010), and provides a method to label the presynaptic terminals in the zebrafish spinal cord (Easley-Neal, 2013). PSD-95, PSD-93, and Sap-97A belong to the membrane associated guanylate kinase (MAGUK) family of proteins and are important scaffolding molecules at glutamatergic synapses (reviewed in Montgomery, 2004). Together, the colocalization of these proteins provides information on the number of glutamatergic synapses present on primary motor neurons (Figure 3A). We found a significant decrease in the number of pan-MAGUK puncta on primary motor neurons in 4.1B-a MO injected embryos compared to control MO injected embryos (30% decrease, $p < 0.01$). This effect was rescued by coinjecting mRNA encoding zebrafish 4.1B-a. Interestingly, this effect was also rescued by coinjecting mRNA encoding zebrafish 4.1B-b or human 4.1B. Surprisingly, we also saw a decrease in the number of synapsin 1/2 puncta (58% decrease, $p < 0.01$; Figure 3B) that was rescued by injection of mRNA encoding 4.1B-a, 4.1B-b, or human 4.1B (Figure 3C). This was surprising as no study to date has described a role for 4.1 proteins at the presynapse. Finally, we found an overall decrease in the number of colocalized puncta on primary motor neurons (62% decrease, $p < 0.01$) that was rescued by injecting each mRNA constructs tested (Figure 3D). No observable difference was seen in the number of synapsin 1/2, pan-MAGUK, or colocalized puncta when 4.1B-a was overexpressed (Figure 3B, C, D). These results

suggest 4.1B-a can affect the localization of pre- and postsynaptic proteins due to either a direct loss of 4.1B-a function in both pre- and postsynaptic cells, or due to a transsynaptic effect across the synaptic cleft. These results also suggest the SAB domain may not be necessary for the function of 4.1B as 4.1B-b, which lacks the SAB domain, can rescue the phenotypes. It is important to note that although 4.1B-b lacks the defined SAB domain (Gimm, 2002), we cannot exclude the possibility that other sequences in 4.1B-b may have evolved the ability to interact with the actin-spectrin cytoskeleton.

To date, studies of 4.1 protein function have focused solely on postsynaptic protein recruitment and stabilization. It was therefore interesting to see an effect on the presynaptic marker synapsin when 4.1B-a was knocked-down. To characterize the presynaptic phenotype further, we examined the localization of the presynaptic proteins Synaptic vesicle protein 2 (SV2) and Synaptotagmin 2b (Figure 3E and F respectively). SV2 is required for normal neuronal transmission and is thought to play a role in regulating exocytosis (Chang, 2009; Schivell, 2005). Synaptotagmins are calcium sensing proteins involved in synaptic vesicle exocytosis and subsequent neurotransmitter release (Fernandez-Chacon, 2001). Synaptotagmins can interact with SV2 to regulate calcium sensing (Pyle, 2000), and thus provides a model of protein complex formation at presynaptic terminals. We found an overall decrease in the number of SV2 (44% decrease, $p < 0.01$; Figure 3H) and synaptotagmin 2b (37% decrease, $p < 0.01$; Figure 3I) puncta on primary motor neurons. Both phenotypes were rescued by coinjecting each 4.1B mRNAs with no observable difference seen with the overexpression of 4.1B-a. These results provide evidence that 4.1B-a may be required for the formation of the active zone at presynaptic terminals.

Because 4.1B has been found at excitatory postsynaptic densities (Scott, 2001), we decided to determine whether the effect of 4.1B-a knockdown is specific to excitatory synapses. To do this, we labeled inhibitory synapses with the inhibitory marker gephyrin (Figure 3G). Gephryin mediates the recruitment and stabilization of glycine receptors and GABA receptors at inhibitory synapses (Kneussel, 2000). We found no decrease in the number of gephryin puncta on primary motor neurons, thus suggesting 4.1B-a is specifically involved in the formation of glutamatergic synapses (Figure 3J).

4.1B-a Knockdown Causes Kinetic Differences During Touch-evoked Coiling

Our immunolabeling results suggest 4.1B-a knockdown affects the number of synapses on primary motor neurons at 26 hpf. At this developmental stage, zebrafish embryos have already developed the touch response neuronal circuit that is dependent on innervation of dorsal and ventral myotome by primary motor neurons (Westerfield,

---

Figure 3 (next page): **Knockdown of 4.1B-a Causes a Reduction in the Number of Synapses at Primary Motor Neurons.** (A) Lateral view of immunofluorescence labeling in Mnx1:GFP embryos expressing GFP and labeled with antibodies to synapsin 1/2 and pan-MAGUK. Arrows indicate site of colocalization. (B - C) Quantification of (B) synapsin 1/2 labeling, and (C) pan-MAGUK labeling at primary motor neurons. Two primary motor neurons were analyzed per embyo. The data represents the average number of puncta per individual primary motor neuron. The number of puncta per cell was quantified with the puncta analyzer plugin for ImageJ developed by Ippolito and Eroglu 2010. (D) Quantification of colocalized puncta per cell. Analysis of colocalization was carried out with puncta analyzer plugin in ImageJ. (E – G) Lateral view of immunofluroescence labeling in Mnx1:GFP fish with antibodies to (E) SV2, (F) Synaptotagmin 2b, and (G) Gephyrin. (H - J) Quantification of immunofluourescence labeling for (H) SV2, (I) Synpatotagmin 2b, and (J) gephyrin. All fish analyzed for an individual condition were averaged and standard deviation, standard error, and One-way ANOVAs were calculated from the data set. Error bars represent standard error. * indicates p-value of < 0.05 and ** indicates p-value of < 0.01. Data shown represents one experiment; all experiments were repeated a minimum of three times. $n \geq 8$ embryos. Scale bar, 5 µm. Abbreviations: Ctl MO = control morpholino; 4.1B-a MO = 4.1B-a morpholino; Dr 4.1B-a RNA = *Danio rerio* 4.1B-a RNA; Dr 4.1B-b RNA = *Danio rerio* 4.1B-b RNA; Hs 4.1B RNA = *Homo sapiens* 4.1B RNA.

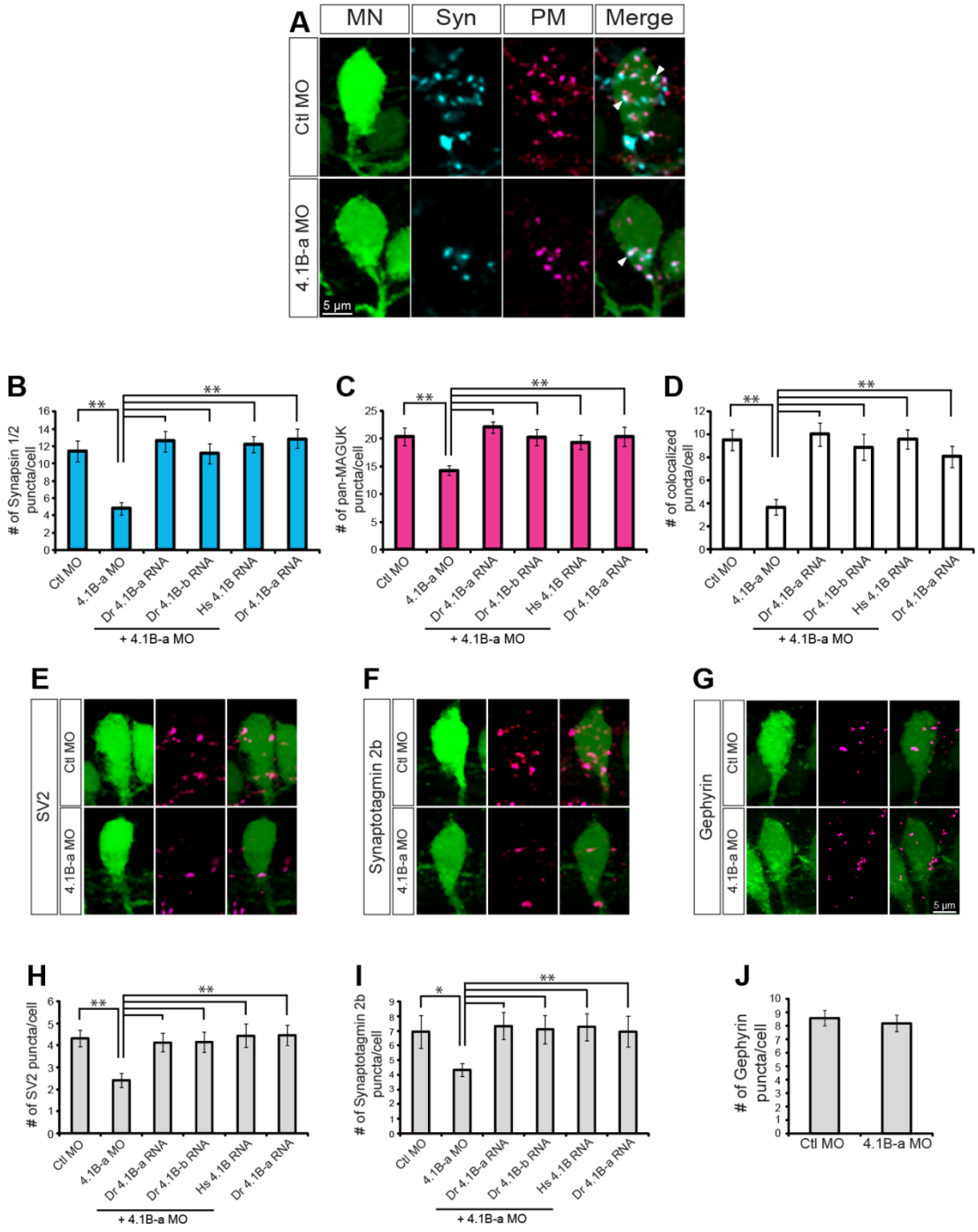
A
MN
Syn
PM
Merge
Ctl MO
4.1B-a MO
5 µm
B
# of Synapsin 1/2 puncta/cell
C
# of pan-MAGUK puncta/cell
D
# of colocalized puncta/cell
Ctl MO
4.1B-a MO
Dr 4.1B-a RNA
Dr 4.1B-b RNA
Hs 4.1B RNA
Dr 4.1B-a RNA
+ 4.1B-a MO
**
E
SV2
F
Synaptotagmin 2b
G
Gephyrin
5 µm
H
# of SV2 puncta/cell
I
# of Synaptotagmin 2b puncta/cell
*
J
# of Gephyrin puncta/cell

1986). We therefore hypothesized that loss of these synapses due to 4.1B-a knockdown would affect touch-evoked behaviors. It is also important to note that spontaneous coiling is significantly reduced by this developmental time point, thus reducing the likelihood of misidentifying touch evoked responses as spontaneous responses. To begin our assessment, we first needed to ensure that any phenotype we saw was due to loss of synaptic number and not due to an effect on motor neuron or muscle development. We first analyzed the structure of caudal primary motor neurons (CaPs) as they are easily identifiable due to their long ventral projecting axon (Eisen 1986; Westerfield, 1986; Figure 4A). We used a MATLAB program designed by Kutzing et al. (2010) to determine if there were any morphological differences in the number and length of axonal projections. We saw no structural differences between control MO and 4.1B-a MO injected embryos (Figure 4A; data not shown). We also assessed the structure of muscle fibers by immunolabeling embryos with Alexa Fluor 488-Phalloidin and saw no observable differences in the structure or organization of the myotome (Figure 4A). Finally, we assessed the number of acetylcholine receptor clusters at the neuromuscular junction by labeling embryos with α-bungarotoxin (Figure 4A). We found no observable differences in the number of puncta between control morpholino and 4.1B-a morpholino injected embryos (Figure 4A; data not shown). Together, these results show no deficits in the structural organization of tissues involved in the touch response neuronal circuit.

To investigate the role of 4.1B-a during touch-evoked behaviors, we performed a kinematic analysis using high-speed video recordings (Figure 4B). We found a significant increase in the latency (defined as the time it takes for the fish to respond to a mechanical stimulus) between control MO and 4.1B-a MO injected embryos (55% increase, $p < 0.01$;

Figure 4C). This phenotype was rescued by coinjection of each 4.1B mRNA. We also saw a significant decrease in the velocity of single C-bends (52% decrease, $p < 0.01$; Figure 4D). The velocity is defined as the displacement of the tip of the tail (beginning at the first observable sign of voluntary muscle contraction until max height is reached) divided by the time it takes for the embryo to complete one C-bend. This phenotype was also rescued by each 4.1B mRNA. 4.1B-a overexpression did not alter the latency or the velocity of touch-evoked behaviors.

We next examined high-speed video recordings of spontaneous coils at 19 hpf. Spontaneous coiling at 19 hpf is primarily mediated by gap proteins (Saint-Amant, 2000). This provides a measure of the ability of motor neurons to induce muscle contraction independent of chemical synapses. We saw no differences in the number of spontaneous contractions per minute (Figure 4E) nor did we see a difference in the velocity of C-bends (Figure 4F). Taken together, we conclude 4.1B-a is important for the formation of excitatory chemical synapses involved in the touch response neuronal circuit.

4.1B-b Is Necessary for Organizing Muscle Fibers in the Developing Myotome

Our expression analysis of *epb41l3b* shows this gene is specifically expressed within muscle tissue. We also showed 4.1B-b was capable of rescuing phenotypes associated with 4.1B-a knockdown, suggesting that the SAB domain is not necessary for synapse development involved in touch-evoked behaviors. As a result, we next focused on the function of 4.1B-b in muscle tissue. We knocked down the function of 4.1B-b with a MO and immunolabeled 26 hpf embryos with Alexa Fluor 488 Phalloidin to determine the integrity of the skeletal muscle tissue (Figure 5A). We observed severe muscle

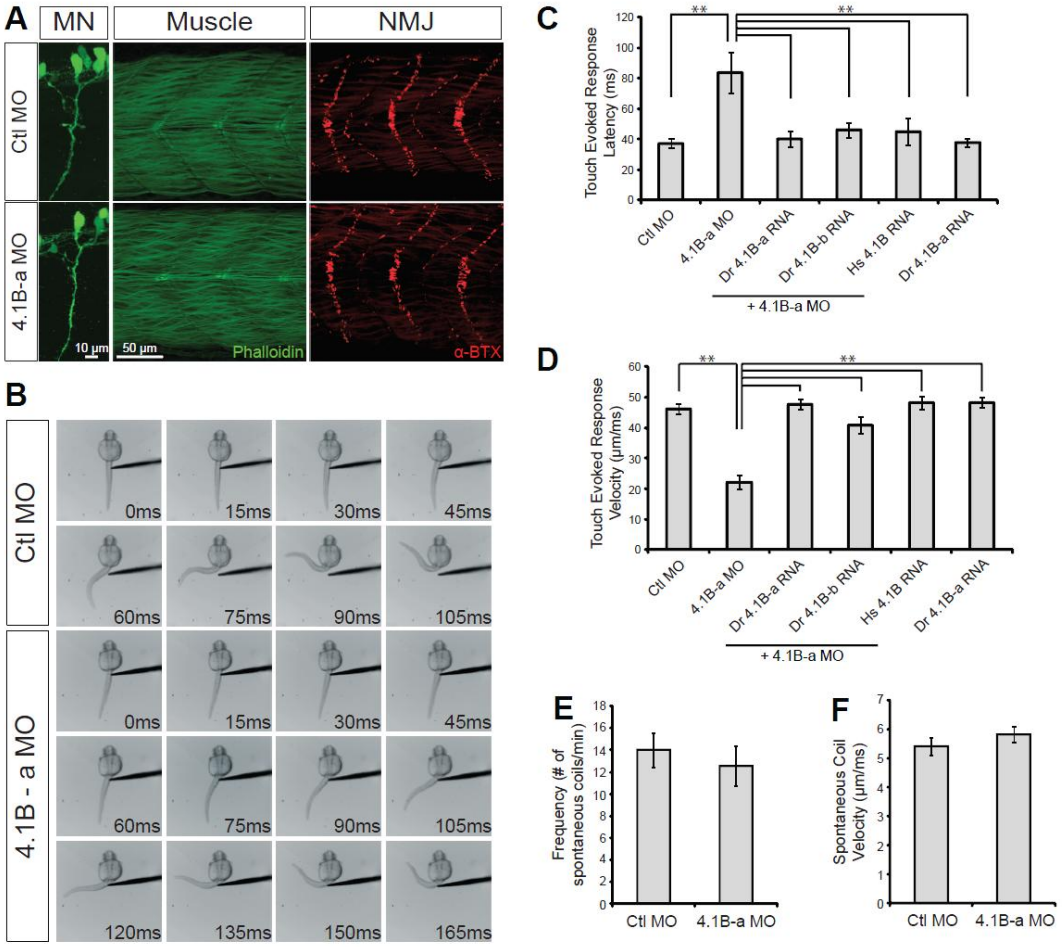

Figure 4: **4.1B-a Knockown Causes Kinetic Differences During Touch-evoked Coiling.** (A) Lateral view of primary motor neurons, the myotome, and the NMJ in the trunk of 26 hpf Ctl MO and 4.1B-a MO injected embryos. Motor neuron structure was analyzed in Mnx1:GFP embryos expressing GFP in primary motor neurons. Scale bar, 10 µm. The myotome and NMJ were analyzed by labeling Mnx1:GFP embryos not expressing GFP with Alexa Fluor 488 Phalloidin (myotome) and α-BTX (NMJ). Scale bar, 50 µm. (B) Example of touch-evoked response in control and 4.1B-a MO injected embryos at 26 hpf. The time series represents the full response used in analysis of (C) latency and (D) velocity. (C) Latency for touch-evoked responses in 26 hpf embryos. Latency was measured from the time the mechanical stimulus touched the outer surface of the skin until voluntary muscle contraction was observed. (D) Velocity measurements of touch-evoked responses at 26 hpf. The first five responses for an individual fish were analyzed beginning at the tip of the tail at rest to the tip of the tail at max height and averaged to give a single velocity for each individual embryo. (E) Frequency of spontaneous coils represented as the number of spontaneous coils per minute at 19hpf. (F) Kinematic analysis of individual C-tail bends at 19hpf. Error bars represent standard error. ** indicates a p-value of < 0.01. $n \geq 8$ embryos.

disorganization in 4.1B-b MO injected embryos compared to control MO injected embryos. Individual segments were irregularly shaped, with some segments narrower rostral-caudally. Muscle fibers were also detached from each other, creating irregular patterns of muscle fiber organization. Upon analysis of 3D renderings, it did not appear that muscle fibers were detached from the myosepta. These phenotypes were rescued by mRNAs encoding 4.1B-b, 4.1B-a and human 4.1B (data not shown). This suggests 4.1B-b has a major role in the formation of muscle fiber attachment to the extracellular matrix.

Motor neuron axons grow toward their muscle fiber targets due to cues within the environment (Bonanomi, 2010). Loss of these cues within muscle cells prevent targeting of axonal projections to the muscle and thus loss of the synaptic connection between them (Eisen, 1991; Kimmel, 1989; Lewis, 1981; Tosney, 1987). We decided to examine the structure of motor neuron axons and their innervation patterns of muscle tissue. We found that CaPs in 4.1B-b MO injected embryos had stunted axons with unusual patterns of axonal outgrowth (Figure 5A). There was a 52% decrease ($p < 0.01$) in the number of processes that emanated from the main ventral axon (Figure 5B). These phenotypes were rescued by zebrafish 4.1B-b or human 4.1B RNA, but were not rescued by zebrafish 4.1B-a RNA (33% decrease compared to control MO injected embryos; $p < 0.05$). We also observed a 39% decrease ($p < 0.01$) in the total cable length of the entire motor axon (Figure 5C) which was rescued by each of the 4.1B RNA constructs. We next looked at the number of ACh receptor clusters on muscle fibers as this is an indication of proper neuromuscular junction (NMJ) formation, and thus proper axonal innervation (Figure 5A). We found a 45% decrease in the number of ACh receptor clusters in 4.1B-b MO injected embryos which was rescued by each 4.1B RNA ($p < 0.01$; Figure 5D). 4.1B-b

overexpression did not cause any observable phenotypes nor did our analysis suggest a significant difference in the various parameters analyzed. These data suggest two possibilities for the role of 4.1B-b in motor neuron development. First, 4.1B-b knockdown disrupts adhesion sites necessary for muscle fiber attachment to the extracellular matrix. This leads to muscle fiber disorganization and subsequent disruption of cues within the myotome necessary for motor neuron axon pathfinding. Second, 4.1B-b knockdown may directly affect motor neuron axon pathfinding. Further studies will be needed to tease the two possibilities apart.

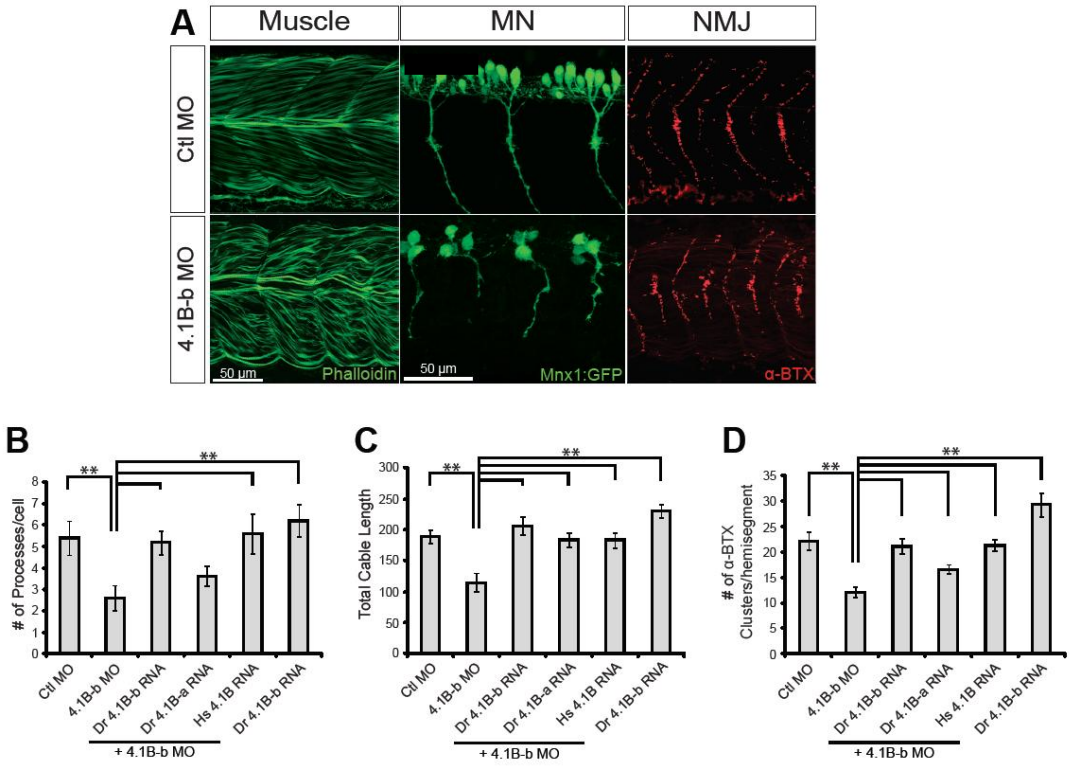

Figure 5: **4.1B-b Is Necessary for Organizing Muscle Fibers in the Developing Myotome.** (A) Lateral view of primary motor neurons of Mnx1:GFP embryos, the myotome, and the NMJ at 26 hpf for Ctl MO and 4.1B-b MO injected embryos. Scale bar, 50 µm (B - C) Quantification of the (B) number of processes per cell and (C) the total cable length of axonal projections. 10 axons were analyzed for each condition. The data was analyzed with the BONFIRE program developed by Kutzing et al. 2010. (D) Quantification of α-BTX per hemisegment. Analysis was conducted with the puncta analyzer plugin in ImageJ. ** indicates a p-value < 0.01. $n \geq 8$.

Knockdown of 4.1B-b Alters Locomotor Behaviors

Our immunolabeling experiments show 4.1B-b may be necessary for the proper formation of the NMJ, axon pathfinding, and/or muscle development. Since these structures and processes are important for the proper development of zebrafish locomotor behaviors, we hypothesized that 4.1B-b knockdown would lead to altered spontaneous and touch-evoked responses. We first examined the frequency and velocity of spontaneous coils at 19 hpf. We observed a 31% decrease in the number of spontaneous coils per minute in 4.1B-b MO injected embryos compared to control MO injected embryos ($p < 0.05$; Figure 6B). This was rescued by each 4.1B RNA construct except 4.1B-a (24% decrease compared to control injected embryos; $p < 0.05$). Surprisingly, we saw no differences in the kinetics of C-bend velocities at 19 hpf (data not shown). We next examined touch-evoked coiling at 26 hpf (Figure 6A). We observed a 64% increase in the latency ($p < 0.01$; Figure 6C) and a 50% decrease in the velocity of touch evoked coiling ($p < 0.01$; Figure 6D). All phenotypes were rescued by 4.1B-b and human 4.1B RNA but not with 4.1B-a RNA. Embryos rescued with 4.1B-a RNA showed a 57% increase in the latency compared to control MO injected embryos as well as a 45% decrease in the velocity of C-bend coiling ($p < 0.01$). This provides evidence that 4.1B-b may be functionally different than 4.1B-a, and thus 4.1B-a cannot rescue all phenotypes associated with myotome development and/or axon pathfinding. Overexpression of 4.1B-b caused a significant increase in the velocity of C-bend behaviors ($p < 0.01$ Figure 6D), with no other significant effects on touch-evoked or spontaneous behaviors. Interestingly, we also observed abnormal behaviors of muscle contraction in 4.1B-b MO injected embryos, particularly in their ability to relax the muscle at the apex of the C-bend. 4.1B-b

embryos exhibited a 60% increase ($p < 0.01$) in the duration of time the tail remained in a state of contraction (Figure 6E); this phenotype was rescued by each 4.1B RNA construct. We also found several examples of embryos who displayed erratic release of the contraction. Immediately upon relaxation, embryos would contract and remain in a state of tetanus. This occurred between one and three times before finally relaxing their tail (data not shown). These data clearly demonstrate that the loss of 4.1B-b affects the formation of the NMJ, motor neuron axon pathfinding, and muscle development, which leads to altered locomotor behaviors during early development.

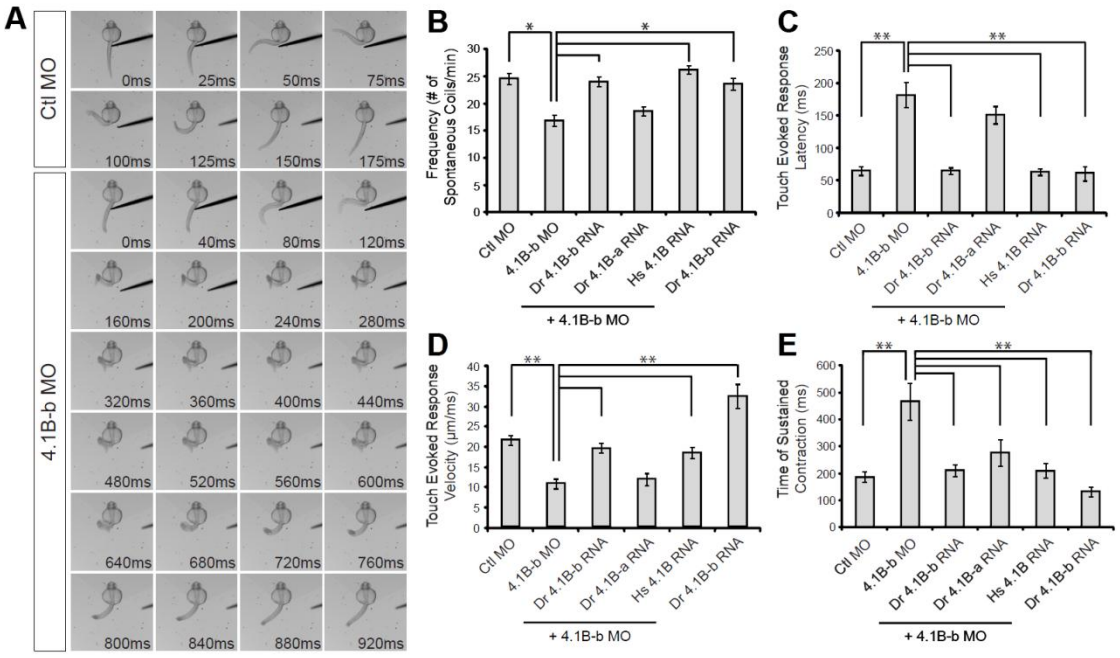

Figure 6: **Knock-down of 4.1B-b Alters Locomotor Behaviors.** (A) Representation of the full touch response from the time of touch with the stimulus to the end of relaxation of tail contraction. Note the difference in time scales between Ctl MO injected embryos with 4.1B-b MO injected embryos. (B) Frequency of spontaneous coils at 19hpf. (C) Latency of touch evoked responses at 26 hpf. (D) Velocity of touch-evoked responses at 26 hpf. (E) Duration of sustained contraction at max height. The length of the sustained contraction began when the tip of the tail reached max height and ended when muscle relaxation occurred. * indicates p-value < 0.05 and ** indicates p-value < 0.01. $n \geq 8$.

Discussion

In the present study, we characterized the function of 4.1B in developing zebrafish embryos. We identified two homologues within the zebrafish genome (Figure 1), *epb41l3a* (protein 4.1B-a) and *epb41l3b* (protein 4.1B-b) that display unique expression patterns within the trunk. *epb41l3a* was expressed within the spinal cord at 19 and 28 hpf, with expression in identified primary motor neurons at 28 hpf (Figure 2B, C). *epb41l3b* on the other hand, was expressed within the myotome at all ages examined (Figure 2B, D). The differential expression patterns of these genes allowed us to study their functions without concern for redundancy, although we cannot rule out that redundant mechanisms may exist due to the functions of the other 4.1 proteins. First, we knocked down 4.1B-a protein levels with an antisense MO and immunolabeled embryos at 26 hpf. We found the markers to the presynaptic proteins SV2, Synaptotagmin 2b, and Synapsin, as well as the postsynaptic marker pan-MAGUK, were all reduced (Figure 3). The colocalization of synapsin with pan-MAGUK revealed a reduction in synapse number, and this correlated with altered kinetics of touch-evoked responses (Figure 4). To test the function of 4.1B-b, we knocked-down the protein with an antisense MO and immunolabeled 26 hpf embryos with an antibody to F-actin filaments. This allowed us to visualize the organization of the myotome which was irregular, not bilaterally symmetrical, and severely disorganized in 4.1B-b knockdown embryos (Figure 5A). Further analysis revealed the primary motor neuron axons were highly aberrant and failed to traverse the stereotyped pathway (Figure 5A, B, C; Eisen, 1986); this lead to a reduction in the number of ACh receptor clusters at sites of neuromuscular contact (Figure 5A, D). These results show a relationship to the uncharacteristic kinetics of

spontaneous and touch evoked behaviors during development (Figure 6). Taken together, we conclude that the zebrafish 4.1B proteins have retained their function of stabilizing macromolecular complexes at plasma membranes. We identify 4.1B-a as an important component for the formation of complexes at synaptic membranes, whereas 4.1B-b is an important component for the formation of complexes at the sarcolemma of muscle cells. Together, these data suggest that the 4.1B proteins in zebrafish may be involved in stabilizing protein complexes at membranes and thus are evolutionarily conserved with their mammalian homologues.

Model of Synapse Formation

Our studies of 4.1B-a were surprising for two reasons. First, no study to date has suggested a role for 4.1B at presynaptic sites. It is possible that the effect we see is due to either direct loss of 4.1B-a at presynaptic terminals, or it could be due to a transsynaptic effect caused by loss of 4.1B-a on the postsynaptic terminal. Given the relatively wide expression of 4.1B-a in the spinal cord and developing hindbrain, we cannot rule out the possibility that 4.1B-a is expressed in presynaptic cells, and thus may be directly involved in stabilizing macromolecular complexes at the presynaptic terminal. Further studies will be needed to elucidate the expression and function of 4.1B-a in presynaptic cells. Second, we were surprised to find that we could rescue the phenotype with 4.1B-b which lacks the SAB domain. This suggests the SAB domain is dispensable for the recruitment and/or stabilization of proteins at synaptic contacts, and provides further evidence that the main function of 4.1 proteins is to interact with its binding partners through the FERM and CTD domains. It is likely the SAB domain evolved as a

mechanism to further enhance the stabilization of these contacts, but is not the only or main mechanism that exists at these contact sites.

4.1B has been shown to interact with the cell adhesion molecule SynCAM1 to specifically recruit NMDARs to synaptic sites in nonneuronal and neuronal cultured assays (Hoy, 2009). It has also been shown that recordings from motor neurons in zebrafish (Ali, 2000) and in *Xenopus* (Li, 2003) display either mixed AMPA/NMDA receptor or just NMDA receptor currents at newly formed synapses. The latter are considered to be silent synapses and are characteristic of an immature synapse. It was shown that blocking NMDA receptor mediated transmission with the antagonist MK-801 caused an increase in the latency and a decrease in the velocity of 24 hpf embryos (Pietri, 2009). The authors conclude that their data is consistent with the presence of silent synapses within the spinal cord. Given this information, we propose a model for 4.1B-a function at the postsynapse. We hypothesize 4.1B-a is involved in stabilizing NMDA receptors at mixed synapses. First, a mixed synapse contains both gap junctions and synaptic vesicles/neurotransmitter receptors (reviewed in Pereda, 2014). Given the fact that there is a transition between spontaneous coiling, which is dependent on electrical synapses, to touch evoked coiling, which is dependent on chemical transmission (Pietri, 2009), it is reasonable to hypothesize that the synapse between the presynaptic cell and the primary motor neuron is a mixed synapse. Second, our data show an increase in the latency and a decrease in velocity similar to the data obtained from the pharmacological knockdown of NMDA receptors. Immunoprecipitation studies have also shown that human 4.1B can interact with NMDA receptors (unpublished data), and given the fact

that human 4.1B mRNA can rescue all phenotypes in this study, we can conclude that 4.1B-a may stabilize NMDA receptors at this particular synapse.

In our model, we propose that at 19 hpf, an electrical synapse between the presynaptic cell and the primary motor neuron has formed, thus allowing spontaneous contractions to occur. NMDA receptors may or may not be present at this time. Blockers of NMDA and AMPA receptors do not affect spontaneous coils at 19 hpf (Pietri, 2009; Saint-Amant, 2000) thus suggesting there is no chemical transmission at this time. It is possible NMDA receptors are present at this time, however, but they remain silent. A silent synapse is an immature chemical synapse consisting of only NMDA receptors; the synapse remains nonfunctional. As the synaptic contact develops, an accumulation of NMDA receptors begin to cluster at the synaptic site between 19 and 21 hpf, when touch-evoked responses can first be observed (Saint-Amant, 1998). For NMDA receptors to become active during neuronal transmission, two things have to occur. The neurotransmitter glutamate has to bind to the receptor, and the cell has to be sufficiently depolarized to overcome the magnesium block that resides within the pore of the NMDA channel (Seeburg, 1995). Depolarization through the gap junction should be sufficient to remove the magnesium block from NMDA receptors. Glutamate can come from several sources. Formation of the presynaptic terminal in a chemical synapse usually occurs within 30 minutes after initial contact. During this time, synaptic vesicles are being stabilized at the presynapse by various active zone components, and the mechanisms that underlie neurotransmitter release are being established (Friedman, 2000). As early as 45 minutes after the initial contact is made, NMDA receptors begin to cluster at the postsynapse. It can take up to 120 minutes after the initial contact to recruit a large

number of NMDA receptors to postsynaptic sites (Friedman, 2000). Since the presynaptic terminal has already formed and is electrically active, glutamate can be released from the presynaptic terminal, and therefore may provide the glutamate necessary for NMDA receptors to become active. The time course of these events correlates with the transition from spontaneous coils (19 hpf) to touch evoked coils (21 hpf).Other sources of glutamate may come from release of glutamate from the vesicular glutamate transport protein, vGlut1, during synaptic vesicle recycling (Sabo, 2003; 2006), although we suggest it is more likely that glutamate is being released from the presynaptic terminal. As continued depolarization and glutamate release occurs from the presynaptic cell, both calcium and sodium can rush into the primary motor neuron. Calcium initiates a signaling cascade that allows the recruitment of AMPA receptors to synaptic contact sites (Opazo, 2011); this allows the synapse to mature and become fully functional. Therefore, activation of the NMDA receptor drives AMPA receptor recruitment to these synaptic sites, and thus establishes the touch evoked neuronal response at 21 hpf. This supports Pietri et al. (2009) who showed the touch response was dependent on AMPA mediated transmission.

In further support of this model, we would expect that during the transition from electrical to chemical transmission, the number of NMDA receptors would increase. At 19 – 21 hpf, there may be very few NMDA receptors present. As the contact continues to mature however, more NMDA receptors are recruited to the synapse. At the same time, competition between the electrical and chemical synapses can drive synapse elimination, thus allowing the chemical synapse to outcompete the electrical synapse and ultimately cause its decline (Coleman, 1993). As NMDA receptors are recruited and gap junctions

are eliminated, depolarization through the NMDA receptor begins to be more important. Thus, when NMDA receptors are blocked at 24 hpf, a small observable decrease in conductance occurs that causes an increase in the time constant and thus an increase in the time it takes the cell to reach threshold. This correlates with the increase in latency observed in the work done by Pietri et al. (2009). If it is also true that 4.1B-a interacts with NMDA receptors to stabilize them at synaptic sites, then loss of 4.1B-a would cause the same result: an increase in the latency of touch-evoked responses. Also, if depolarization in the presynaptic cell is not sufficient to release enough neurotransmitter at the neuromuscular junction, individual motor units may not be activated. Each motor unit, consisting of a single muscle fiber innervated by a single primary motor neuron, has their own threshold of which they must overcome to allow contraction of that fiber; this provides smooth muscle contraction. If fewer motor units are being recruited, then the velocity of overall muscle contraction would be reduced, consistent with NMDA and 4.1B-a knockdown. Thus, we suggest the synapse between the presynaptic cell and primary motor neuron provides a model to study long term potentiation, which is the persistent strengthening of synaptic contacts due to patterns of electrical activity. Further, these data suggest that long term potentiation itself may be a general mechanism of synapse formation.

It is important to note that the model presented is based off of an accumulation of data gathered from various studies using various model systems and looking at various time points. It is therefore very possible that this may not be the function of this synapse. An enormous amount of work is needed to establish this synapse as a model to study long term potentiation, but we suggest there is a lot of promise in characterizing this synapse

further. Even if this synapse is not involved in long term potentiation, this synapse gives us the ability to study electrical synapse formation, chemical synapse formation, mixed synapses, and synapse competition, which can be directly correlated to simple motor behaviors. Thus, it provides an elegant model to study the initial events of synapse formation.

We must also note that it is possible that the effects we see in our studies are due to defects at the presynapse. Our evidence showed Synaptotagmin 2b and SV2 were downregulated at 26 hpf; these proteins are important for calcium sensing and subsequent neurotransmitter release. With fewer quanta released at the presynaptic terminal, it may activate fewer neurotransmitter receptors to cause a smaller depolarization, producing the same behavioral phenotypes we observed. We did not propose this as a hypothesis however, because no data suggest 4.1B is involved in forming the presynaptic terminal. It is more likely that because 4.1B also interacts with cell adhesion molecules through the FERM domain (Hoy, 2009), important for stabilizing synaptic contacts, loss of 4.1B may have a transsynaptic effect, thus affecting the formation of the active zone and subsequent mislocalization of SV2, synaptotagmin 2b, and synapsin. Further studies will be needed to resolve the role of 4.1B at pre- and postsynapses.

Interestingly, 4.1B has also been shown to contribute to the stabilization and organization of membrane proteins in peripheral myelinated axons (Cifuentes-Diaz, 2011). This fact, however, does not affect our model as studies have shown zebrafish axons are not myelinated at early developmental stages. The first genes associated with myelin formation are observed at 2 dpf, and actual myelin wrapping around axons begins at 4 dpf (Brosamle, 2002). Our observations, and thus our proposed model, all occur

before 30 hpf, before axons have been myelinated. This gives us the opportunity to study the role of 4.1B-a during synaptogenesis without confounding results due to its role in myelination.

Model for Muscular Dystrophy

Our knock-down studies of 4.1B-b show severe muscle fiber disorganization within the myotome of early developing embryos as well as aberrant motor neuron axons and reduced NMJ synapses (Figure 5); these data correlated with erratic motor behaviors seen at 26 hpf (Figure 6). It is interesting to note that 4.1B-b does not contain the SAB domain as discussed above. We suspect that in muscle, loss of this domain prevents 4.1B-b from interacting with actin filaments important for the contraction of the muscle fiber. Expression studies of 4.1R and 4.1B in muscle however, suggest that an isoform with a more complete SAB domain exists. The necessity of this longer isoform, however, has not been studied, and therefore we cannot draw any conclusions as to the evolutionary basis of this domain or the necessity of it in other vertebrate muscle tissue.

We also found 4.1B-b knockdown affects the frequency of spontaneous coils but not the velocity. It has been shown that muscles are tightly electrically coupled at early developmental stages and is thus a syncitium of muscle fibers (Buss 2000; Drapeau, 2002). We suspect then that when the muscle is activated, the muscles contract more like a single unit, and therefore differences in velocity measurements may be harder to detect. This is suggested by the data as the average tail velocity and standard error are very similar (Ctl MO: mean = 3.67 μm/ms ± 0.2 μm/ms, n = 11; 4.1B-b MO mean: 3.65 μm/ms ± 0.3 μm/ms, n = 10). As for the frequency, there are two possibilities as to why

the frequency may be reduced. First, disorganization of the muscle at 19 hpf may have disrupted the cues in the environment for the motor neuron axons to find their target. This would lead to less depolarization of the muscle cell and therefore reduced frequency. It is also possible that loss of communication between muscle cells within this syncitium would cause a decoupling of the electrical signal and a reduced frequency. Given our data at 26 hpf, we suspect it may be a combination of both. Taken together, we propose loss of 4.1B-b prevents correct muscle communication between muscle fibers as well as between motor neurons which causes the embryo to contract its muscles less often. Once the contraction has been initiated, the muscle contracts in an apparent all or none fashion with no quantifiable effects seen on velocity.

In addition, we observed that 4.1B-a cannot rescue all phenotypes associated with 4.1B-b knockdown. Considering our data that show 4.1B-b can rescue all phenotypes associated with 4.1B-a knockdown, we suggest that 4.1B-b has either gained specific interacting partners that allow it to form a network of proteins at the sarcolemma, or 4.1B-a lost the ability to interact with proteins at the sarcolemma. This provides evidence of tissue specific functions for these genes. From our data, we can conclude that 4.1B-b is necessary for muscle fiber attachment to the extracellular matrix at the sarcolemma. Phenotypes associated with axon pathfinding and NMJ formation will need to be investigated further.

Several myopathies, such as Duchenne and Becker muscular dystrophies, arise from disruptions in cell adhesion between muscle fibers (Goody, 2011). Specifically, proteins localized to the sarcolemma of a muscle fiber will interact with components of the extracellular matrix, which are imperative for forming organized muscle structures.

Loss of this complex weakens the interaction between the muscle fibers and the extracellular matrix, and causes the muscle fiber to eventually atrophy after repeated cycles of contraction. Two macromolecular complexes important for this process include the dystrophin-glycoprotein complex and integrin α7β1 heterodimers (Campbell, 1989; Hodges, 1997). Studies of 4.1R in skeletal muscle show distinct colocalization with Dystrophin, a protein involved in stabilizing protein complexes at the sarcolemma of muscle fibers (Delhommeau, 2005; Ervasti 2006). Complete loss of Dystrophin leads to Duchenne muscular dystrophy (DMD), whereas a reduction of Dystrophin leads to Becker muscular Dystrophy (BMD). DMD and BMD patients experience weakness and loss of muscle tissue over time with phenotypes more severe in DMD patients. Delhommeau et al. (2005) found that 4.1R was completely lost in muscle tissue from DMD patients, and was slightly reduced in BMD muscle tissue. This is consistent with Dystrophin expression levels seen in these tissues. Further, 4.1R was colocalized with the low levels of Dystrophin expressed within BMD muscle tissue. The authors suggest 4.1R may be a critical component for stabilizing dystrophin to the sarcoleamma, although no direct evidence has been shown. Interestingly, phenotypes associated with DMD/BMD have not been seen in 4.1R knockout mice or in patients who suffer from hereditary elliptocytosis due to mutations in 4.1R (Conboy, 1993; Shi, 1999).

Integrins have also been associated with muscular dystrophies and are important for connecting the muscle fiber to the extracellular matrix (Hodges, 1997; Vachon, 1997). 4.1R associates with β1-integrin in keratinocytes, where loss of 4.1R causes a reduction of the surface expression and the activity of β1-integrin (Chen, 2011). Studies of 4.1B have also shown an association with β1-integrin important for integrin-mediated cell

spreading in Cos7 cells (Jung, 2012). Jung et al. also found, however, that loss of 4.1B in astrocytes does not cause a reduction in integrin surface expression as is seen for keratinocytes (Chen, 2011). Differences in results could lie within the model systems used as many protein interactions are spatially and temporally regulated by the proteins that exist within a given cell. Differences can also lie within the specific proteins (4.1R vs 4.1B) and isoforms used within these studies as sequence differences allow for unique interactions. Finally, 4.1B has also been shown to directly interact with αvβ8 integrin through the CTD, and this is important for CNS function (McCarty, 2005). Thus, it may be possible for 4.1B to directly interact with integrins to support adhesion between muscle fibers and the extracellular matrix.

Studies of dystrophin and integrin have also shown that loss of dystrophin can lead to an up regulation of α7β1 integrin (Burkin, 2001; Hodge, 1997; Vachon, 1997), suggesting the two pathways are in tight association with each other. Given that various 4.1 proteins have been shown to associate with both dystrophin and integrin, it is likely that 4.1B-b aids in the process of stabilizing one or both of the complexes at the sarcolemma. This can occur either through direct interactions with 4.1B-b and dystrophin/integrin or through interactions with other proteins that exist within the macromolecular complexes that these two components constitute. We cannot rule out the possibility that 4.1B-b can interact with other proteins that do not exist within these complexes for support of the sarcolemma with the extracellular matrix, although no evidence has suggested this. It will be necessary to further study the interactions of dystrophin and integrin with 4.1 proteins to determine the exact role of 4.1 in stabilizing these protein complexes. Our studies may provide a model to study their direct

relationship with respect to muscle fiber organization, and possibly as a model for studying various muscular dystrophies.

Summary

Taken together, our data suggest that the functions of the duplicated 4.1B proteins in developing zebrafish are conserved with their mammalian homologue; they are important for stabilizing protein complexes at sites of adhesion. We identified the protein 4.1B-a as an important component of synapses. The loss of synapses correlated with altered kinetics of touch evoked responses, and thus suggests 4.1B-a is required for establishing functional neuronal circuits. These data, coupled with a variety of studies of synapse formation and zebrafish behaviors and development, allowed us to propose a model for various aspects of synapse formation, including electrical synapses, chemical synapses, synapse competition/elimination and long term potentiation. We also identified protein 4.1B-b as an important component of individual muscle fibers, presumably by stabilizing protein complexes at the sarcolemma necessary for adhesion to the extracellular matrix. The loss of muscle fiber organization correlated with various disruptions observed during locomotor behaviors, and thus may provide a model to study myopathies such as DMD. These data also suggest the two proteins have partitioned the function of 4.1B (subfunctionalization) since human 4.1B can rescue all phenotypes associated with 4.1B-a and 4.1B-b knockdown. This gives us the opportunity then to study the function of human 4.1B within the zebrafish.

Experimental Procedures

Identification of epb41l3 Genes

To obtain transcripts of the zebrafish *epb41l3* genes, predicted sequences were identified from the zebrafish genome assembly Zv9 from the Sanger Institute (http://uswest.ensembl.org/Danio_rerio/Info/Index) using mouse *epb41l3* mRNA sequence for comparison (NM_013813.1). This search revealed two *epb41l3* genes that we confirmed by syntenic analysis (http://teleost.cs.uoregon.edu/acos/synteny_db/) (Catchen, 2009) and named *epb41l3a* and *epb41l3b* in accordance with the guidelines published by the Zebrafish Model Organism Database (www.zfin.org). Deduced mRNA and protein sequences were aligned to 4.1B, 4.1N, 4.1G, and 4.1R from various organisms using ClustalW to predict nucleic acid and amino acid sequence homology of individual exons and domains respectively (Subramaniam, 1998). To generate the phylogenetic tree, sequences were trimmed to include unambiguously aligned regions and were analyzed by Phylogeny.fr (Dereeper, 2008). Image clones of both *epb41l3* genes were obtained (Open Biosystems; *epb41l3a:* NM_001003987.1; *epb41l3b*: NM_214812.1) and subsequently cloned into pXT7 for capped mRNA synthesis. mRNA was transcribed with the mMESSAGE mMACHINE T7 transcription kit (Life Technologies, Grand Island, NY)

In Situ Hybridization

Zebrafish embryos (AB/Tübingen and Mnx1:Gal4:UAS:GFP (Mnx1:GFP) strains) were raised at 28.5°C according to standard protocols (Westerfield, 2007) and treated with 0.003% 1-phenyl-2-thiourea to prevent pigmentation. Embryos were staged

according to Kimmel et al. (1995) at 19, 28, and 72 hours post fertilization (hpf). Sense and antisense probes were synthesized from cDNA of 24 hpf embryos (AB/Tübingen) with primers that contained T7 or T3 promoter sites. Probes were designed to unique regions of the *epb41l3* genes that were confirmed for specificity by BLAST analysis. The probes were subsequently tagged with digoxigenin and whole mount *in situ* hybridization was carried out as previously described with minor modifications (Pietri, 2008). Briefly, embryos were hybridized with digoxigenin labeled probes at 65°C overnight (O/N) in Pre-Hyb solution (50% formamide, 5X SSC, 100µg/mL yeast RNA, 50µg/mL Heparin, 0.125% tween-20, citric acid to pH 6). Digoxigenin antibodies conjugated to alkaline phosphatase were used and detected with NBT/BCIP (Roche, Mannheim, Germany). Images were acquired on a Leica M165 FC stereomicroscope using a Leica DFC425 C digital microscope camera. Fluorescent *in situ* hybridization was carried out as in Welten et al. (2006) with minor modifications. Briefly, embryos were hybridized with digoxigenin labeled probes at 65°C O/N in Pre-Hyb solution. Digoxigenin antibodies conjugated to horse radish peroxidase were added to embryos at 1:1000 and developed with 1:50 Tyr-Cy3. Following the *in situ*, embryos were incubated with either Rb-GFP (1:500; Life Technologies, Grand Island, NY) or Ck-GFP (1:500; Abcam, Cambridge, MA) and labeled with Rb-488 or Ck-488 (Life Technologies, Grand Island, NY) for visualization. Images were acquired on an Olympus FV1000 confocal microscope and processed in Adobe Photoshop.

Reverse Transcriptase PCR

RNA was isolated from AB/Tübingen embryos at the 16-cell, 90% epiboly, 3-somite, 16, 24, 48, 72 hpf, and 7days post fertilization (dpf) stages using Trizol Reagent (Invitrogen, Carlsbad, CA). cDNA was synthesized with the SuperScriptIII First-Strand Synthesis system (Invitrogen, Carlsbad, CA). Concentrations of the cDNAs were determined and adjusted using primers specific to the tubulin-alpha gene (forward primer 5' – CTGTTGACTACGGAAAGAAGT – 3' and reverse primer 5' – TATGTGGACGCTCTATGTCTA – 3'). Primers were designed to unique regions of *epb41l3a* (forward primer 5' – TGGATACGCAGGAGAACAACAG – 3' and reverse primer 5' – CGGCCGCTCCTCTTCT – 3') and *epb41l3b* (forward primer 5' – CCAGCTGCGGGATGA – 3' and reverse primer 5' – GGAGAGTTTCTTTGCGTTTTCC – 3'). PCR products for 16-cell, 90% epiboly, 24 hpf, and 7 dpf embryos were sent for sequencing to confirm the *epb41l3a* and *epb41l3b* genes were being expressed.

4.1B-a and 4.1B-b Morpholino Knockdown

An antisense morpholino oligonucleotide (MO) was designed to each gene (*epb41l3a*: AGAGGTGCAGATGTTACCTGATCCT; *epb41l3b*: ATATGTGGGAATCTCACCTTTCTGT; Gene Tools, Philomath, OR) and was injected into embryos at the one cell stage using a MPPI-2 pressure injector (ASI, Eugene, OR). MOs were injected at a concentration of 0.8mM. This concentration did not have any adverse effects on overall embryonic development and was determined to give the least amount of cell death based on an acridine orange stain assay (Williams, 2000).

Confirmation of knockdown was performed by RT-PCR from 28 hpf embryos using primers designed to exon 1 and exon 7 for *epb41l3a* (forward primer 5' – CAGAGGGTAAAGCAGAGC – 3' and reverse primer 5' – CTGATTCTCCACATCGCG – 3') and exon 1 and exon 2 for *epb41l3b* (forward primer 5' – CCAGAACCGGACGTCCATA – 3' and reverse primer 5' – CACAGTGCAGGTGTAGTCG – 3'). PCR products were sent for sequencing to confirm inclusion of intron 1. All comparisons were made to embryos injected with a control MO (Gene Tools, Philomath, OR). Rescue of morpholino-mediated knock-down was performed by co-injecting *in vitro* transcribed mRNA encoding zebrafish image clones of *epb41l3a* or *epb41l3b* or encoding human *epb41l3* at 8ng/µL; overexpression experiments were performed by injecting *epb41l3a* or *epb41l3b* zebrafish image clone RNA at 8 ng/µL.

Immunolabeling and Quantification

Immunofluorescence labeling was performed with the following primary antibodies and dilutions: mouse anti-panMAGUK (1:100; NeuroMab, Davis, CA), rabbit anti-Synapsin 1/2 (1:1000; Synaptic Systems, Goettingen, Germany), chicken anti-GFP (1:500; Abcam, Cambridge, MA), mouse anti-Synaptotagmin2b (znp-1; 1:750; Developmental Studies Hybridoma Bank, University of Iowa), mouse anti-SV2 (1:1000; Developmental Studies Hybridoma Bank, University of Iowa), mouse anti-Gephyrin (1:500; Synaptic Systems, Goettingen, Germany), Tetramethylrhodamine α-Bungarotoxin (1:500; Life Technologies, Grand Island, NY), and Alexa Fluor 488 Phalloidin (1:20; Life Technologies, Grand Island, NY). Secondary antibodies used were anti-Chicken

488, anti-mouse IgG 546, and anti-rabbit 633 (Molecular Probes, Eugene, OR). Embryos were staged at 28 hpf and fixed for either 1.5 hrs at 4°C (panMAGUK, Synapsin 1/2, GFP), for 3 hrs at 4°C (Gephyrin, Phalloidin, α-Bungarotoxin, GFP) or overnight at 4°C (SV2, Synaptotagmin, GFP) in 1X Fish Fix Buffer (Westerfield, 2007) and 4% Paraformaldehyde. Embryos were then washed in PBDTx (10% PBS, 0.01% BSA, 0.01% DMSO, 0.1% Triton-X 100; pH 7.3) and blocked in PBDTx plus 2% normal goat serum. Embryos were incubated overnight with respective primary antibodies at 4°C. The next day, embryos were washed in PBDTx and then incubated in respective secondary antibodies in the dark for 5 hrs at room temperature. Embryos were then washed in PBDTx and stored in 80% glycerol overnight at 4°C. Images were taken of the spinal cord from somites 12 – 16 on an Olympus Fluoview FV1000 confocal microscope with a 63x oil-immersion objective. Images acquired through the Olympus FV1000-ASW software were opened in ImageJ version 1.43 with the loci tools plugin. Images were processed into a flattened RGB composite as a maximum intensity projection and saved as tiff files. These images were then opened in ImageJ version 1.29 and analyzed using the puncta analyzer plugin graciously given to us by Dr. Cagla Eroglu (Ippolito, 2010). All data were analyzed in Excel using the data analysis tool pack to perform an analysis of variance test (F-test), a two-tailed unpaired student t-test, and one way-ANOVA to test the significance between data sets; $p < 0.05$ was considered to be significant. All results are expressed as the mean ± standard error.

Video Recording and Kinematic Analysis

Analysis of embryos was done as previously described (Pietri, 2009). Briefly, embryos were anesthetized in 0.003% MS-22 and mounted in 1.5% low melt agarose. The embryos were then submerged in embryo media and the agarose surrounding the tail was removed. The movements of embryos were recorded under a stereomicroscope (Leica LZMFIII) using a Phantom v4.2 camera at a rate of 200fps. We recorded 20 hpf embryos for 1 minute and counted the frequency of tail swings. Velocity measurements were taken using the Image Pro Plus software (Media Cybernaetics, Bethesda, MD) on the first five tail swings of each embryo. For touch evoked responses, the experiment was carried out as above on 28 hpf embryos. These embryos were subjected to a mechanical stimulus (insect pin attached to a micromanipulator) five times. Latency and velocity measurements were taken in Image Pro Plus. Statistical analysis including F-tests, student t-tests, and one-way ANOVA's were carried out in Excel. All graphs and images were prepared in Adobe illustrator.

Bridge

Synaptogenesis is a very complex process involving the recruitment and stabilization of thousands of proteins at pre- and postsynaptic sites. In the previous study, we identified the protein 4.1B-a as being a necessary component for the proper formation of synapses, possibly aiding in the formation and stailization of macromolecular complexes. We next turn our attention to the initial formation of synapses and how various proteins get recruited to the presynaptic terminal.

CHAPTER III

LATE RECRUITMENT OF SYNAPSIN TO NASCENT SYNAPSES IS REGULATED BY CDK5

This work was previously published in Cell Reports, Volume 3, pages 1199-1212 in April, 2013. The work described in this chapter was co-authored by myself, Courtney Easly-Neal, JoAnn Buchanan, and Philip Washbourne. I carried out the Cdk5 experiments and contributed to the writing and editing of the manuscript. JoAnn Buchanan carried out the electron microscopy experiments and Courtney Easly-Neal performed the live imaging experiments and wrote the manuscript. Philip Washbourne contributed to the design of this project and the preparation of the manuscript.

Introduction

Chemical synapses are highly complex sites of neuronal contact at which unidirectional communication occurs. Both pre- and postsynaptic sides of the contact contain up to 1000 distinct proteins (Valor and Grant, 2007), that must be correctly assembled for the synapse to function. Understanding the mechanisms by which these components are transported and then stabilized at synapses is critical to unraveling developmental disorders such as autism, mental retardation and schizophrenia (Zoghbi, 2003).

Synapsins are an important component of mature synapses, based on their localization to >99% of synapses in mouse cortex (Micheva et al., 2010). In mammals, these proteins are encoded by three genes, *Synapsin1*, *2* and *3* (Fornasiero et al., 2010).

The Synapsins regulate the releasable pool of SVs (Bonanomi et al., 2005), and are phosphorylated by at least six kinases including Cyclin dependent kinase 5 (Cdk5) and Calcium/calmodulin kinase II (CaMKII) (Fornasiero et al., 2010). Phosphorylation can regulate the association of these cytosolic proteins with synaptic vesicles (SVs) and actin (Fornasiero et al., 2010). Although the Synapsins were the first SV-associated proteins identified (Fornasiero et al., 2010), the transport of these proteins to synapses has remained understudied. Due to the strong association between SVs and Synapsins (Huttner et al., 1983), it has been assumed that they are transported together (Ahmari et al., 2000). Recent imaging studies show that this can be the case (Scott et al., 2011), but quantitative analysis of Synapsin transport and an understanding of the mechanisms governing transport and recruitment of Synapsins to synapses still remain elusive, especially *in vivo*.

There are four possible modes of transport by which the Synapsins could be conveyed to presynaptic terminals: (1) cytosolic diffusion (Scott et al., 2011), (2) association with SV protein transport vesicles (STVs) (Ahmari et al., 2000; Scott et al., 2011), (3) association with Piccolo-containing active zone precursor transport vesicles (PTVs) (Tao-Cheng, 2007; Zhai et al., 2001) or (4) with an as yet unknown transport complex. STVs transport an array of SV proteins including VAMP2/Synaptobrevin2 (VAMP2), Synaptotagmins, and SV2 (Ahmari et al., 2000; Takamori et al., 2006). STVs vary widely in size from clusters the size of a few SVs to larger tubulovesicular aggregates of SV material (Ahmari et al., 2000; Kraszewski et al., 1995). In contrast, PTVs are more uniform 80nm dense-core vesicles that carry active zone cytomatrix proteins, as well as proteins involved in calcium sensing and vesicle fusion, such as

Piccolo, Bassoon, N-cadherin, and SNAP-25 (Shapira et al., 2003; Zhai et al., 2001). Both STVs and PTVs are transported bi-directionally along axons, pausing for varying lengths of time (Ahmari et al., 2000; Bury and Sabo, 2011; Kraszewski et al., 1995; Sabo et al., 2006; Shapira et al., 2003; Zhai et al., 2001). Co-transport of Synapsins with either STVs or PTVs would constitute an efficient delivery mechanism for the Synapsins to synapses.

Previous studies examining the trafficking of presynaptic components to CNS synapses have almost exclusively been performed *in vitro*, due to the lack of an appropriate *in vivo* model for synapse assembly. Recent live imaging studies in zebrafish (*Danio rerio*) (Jontes et al., 2000; Jontes et al., 2004) have suggested that this organism possesses the characteristics necessary to facilitate examination of synaptogenesis in a living vertebrate. Rohon-Beard (RB) sensory neurons in the zebrafish spinal cord lend themselves to live-imaging studies as their central axons are linear, allowing fast imaging within a narrow range of focus (Figure 1A and 1B) (Jontes et al., 2004). These cells transduce the sense of touch (Douglass et al., 2008) to mediate touch-evoked coiling behavior by one day postfertilization (dpf) (Saint-Amant and Drapeau, 1998). RB cells form synapses with commissural primary ascending (CoPA) interneurons (Figure 1B) (Downes and Granato, 2006; Gleason et al., 2003) and these AMPA-type glutamate receptor-dependent synapses are sufficient to sustain sensory-motor behavior (Pietri et al., 2009).

In this study, we examined the mechanisms by which Synapsin traffics to sites of nascent synapses between RB and CoPA cells *in vivo*. Live imaging demonstrated that Synapsin1 is transported in discrete puncta. Synapsin transport packets moved

independently of STV and PTV markers, thus presenting a novel transport packet to consider during presynaptic assembly. Synaptic recruitment of all three transport packets was in a defined sequence: STVs arrived at nascent synapses first, followed by PTVs after a ~30 minute delay, and then Synapsin after an additional ~30 minutes had elapsed. We found that Cdk5 was instrumental in regulating recruitment of Synapsin to nascent synapses. Thus, our study examines the kinetics and molecular mechanisms of synaptic recruitment of Synapsin transport packets *in vivo* and demonstrates that presynaptic assembly proceeds in a sequential fashion.

Results

Synapsin Localizes at Synapses Between RB and CoPA Cells

We began our examination of synapses between sensory RB axons and CoPA cells in the spinal cord of zebrafish embryos at 25 hpf (Figure 1A), a developmental stage at which embryos can respond to touch (Saint-Amant and Drapeau, 1998). By this stage, RB central axons expressing GFP from a *neurogenin1*:GFP transgene (ngn1:GFP; Tg[-3.1ngn1:GFP]sb2) extend along the length of the dorsal longitudinal fascicle (dlf; Figure 1B, arrow in Figure 1C). These axons lie directly adjacent to CoPA interneuron cell bodies, as visualized by immunolabeling with con-1 antibody (Figure 1B, arrowhead in Figure 1C) (Bernhardt et al., 1990).

Immunolabeling with antibodies to Synapsins 1 and 2 and postsynaptic density membrane associated guanylate kinase proteins (MAGUKs) PSD-95, PSD-93 and SAP102 (pan MAGUK antibody) (Meyer et al., 2005) was used to examine the localization of Synapsins at synapses between RB axons and CoPA cells at this stage of

development. To identify and visualize CoPA cells, we expressed Tau-GFP fusion protein in a mosaic distribution by injecting a neuronal expression vector into fertilized eggs at the one cell stage. The preferential targeting of Tau-GFP to axons facilitated the identification of CoPA cells by virtue of their ascending, commissural axon (Bernhardt et al., 1990). We observed punctate labeling of both Synapsin 1/2 and pan MAGUK antibodies at the cell bodies of CoPA cells at 24-26 hpf (Figure 1D, left panel). For considerations of MAGUK labeling specificity see Extended Results. When we examined images in which Synapsin and MAGUK immunolabeling was overlayed (Figure 1D), we saw colocalization in distinct puncta at CoPA cell bodies, demonstrating that Synapsins localize at synapses on CoPAs in the developing zebrafish spinal cord.

As axons from several neuronal populations project in the dlf, including the contralateral axons of CoPA cells, it was conceivable that the synapses located on CoPA cell bodies might represent a mixed population of synapses from RBs, CoPAs, and other neurons. The narrowminded mutation (nrd, *prdm1a*$^{m805/m805}$) disrupts the *prdm1a* gene, resulting in a deficit in neural crest cell development, including loss of the RB cells (Hernandez-Lagunas et al., 2005), while sparing all other neurons examined in the spinal cord (data not shown). *prdm1a*$^{m805/m805}$ embryos showed no punctate immunoreactivity for MAGUKs or Synapsin on CoPA cell bodies (Figure 1D, WT n = 4, *prdm1a*$^{m805/m805}$ n = 3). We conclude that all synapses containing Synapsins that impinge on CoPAs are from RBs at this stage of development.

There are between 50 and 78 RB cells along each side of the entire spinal cord (Eisen and Pike, 1991), but on average only 23 CoPA interneurons (Eisen and Pike, 1991). For our further studies of synapse assembly, it was important to take into account

the overall connectivity between RBs and CoPAs. For example, if a given RB synapses with only a subset of CoPA cells, it would be challenging to distinguish the region of axon that synapses with a CoPA cell of interest. To address this, we examined embryos that had been injected with a RB-specific GFP expression vector and in which only a single RB was fluorescently-labeled. Immunolabeling with Synapsin 1/2 and pan MAGUK antibodies revealed that, at 25 hpf, 87.1% of CoPAs (n = 31 CoPAs from 13 embryos; arrowheads in Figure 1E) had formed synapses with single labeled RB axons as indicated by Synapsin immunoreactivity in the RB axon adjacent to the MAGUK puncta. Furthermore, on average, a single synapse (1.3 ± 0.1; n = 18 CoPAs from 8 embryos) was observed between a RB axon and each CoPA cell. By 28 hpf, we observed as many as 39 postsynaptic puncta at a single CoPA (average = 18.7 ± 2.3; see Figure 3), suggesting that eventually every RB may synapse onto every CoPA within a hemi-spinal cord. Importantly for our studies, these results suggest that every RB contacts the overwhelming majority of CoPAs in one side of the spinal cord and that a single synapse forms at each contact site.

Ultrastructure of Immature Synapses on CoPA Cell Bodies

We next examined the ultrastructure of RB-CoPA synapses to determine whether the classical hallmarks of synapses between RB and CoPAs could be resolved at this early developmental time point. We performed transmission electron microscopy on transverse sections of embryos at 25 and 28 hpf. We found that CoPA cells could be identified in cross section due to (1) their cell body shape, (2) their dorso-lateral location within the spinal cord, and (3) their proximity to the dlf (Figure 2A). At 25 and 28 hpf,

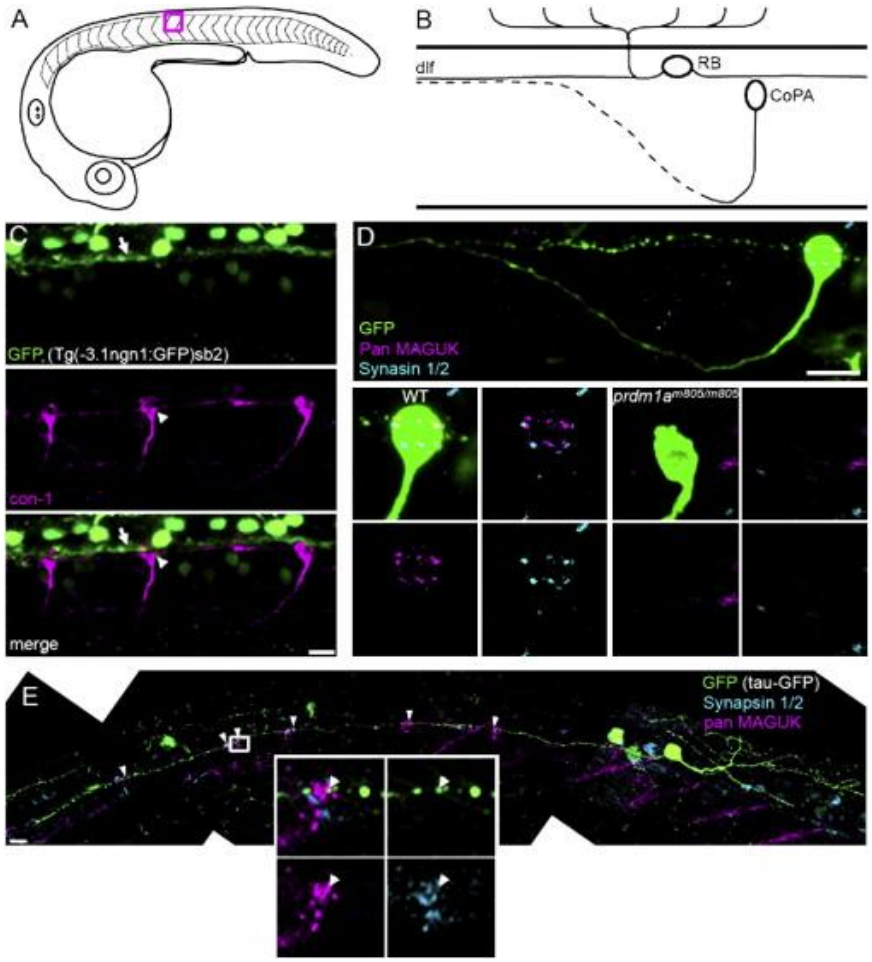

Figure 1. RBs Synapse onto CoPA Interneurons (A) Diagram of a lateral view of a 25 hpf zebrafish embryo. Studies were performed between segments 11 and 15. Red box outlines segment 12, the region represented in (B). (B) Diagram depicting the cell body location and axon trajectories of an RB cell and a CoPA cell, in a lateral view of the developing spinal cord. The dotted axon represents a contralateral projection. (C) CoPA cell bodies (white arrowhead), labeled with con-1 antibody (magenta), were in close proximity to RB axons expressing GFP (white arrow), in ngn1:GFP transgenic embryos. Scale bar represents 10 mm. (D) pan MAGUK (magenta) and synapsin 1/2 (cyan) immunolabeling on WT and prdmm805/m805 embryos with Tau-GFP-labeled CoPA cells. Top panel: shows axon projections and cell body of a CoPA cell in WT embryo. The cell body is shown at higher magnification in bottom left 4 panels, to highlight overlap of pre and postsynaptic puncta. Lower right four panels: no pre- or postsynaptic puncta were seen on CoPA cell bodies in prdmm805/m805 embryos, lacking RB cells. Scale bar represents 10 mm. (E) Composite image of a RB cell expressing GFP (green), including the entire central axon extending rostrally, with labeling for synapsin 1/2 (cyan) and pan MAGUK (magenta). Distinct clusters of colocalized pan MAGUK and synapsin 1/2 immunofluorescence were at CoPA cell bodies, see arrowheads. Inset shows distinct MAGUK and synapsin 1/2 puncta, arrowhead indicates a MAGUK puncta adjacent to a synapsin 1/2 puncta that is within a varicosity in the GFP-expressing RB axon. Scale bar represents 10 mm.

we were able to identify axons forming the dlf lying lateral to CoPA cell bodies. Many of these axons contacted the lateral face of a CoPA cell body (Figures 2B,C). At 25 hpf, some axons were contacted by small filopodial extensions from the CoPA cell body, and these contact sites showed accumulations of SVs (Figure 2D, in 3/3 CoPA-like cells examined). Filopodial extensions from the cell bodies of CoPA cells were not observed at 28 hpf (Figure 2B,C, 4/4 CoPA-like cells).

At 28 hpf, a few axon profiles directly in contact with the cell body (in 4/4 cells examined) demonstrated accumulations of SVs (Profiles 1 and 2 in Figure 2B). Analysis of contacts with accumulations of SVs at higher magnification revealed an even apposition and a thickening of the pre- and postsynaptic membranes (Figure 2E, F). Furthermore, we noted weakly labeled postsynaptic densities, suggesting that these contacts are immature synapses (Ahmari and Smith, 2002). Upon overlay of multiple cell body profiles together with their impinging presynaptic axon terminals, we noticed that synapses were clustered within the region of the lateral face of the CoPA cells contacted by the dlf (Figure 2C). From these experiments, we conclude that at 25–28 hpf synapse formation is ongoing between axons of the dlf, which we previously identified as being from RBs, and CoPA cells in the zebrafish spinal cord.

Delayed Recruitment of Synapsins

We next examined the time course over which Synapsins and SVs accumulated at RB-CoPA synapses. Embryos from transgenic ngn1:GFP zebrafish, which express GFP in RBs, were immunolabeled with antibodies to Synapsins and Synaptotagmin2b (Synaptotagmin), to label SVs and STVs, and to postsynaptic MAGUKs.

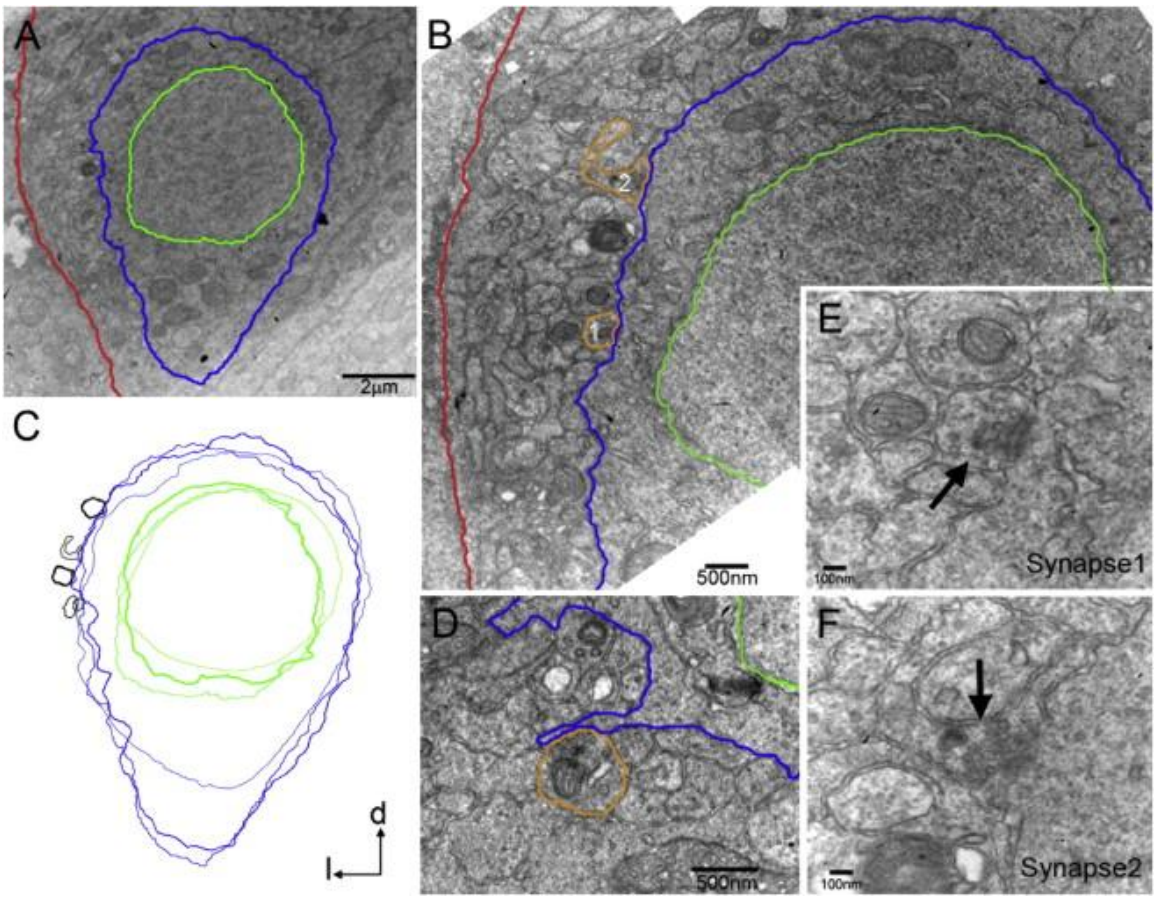

Figure 2. Axosomatic Synapses on CoPA-Like Cells (A) Electron micrograph of a transverse section of the zebrafish embryo at 28 hpf. CoPA-like cells were identified based on their cell body shape and dorso-lateral location in the spinal cord. The plasma membrane and nuclear envelope were traced in blue and green for clarity, respectively. The basal lamina of the spinal cord is in red. (B) Synapses (orange tracing) from axons in the dlf were identified on the CoPA-like cell body in (A) (see E and F for higher magnification). (C) Synapses were found on the lateral face of CoPA-like cells in a stereotypical location, as demonstrated by an overlay of three cell profiles with their synapses (black). (D) At 25 hpf, synapses were located on small filopodial extensions from the cell body. (E and F) Higher magnification images of synapse1 (E) and synapse2 (F) in (B), with accumulations of synaptic vesicles (arrows), smooth apposed synaptic membranes and weakly labeled postsynaptic densities.

Embryos were fixed and labeled at 19, 22, 25, and 28 hpf. These ages flank the onset of the touch response at 21 hpf (Pietri et al., 2009; Saint-Amant and Drapeau, 1998), when we would hypothesize that RB-CoPA synapses form and become functional.

At 19 hpf, punctate immunoreactivity for Synaptotagmin was seen along the dlf. Co-labeling with antibodies that label CoPA cells (con-1) revealed that punctate aggregates of Synaptotagmin were adjacent to CoPA cell bodies where they contacted the dlf (Figure 3A). We found an average of 2 (± 0.27, n = 8 CoPAs) puncta per CoPA with Synaptotagmin immunoreactivity, and this number increased at each developmental time point examined (Figure 3B,D). These results suggest that STVs are present in axons at these stages of development and that the number of STVs adjacent to CoPA cell bodies increases over time.

In contrast to the early appearance of STV immunoreactivity, immunolabeling for Synapsin was first seen at 22 hpf (Figure 3C,D), 3 hours later than SV protein Synaptotagmin. A portion of the Synapsin labeling was diffuse throughout the dlf, but large, intense puncta were occasionally seen in axons, especially at sites adjacent to CoPA cell bodies (Figure 3C). The numbers of Synapsin puncta steadily increased with development (Figure 3C,D). To determine what fraction of Synapsin puncta were indeed synaptic, we examined MAGUK immunoreactivity. This postsynaptic marker was detected earlier than Synapsin, at 19 hpf, and an increasing number of MAGUK puncta were seen in CoPA interneurons at each later time point (Fig. 3*C, D*). Importantly, adjacent Synapsin and MAGUK puncta were seen at CoPA cell bodies at around 22 hpf (arrowhead, Fig. 3*C-F*), a time at which these synapses are presumed functional (Pietri et al., 2009). Only a small proportion (4.79% ± 2.21%, n = 16 CoPAs) of the many

MAGUK puncta were adjacent to Synapsin at 22hpf, but this proportion steadily grew to over 25% over the next 6 hours of development (Figure 3E). In contrast, the proportion of Synapsin puncta that were adjacent to MAGUK proteins was much higher and remained relatively constant over time, averaging 69% - 91% (19 hpf, n = 16 CoPAs; 22 hpf, n = 15; 25 hpf, n = 21; 28 hpf, n = 18) over the ages examined (Figure 3F). Based on the different developmental time points at which markers for STVs and Synapsin appear, our immunolabeling studies suggest that there is a sequential arrival of synaptic proteins at the RB-CoPA synapse. These results also imply that Synapsins and STVs are trafficked independently to synapses. At this level of analysis, it is important to consider that the 3 hour delay in the arrival of Synapsin at RB-CoPA synapses as compared to Synaptotagmin may not be soley due to differential trafficking. This delay could also depend on the developmental expression pattern of *synapsin* genes in the zebrafish

---

Figure 3 (next page). Presynaptic Components Arrive Sequentially During Development (A) Left panel: lateral view of three segments of a 25 hpf embryo expressing ngn1:GFP (green) labeled with antibodies to synaptotagmin2b (magenta) and CoPA neurons (con-1, cyan). Notice synaptotagmin2b puncta were colocalized with CoPA cell bodies at the dlf. Right panels: zoom of box in left panel. Inset shows single plane of boxed region at the level of the dlf and the contacting region of the CoPA cell. Scale bar represents 10 mm. (B) Dorsal view of IF labeling for synaptotagmin2b (magenta) colocalized with CoPA cell bodies (cyan) in ngn1:GFP embryos from 1–28 hpf. Asterisk labels RB cell bodies. Scale bar represents 10 mm. (C) Dorsal view of IF labeling for MAGUKs (magenta) and synapsin 1/2 (cyan) from 19–28 hpf. Asterisk labels RB cell bodies. White arrowheads show sites of colocalization of synapsins and MAGUKs, white arrows indicate localization of synapsins only, and yellow arrowheads indicate localization of MAGUKs only. Outlines of CoPA cell bodies were generated by increasing the gain of the MAGUK IF. Scale bar represents 10 mm. (D) Histogram shows the number of synapsin 1/2, synaptotagmin2b, and MAGUK puncta per CoPA cell from 19–28 hpf. (E and F) Histograms show the percentage of MAGUK puncta colocalized with synapsin puncta, and the percentage of synapsin puncta colocalized with MAGUK puncta, respectively, from 19–28 hpf. Error bars show SEM.

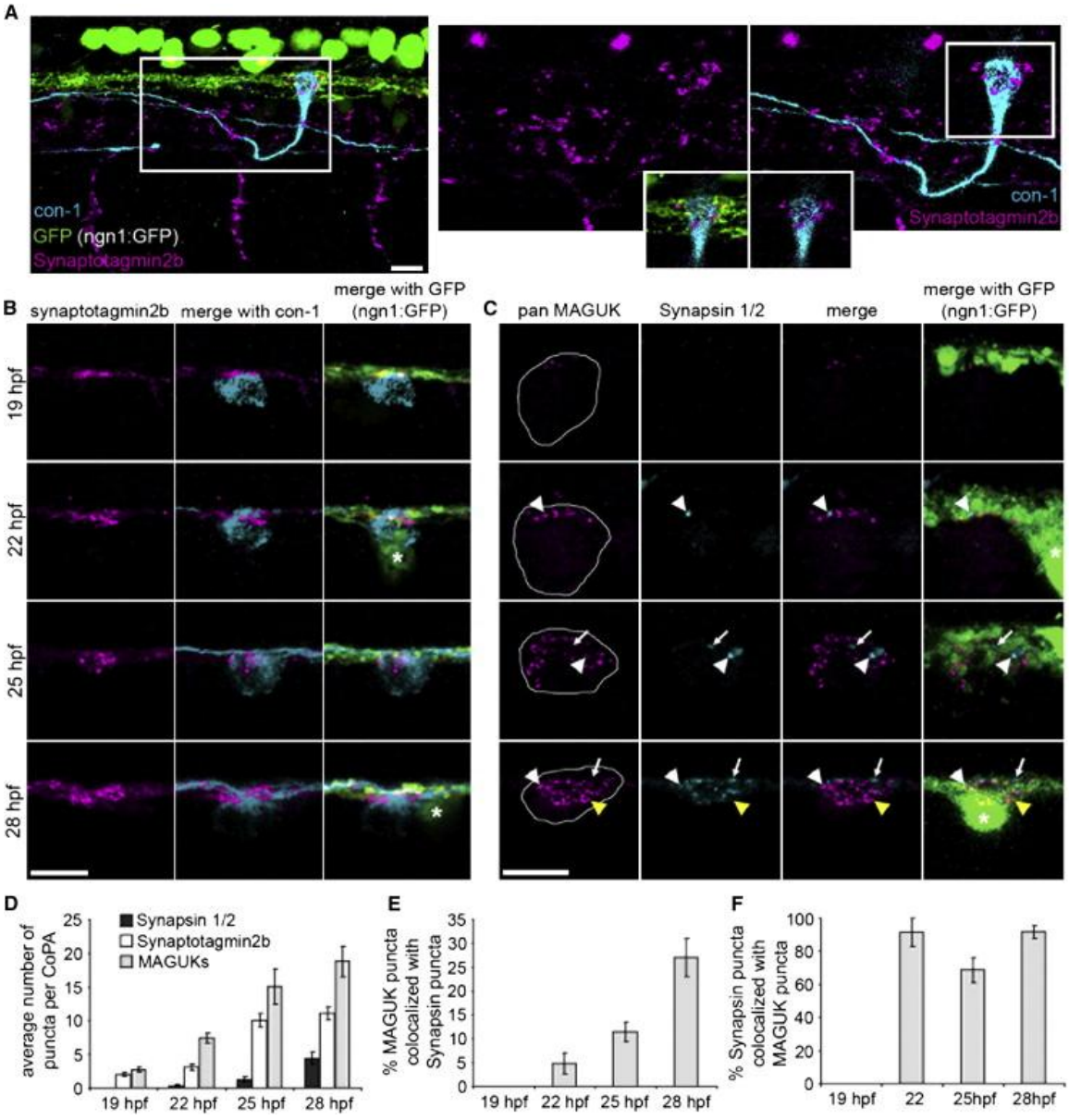
A
con-1
GFP (ngn1:GFP)
Synaptotagmin2b
con-1
Synaptotagmin2b
B
synaptotagmin2b
merge with con-1
merge with GFP (ngn1:GFP)
19 hpf
22 hpf
25 hpf
28 hpf
C
pan MAGUK
Synapsin 1/2
merge
merge with GFP (ngn1:GFP)
D
Synapsin 1/2
Synaptotagmin2b
MAGUKs
average number of puncta per CoPA
19 hpf
22 hpf
25 hpf
28 hpf
E
% MAGUK puncta colocalized with Synapsin puncta
19 hpf
22 hpf
25 hpf
28 hpf
F
% Synapsin puncta colocalized with MAGUK puncta
19 hpf
22
25hpf
28hpf

embryo. We identified and isolated the coding regions of the three zebrafish *synapsin* genes *synapsins1*, *2a* and *2b*. No ortholog of mammalian Synapsin3 was identified in the zebrafish genome, although Synapsin2 was present as duplicate co-orthologs. *In situ* hybridization at 17, 19, 22 and 25 hpf, revealed that transcripts for these genes did not appear until 19 hpf (Figure S1; appendix). Based on our immunolabeling studies (Figure 3C), we conclude that there appears to be a ~3 hour delay in the generation of Synapsin protein. While the developmental expression pattern explains the late arrival of Synapsins at RB-CoPA synapses, it nonetheless underscores the possibility of independent, sequential arrival of STVs and Synapsins at the presynaptic terminal.

Synapsin1 Is Transported in Axons Independently of STVs and PTVs

Although previous studies have suggested that Synapsin is trafficked to synapses with STVs (Ahmari et al., 2000; Scott et al., 2011) or PTVs (Tao-Cheng, 2007), our immunolabeling data suggest that Synapsin may arrive at synapses independently of STVs, and with a delay. To examine how Synapsin is transported in RB axons relative to both STVs and PTVs, we imaged fluorescently-tagged fusion proteins in RBs in the spinal cords of living zebrafish embryos. We co-expressed Synapsin with either fluorescently-tagged VAMP2, a membrane protein of SVs, or fluorescently-tagged Ncadherin, an integral component of PTVs (Bury and Sabo, 2011; Zhai et al., 2001). We used both GFP and mKate2, a red fluorescent protein, as fluorescent tags to enable imaging of two different constructs simultaneously. For validation of our fluorescently-tagged constructs see Supplementary Experimental Procedures and Figure S2.

We examined the transport of Synapsin-GFP in axons of RB cells between 24 and 26 hpf. We noticed diffuse Synapsin-GFP fluorescence throughout the axon and strongly fluorescent puncta of Synapsin-GFP, some of which were stabile, but many of which were motile. On average the diffuse pool of Synapsin1-GFP represented only 17.81% ± 3.75% of the total pool of Synapsin1-GFP fluorescence. This suggests that the majority of Synapsin-GFP is transported as part of a transport packet. We then expressed all chromatically-distinct combinations of VAMP2-mKate2, Ncadherin-GFP, Synapsin1-GFP and Synapsin1-mKate2 to determine whether Synapsin may be transported with STVs or PTVs. When RBs expressing Synapsin1-GFP and VAMP2-mKate2 were imaged, we found that the two were transported independently (Figure 4A,D), confirming that Synapsin1 is not transported by STVs. Puncta expressing only one of the fluorescently-tagged markers could be seen moving along the axon (arrowheads Figure 4A). Paused puncta were often observed where both VAMP2 and Synapsin1 were colocalized, however, in many instances (n = 14), one of the two fusion proteins moved away while the other remained paused (white and yellow arrows in Figure 4A). This same pattern was seen with the other pairs of presynaptic markers. Ncad-GFP and Synapsin1-mKate2 never trafficked together (Figure 4B), and Ncad-GFP and VAMP2-mKate2 rarely did (Figure 4C), suggesting that Synapsin, STVs and PTVs are all transported independently. To quantify this effect, we calculated the numbers of puncta that were motile during a 30 minute imaging session. For each of the singly-labeled presynaptic markers, on average 96.2% of the puncta observed during an imaging session were motile, while very few two-color puncta moved (Figure 4D; n = 58 puncta).

We further examined the kinetics of puncta movement. The instantaneous velocities of Ncad-GFP, VAMP2-mKate2, and Synapsin1-GFP displayed a wide range as seen in the population histogram (from 0.01– 1.44 μm/sec, Ncadherin: n = 74 puncta, VAMP2: n = 71 puncta, Synapsin n = 55 puncta; Figure 4E). However, the maximal velocities of Synapsin1-GFP puncta were significantly below those of Ncad-GFP or VAMP2-mKate2 puncta. Synapsin1-GFP puncta did not move faster than 0.57 μm/sec, whereas more than 8% of VAMP2 and Ncad puncta moved with higher velocities (VAMP2 = 8.4%, Ncad = 8.1%; Figure 4E), reaching 1.14 and 1.44 μm/sec, respectively. This result suggests that Synapsin may be transported by motor proteins distinct from those used by STVs and PTVs. Together with the analysis of co-transport, our data demonstrate that PTVs, STVs and Synapsin are transported independently in axons.

Synapsin Is Recruited 1 Hour After STVs

We next investigated the order and timing of Synapsin recruitment with respect to STVs and PTVs at individual synapses. We monitored the transport and stabilization of STVs and PTVs over time and then examined colocalization of endogenous Synapsins with paused and motile transport packets. Our results suggest that Synapsin is transported independently of STVs and PTVs (Figures 4) and that Synapsin might be recruited with a delay when compared to STVs (Figure 3). Thus, we predicted that live imaging of STVs or PTVs and subsequent immunolabeling of Synapsins should reveal: (1) that motile transport packets do not colocalize with endogenous Synapsins, and (2) that STVs or PTVs, which have stabilized at synapses during imaging, colocalize with Synapsins by the end of the imaging period. Furthermore, the average time between stabilization of

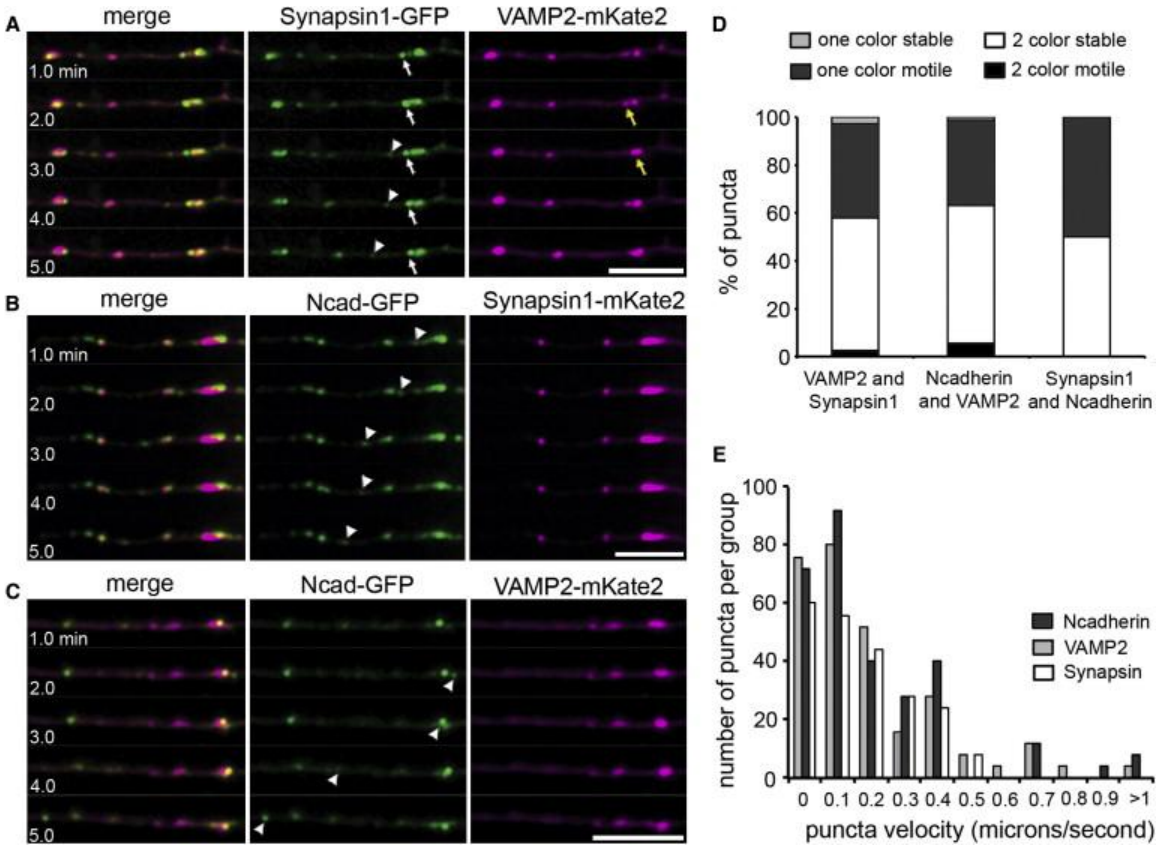

Figure 4. Synapsin1, STVs, and PTVs Are Transported Independently of Each Other (A–C) Selected sequence of five frames, 1 min apart, from 30 min time-lapse movies showing differential transport of synapsin1-GFP and VAMP2-mKate2 (A), synapsin1-mKate2 and N-cadherin-GFP (B), and N-cadherin-GFP and VAMP2-mKate2 (C) in RB axons. Movies acquired between 24–26 hpf. Arrows and arrowheads highlight motile puncta that were positive for only one of the two fluorescent fusion proteins. A VAMP2-mKate punctum was initially paused (yellow arrow in A) and colocalized with a synapsin1-GFP punctum (white arrow), but then moved away (t = 3.0). Scale bars represent 10 mm. (D) Histogram showing the number of two color puncta versus single color puncta that are motile over a 30 min imaging period. Two color puncta are those labeled for both transport packet markers imaged in a given pair, single color puncta are those expressing only one of the two markers. Error bars represent SEM. *$p < 0.005$. (E) Distribution of the number of each type of puncta (N-cadherin, VAMP2, synapsin) at each velocity. The maximum velocity measured for a synapsin1 puncta was 2.49- and 1.98-fold slower than the maximum velocity for an N-cadherin or a VAMP2 puncta, respectively.

transport packets and the fixation and labeling of Synapsin at those puncta would inform us of the time between recruitment of STVs/PTVs and Synapsins.

We performed this analysis by recording STV transport and pausing over a 2 hour time period starting at ~24 hpf (Figure 5A). The movies were used to generate a retrospective stability map; a 'heat' map that indicates the length of time that each punctum was paused prior to the end of the imaging period and fixation (Figure 5B). This analysis revealed a wide variety of stabilities, ranging from puncta that were not paused at the end of imaging (0 hours, dark blue), puncta that paused during imaging and remained there until the end of imaging (e.g. 0.5 hours, arrow, light blue in stability map), to puncta that were paused for the entire imaging period (>2 hours, arrowhead, magenta).

We used labeling of MAGUKs to determine whether paused fusion-protein positive puncta had stabilized at *bona fide* synaptic sites. When colocalization between MAGUK protein IF and VAMP2-mKate2 puncta was analyzed, we did not find any instances in which VAMP2-mKate2 puncta, that had been paused for less than 1.5 hours or that were not paused at the end of the imaging period, colocalized with MAGUK puncta (arrow in Figure 5A-C; n = 7 RB axon segments). Further, we found that only VAMP2-mKate2 puncta that had been paused for at least 1.5 hours prior to fixation were stabilized adjacent to MAGUK puncta (average stability with MAGUK localization = 94.8 min ± 14.7 min, n = 7 RB axon segments and 74 puncta; Figure 5C). Interestingly, the total fluorescence intensity was highest for VAMP2-mKate2 puncta that had been paused for the longest amount of time (Figure 5D), ~50% of which are synaptic sites, as indicated by the presence of postsynaptic MAGUKs. This 2.7 - 7.3 fold increase in

intensity of long-term paused puncta over newly paused puncta suggests that additional VAMP2-mKate2 positive STVs are added to synaptic sites more than 2 hours after initial pausing. These data suggest that STVs stabilize at nascent synaptic sites and that stabilization precedes accumulation of postsynaptic MAGUK scaffolding proteins by about 1.5 hours.

We next examined whether endogenous Synapsin was transported with VAMP2-positive STVs. While many VAMP2-mKate2 transport packets were moving at the end of the imaging session or had paused up to 30 min before the end of the imaging period (62% of all puncta analyzed), none of these were colocalized with Synapsin (arrow Figure 5B,E). This confirms that endogenous Synapsin does not transport with VAMP2-mKate2 positive STVs.

However, Synapsin was colocalized with VAMP2-mKate2 clusters that had been paused for at least one hour (arrowhead Figure 5A,B and E; n = 13 RB axon segments, and 118 puncta). In addition, ~100% of stable VAMP2-mKate2 puncta that had stabilized at MAGUK puncta were also colocalized with Synapsin (arrowhead Figure 5A,B; n = 7 RB axon segments). As CoPA cells have not yet established dendrites and their cell bodies do not monopolize the dlf, we focused our analysis on potential synaptic sites by examining axonal regions adjacent to CoPA cell bodies (within 2 μm). This analysis revealed that only 30% of motile puncta (t = 0) were in proximity to a CoPA at the time of fixation (Figure 5F). In contrast, the probability that a VAMP2-positive punctum was immobilized at a CoPA was above 50% if it was paused for at least 30 min (Figure 5F). Puncta that had paused for over 2 hours had over 70% probability of being colocalized with a CoPA cell (Figure 5F). We analyzed the percentage of puncta that had paused at

CoPAs and that were colocalized with Synapsins. 100% of long-term paused puncta at CoPA cells (>2hrs) and ~43% of puncta that had been paused at CoPA cells for around 2 hours were colocalized with Synapsin (Figure 5E, grey bars). These data suggest that Synapsin is recruited to synaptic sites that have already assembled STVs. Furthermore, we conclude that Synapsin and postsynaptic MAGUK proteins are recruited to new synapses with a similar time course.

PTVs Are Recruited before Synapsin

We next examined the time course of Synapsin recruitment to the RB-CoPA synapse as compared with PTVs. Live imaging of Ncad-GFP and post-imaging IF labeling for Synapsin and MAGUKs were performed as previously described. Again, we

---

Figure 5 (next page). Delayed Synapsin Recruitment to Paused VAMP2-mKate2 Puncta (A) Selected frames from a 2 hr time-lapse movie (from 24–26 hpf) of VAMP2-mKate2 expressed by a RB cell. Although some puncta remained stable for the entire imaging period (arrowheads) others stabilized during imaging (arrow). Scale bar represents 10 mm.(B) Postimaging IF labeling demonstrates the presence of MAGUKs (green) at a VAMP2-mKate2 punctum that was paused for at least 2 hr (arrowhead), but not at a punctum paused for 29 min (arrow). The stability map uses a color code to report the time each punctum was paused before the end of imaging. Bins were as follows: nonpaused puncta (0.0, dark blue), paused for 0–0.5 hr (0.5), 0.5–1 hr (1), etc. to puncta paused for the entire imaging period (>2.0, magenta). Scale bar represents 10 mm. (C) Stability histogram shows quantification of the percentage of VAMP2-mKate2 puncta colocalized with MAGUKs over the total of all axon segments analyzed. Bins are as described for the stability map above. n = 7 RB axon segments analyzed. (D) Intensity histogram shows the total fluorescence intensity for VAMP2 puncta. A significant increase in total fluorescence intensity was seen at puncta paused for >2 hr. Error bars show SEM. (E) A stability histogram quantifying the percentage of synapsin 1/2 that colocalized with VAMP2-mKate2 puncta reveals that, on average, recruitment of VAMP2-mKate2 preceded that of synapsin by 83.7 min (±12.5 min). n = 13 RB axon segments analyzed. (F) A stability histogram quantifying the percentage of VAMP2-mKate2 puncta that are localized within 2 mm of a CoPA cell.

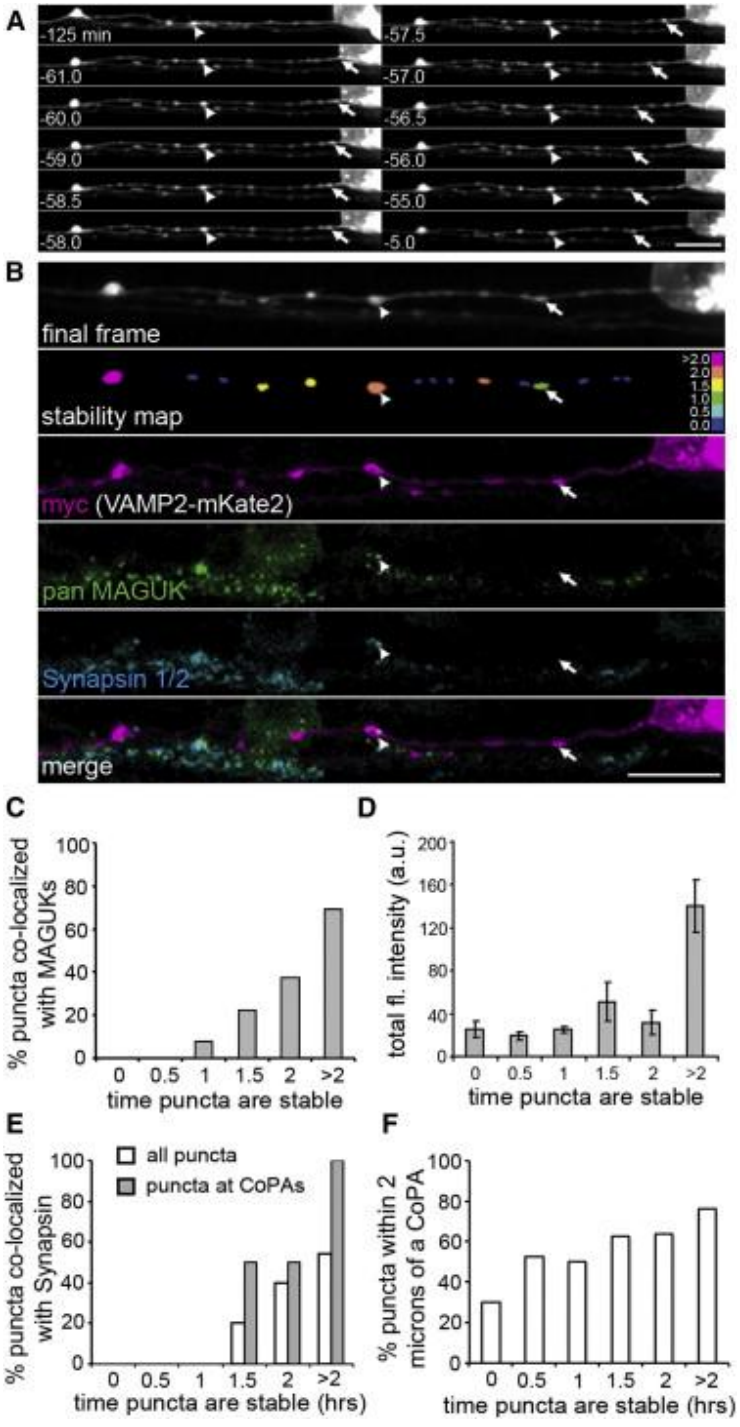
A
-125 min
-61.0
-60.0
-59.0
-58.5
-58.0
-57.5
-57.0
-56.5
-56.0
-55.0
-5.0
B
final frame
stability map
>2.0
2.0
1.5
1.0
0.5
0.0
myc (VAMP2-mKate2)
pan MAGUK
Synapsin 1/2
merge
C
% puncta co-localized with MAGUKs
time puncta are stable
D
total fl. intensity (a.u.)
time puncta are stable
E
all puncta
puncta at CoPAs
% puncta co-localized with Synapsin
time puncta are stable (hrs)
F
% puncta within 2 microns of a CoPA
time puncta are stable (hrs)

analyzed puncta that were in close proximity to CoPA cells. Puncta that had been actively trafficking at the end of the imaging period almost never colocalized with Synapsin and MAGUKs (Figure 6A-C), suggesting that endogenous Synapsin is not transported with PTVs. We found that Ncad-GFP puncta colocalized with Synapsin, on average, 37.6 ± 8.0 min after stabilizing at CoPAs (see arrows Figure 6D; n = 13 RB axon segments and 92 puncta). In comparison, the average time of colocalization after stabilization for VAMP2 was 73.8 ± 12.5 min (Figure 6D; $p<0.05$, n = 13 RB axon segments and 118 puncta). 100% of Ncad-GFP puncta that colocalized with Synapsin were also found to be adjacent to MAGUK puncta. These data suggest that PTVs arrive at synapses around 30 minutes prior to Synapsin, and with a distinct time course to VAMP2 transport packets.

Neuronal Activity Does Not Regulate Synapsin Recruitment

Synapsin localization at mature synapses is tightly regulated by neuronal activity (Lazarevic et al., 2011). To examine the effect of activity on Synapsin recruitment to

Figure 6 (next page). N-Cadherin Recruitment Precedes Synapsin (A) Selected frames from a 2 hr time-lapse movie (from 24–26 hpf) of Ncad-GFP expression in a RB cell. Some puncta were paused for the entire imaging period (arrowhead), whereas others paused during imaging (arrow). Scale bar represents 10 mm. (B) Postimaging IF labeling demonstrates the presence of synapsin 1/2 (cyan) and MAGUKs (magenta) at an N-cadherin-GFP (green) punctum that was paused for the entire imaging period (arrowhead) and for 34.5 min preceding the end of imaging (arrow), but not at a punctum that was paused for only 29.5 min preceding the final frame (yellow arrow). A stability map (with bins as described in Figure 5) reports the time each puncta was paused preceding the end of imaging. Scale bar represents 10 mm. (C) A stability histogram quantifying the percentage of synapsin 1/2 puncta that colocalized with N-cadherin-GFP (white bars) reveals that recruitment of N-cadherin precedes synapsin by 37.6 min (±8.0 min). Gray bars show data for VAMP2-mKate2 from histogram in Figure 5C to emphasize the difference in the time delay with which synapsin colocalization is first seen. Bins were as described for Figure 5. (D) Histogram quantifying the average amount of time (in min.) NCad and VAMP2 puncta were stable prior to the end of imaging and colocalized with synapsin. n = 13 RB axon segments analyzed. Error bars show SEM. *$p < 0.05$.

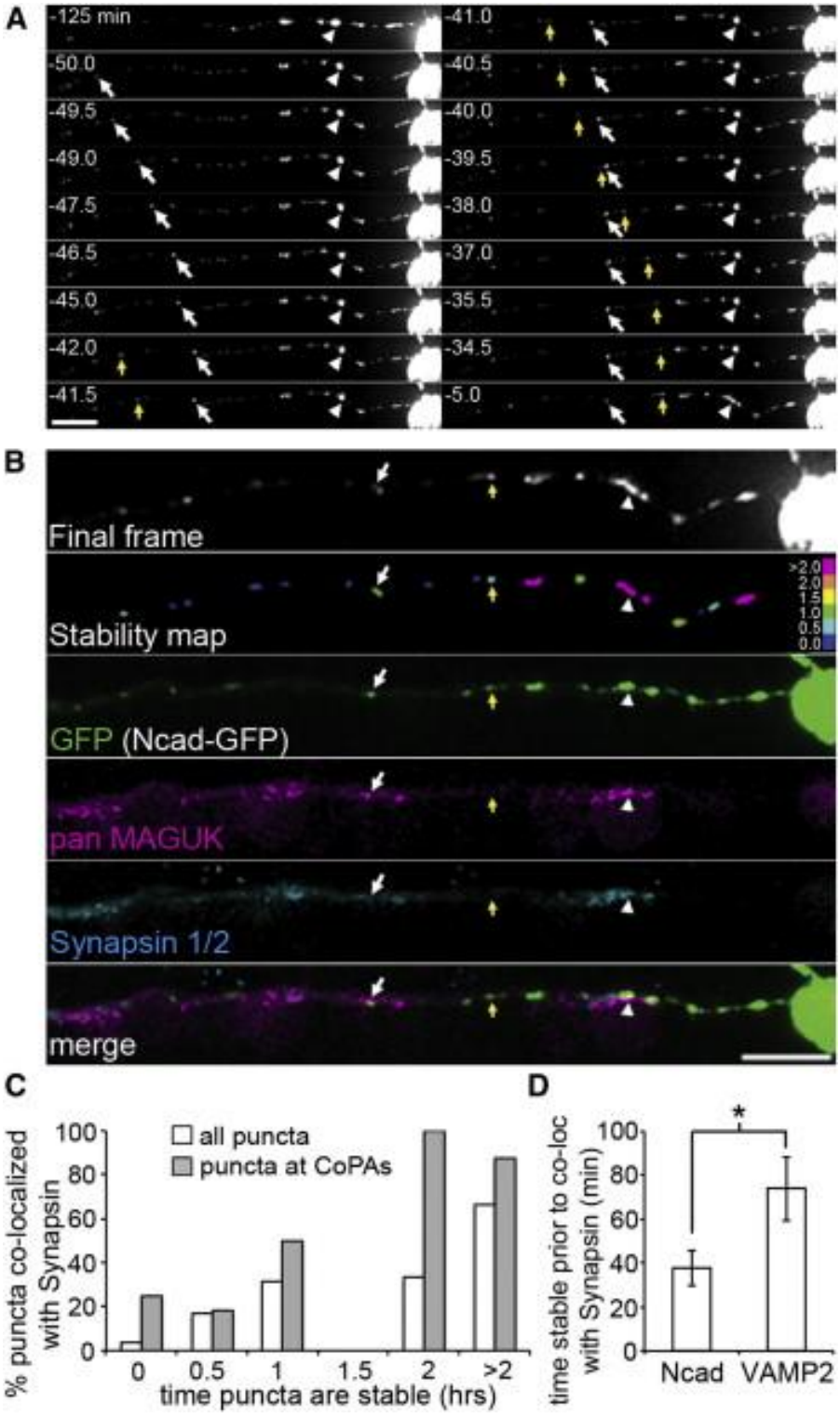
A
-125 min
-50.0
-49.5
-49.0
-47.5
-46.5
-45.0
-42.0
-41.5
-41.0
-40.5
-40.0
-39.5
-38.0
-37.0
-35.5
-34.5
-5.0
B
Final frame
Stability map
>2.0
2.0
1.5
1.0
0.5
0.0
GFP (Ncad-GFP)
pan MAGUK
Synapsin 1/2
merge
C
% puncta co-localized with Synapsin
all puncta
puncta at CoPAs
time puncta are stable (hrs)
D
time stable prior to co-loc with Synapsin (min)
Ncad
VAMP2
*

nascent synapses, we immunolabeled Synapsin1/2 and MAGUKs in zebrafish carrying the *macho* mutation (*mao*$^{tt261/tt261}$). This mutation results in a lack of action potentials in RB cells and other sensory neurons due to a reduction in voltage-gated sodium currents (Pineda et al., 2005). Homozygous mutants, as identified by a lack of touch response (Ribera and Nusslein-Volhard, 1998), demonstrated similar numbers of Synapsin puncta at CoPA cells (3.9 ± 0.8 versus 3.2 ± 0.8, $p>0.5$, n = 5 embryos each) and equivalent colocalization of MAGUK puncta with Synapsin (21.3 ± 4.4% versus 25.1 ± 5.6, $p>0.5$, n = 5 embryos), as compared to sibling embryos with touch sensitivity (data not shown). This analysis suggests that the transport and stabilization of Synapsins at synapses is not dependent on the activity level of RB cells.

Cdk5 Regulates Synapsin Recruitment

A key function of Synapsin is to maintain the SV reserve pool, a role that is shared with Cdk5 (Kim and Ryan, 2011). Cdk5 is expressed in zebrafish embryos from the beginning of development, and Cdk5 expression has been shown in the spinal cord at 24hpf (Kanungo et al., 2007). Furthermore, Cdk5 is highly expressed in RB cells (Kanungo et al., 2009), so we hypothesized that Synapsin1 recruitment might be regulated by Cdk5. We tested this hypothesis by inhibiting Cdk5 activity with roscovitine and examined Synapsin1 transport or stabilization at synapses. Since Synapsins are tightly associated with the actin cytoskeleton at synapses (Fornasiero et al., 2010), we considered other kinases that regulate actin. Thus, we tested an inhibitor of Focal Adhesion Kinase (FAK14), a kinase that stabilizes the presynaptic cytoskeleton (Fabry et al., 2011). We also tested an inhibitor of p38 MAPK (SB203580), a kinase involved in

synapse development through cadherins (Ando et al., 2011), which also stabilize the presynaptic actin cytoskeleton (Bozdagi et al., 2004).

We imaged embryos expressing Synapsin1-GFP in RB axons that were treated with the inhibitors for 1-3 hours and found that roscovitine treatment caused a significant decrease in the number of paused puncta and a concomitant increase in the number of motile puncta (Figure 7A, B; control n = 5 axons and 42 puncta, roscovitine n = 5 axons and 48 puncta). None of the other kinase inhibitors affected transport or pausing of Synapsin1-GFP (Figure 7B; SB203580 n = 6 axons and 59 puncta, FAK14 n = 5 axons and 38 puncta). There was no significant difference in the total number of puncta in any condition. Roscovitine treatment did not perturb puncta motility or pausing of VAMP2-mKate2 and Ncadherin-GFP (Figure 7C, D), suggesting that Cdk5-regulated stabilization is specific to Synapsin transport packets.

To characterize the effect of roscovitine on endogenous Synapsin and STVs, we examined immunoreactivity for Synapsin1/2, Synaptotagmin2b, and MAGUKs in WT embryos treated with roscovitine from 23-26 hpf. The colocalization of MAGUK puncta with Synapsin puncta was significantly decreased in the roscovitine treated embryos (Figure 7E, F; control n = 9 embryos, roscovitine n = 10 embryos). The average number of puncta per CoPA in the roscovitine treatment condition was not significantly affected for any of the markers (Figure 7G; control: Synapsin1/2 n = 29, Synaptotagmin2b n = 6, MAGUKs n = 29, roscovitine: Synapsin 1/2 n = 42, Synaptotagmin2b n = 10, MAGUKs n = 42), although there was a small, but insignificant, decrease in the total number of Synapsin puncta in the roscovitine treatment condition ($p = 0.096$; Figure 7G). These

results implicate Cdk5 kinase activity in the stabilization of Synapsin transport packets at nascent synapses.

Roscovitine can also inhibit Cdk1 and 2 (Knockaert et al., 2002), so to further characterize the role of Cdk5 in the recruitment of Synapsin to synapses we used morpholine-modified antisense oligonucleotides (MOs) to specifically knock-down Cdk5 levels (Tanaka et al., 2012). We monitored the transport of Synapsin1 transport packets in RB axons in the presence of MO. Cdk5 knock-down caused a reduction in the ratio of immotile to total puncta (Figure 7H; control = 0.5 ± 0.07, MO = 0.3 ± 0.01, $p<0.05$, n = 7 axons for all conditions), similarly to roscovitine treatment (Figure 7B). This effect was rescued by co-injecting mRNA encoding human Cdk5 (MO+RNA = 0.5 ±0.04, $p<0.05$). Furthermore, knock-down reduced the colocalization of endogenous Synapsins and postsynaptic MAGUKs, as revealed by immunolabeling of Cdk5 MO-injected embryos (Figure 7I; $p<0.05$; control n = 12, MO n = 11, MO + RNA n = 14 CoPAs). Cdk5 knock-down also resulted in a significant reduction in the number of Synapsin puncta on CoPA cells (Figure 7J; $p<0.001$), but did not result in a significant reduction in the other presynaptic marker, Synaptotagmin (Figure 7J; $p>0.05$). Taken together these data suggest that Cdk5 specifically regulates the stabilization of Synapsin transport packets at synapses.

Cdk5 could play a permissive role in allowing Synapsin transport packets to stop at synapses. Alternatively, Cdk5 might take on an instructional role in the recruitment of Synapsin to nascent presynaptic terminals. In this case, local activation of Cdk5 would be necessary for stabilization of Synapsins. To distinguish between the two possibilities, we ectopically and constitutively activated Cdk5 by expressing RNA encoding human Cdk5

and human p25C in developing zebrafish embryos and analyzed localization of Synapsins at synapses. p25C is a cleavage fragment of p35, an activator of Cdk5. Association of p25C with Cdk5 results in prolonged, ectopic activation of Cdk5 (Cheung and Ip, 2007). Expression of Cdk5 or p25C alone had no significant effect on the localization of Synapsins at synaptic sites (Fig. 7I, $p > 0.05$). In contrast, coexpression of Cdk5 and p25C resulted in a significant reduction in the colocalization of Synapsin with postsynaptic MAGUKs (Fig. 7I, $p < 0.005$). The localization of MAGUK puncta at CoPA cells was not affected by these manipulations (Fig. 7J, $p > 0.05$). While Cdk5 knock-down did not affect the localization of Synaptotagmin puncta at CoPA cells, all manipulations resulting in Cdk5 hyperactivity (i.e. Cdk5 RNA or p25C RNA injection) resulted in a ~25% decrease in Synaptotagmin puncta number (Fig. 7J). This suggests that Cdk5 activity may be sufficient, but not necessary, to restrict STV recruitment. This mechanism is distinct from the role of Cdk5 on Synapsin localization at synapses in that it persists when Cdk5 activity is ectopic. Our data suggest that the activation of Cdk5 is tightly controlled, and that the localization of Cdk5 activity is critical for Synapsin localization to synapses.

Discussion

In the current study, we have made three important advances in understanding the recruitment of presynaptic components to nascent synapses. (1) We have shown that Synapsin1, an important regulator of SV release and the SV reserve pool, is transported as part of a distinct complex to nascent synapses, independently of STVs and PTVs. (2) Our studies have revealed a defined sequence in the recruitment of presynaptic transport packets to a nascent synapse. (3) We identify Cdk5 as a specific regulator of Synapsin

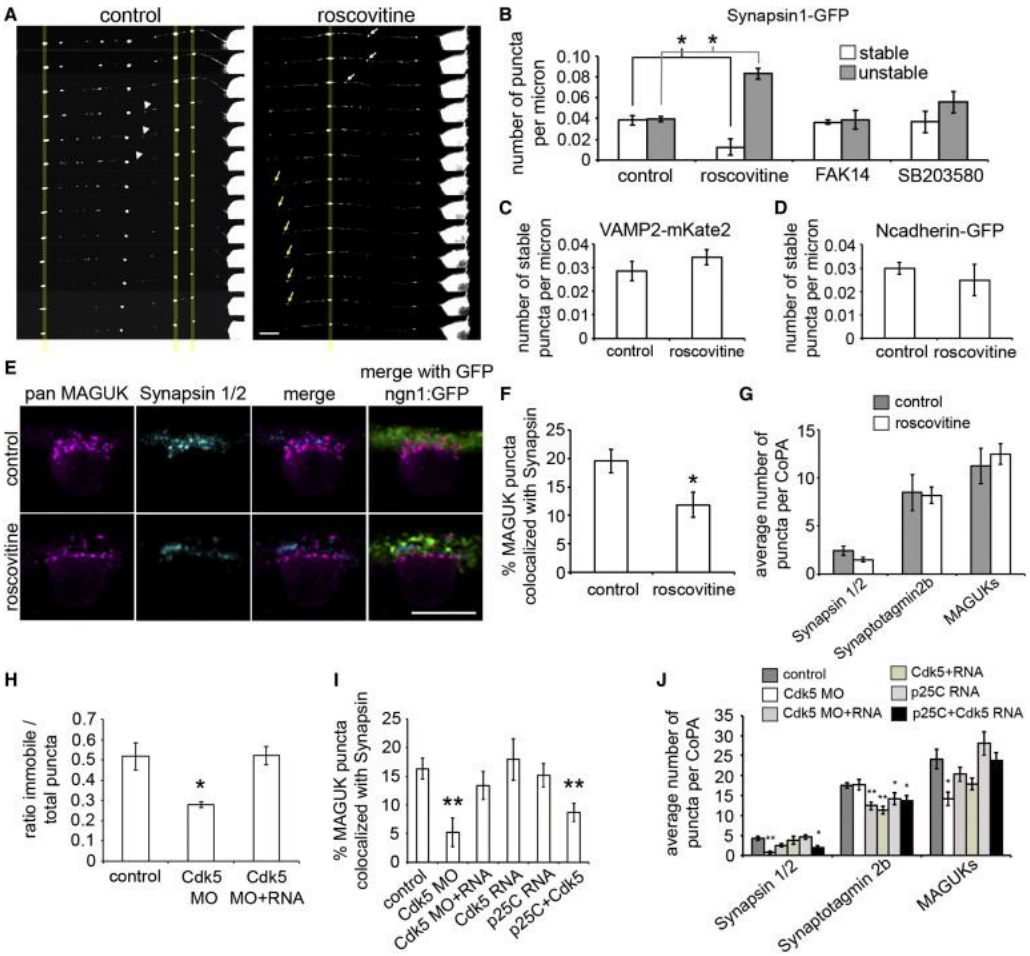

Figure 7. Cdk5 Regulates Synapsin Stabilization at Synapses (A) Selected frames from 1 hr time lapse movies of synapsin1-GFP expressing RB axons treated with either vehicle (control, left panel) or roscovitine (right panel). Scale bar represents 10 mm. (B) Histogram quantifying the number of stable and unstable puncta per micron for each treatment condition. (C and D) Histograms showing the number of stable puncta per micron in control and roscovitine treatment conditions in VAMP2-mKate2 expressing RB axons (C) and in N-cadherin-GFP expressing axons (D). (E) Dorsal view of IF labeling in 26 hpf ngn1:GFP (green) expressing embryos with antibodies for pan MAGUK (magenta) and synapsin 1/2 (cyan). Scale bar represents 10 mm. (F) Histogram showing the percentage of MAGUK puncta colocalized with synapsin puncta. (G) Histogram showing the average number of synapsin 1/2, synaptotagmin2b, and MAGUK puncta per CoPA cell for both control and roscovitine treatment conditions. (H) Histogram showing the ratio of stable to total synapsin1-GFP puncta in control, Cdk5 MO, and Cdk5 MO and RNA-injected embryos. (I) Histogram showing the percentage of MAGUK puncta colocalized with synapsin puncta in control, Cdk5 MO, Cdk5 MO and RNA, Cdk5 RNA, p25C RNA, and p25C and Cdk5 RNA-injected embryos. (J) Histogram showing the average number of synapsin 1/2, synaptotagmin2b, and MAGUK puncta for control, Cdk5 MO, Cdk5 MO and RNA, Cdk5 RNA, p25C RNA, and p25C and Cdk5 RNA-injected embryos. Error bars show SEM. *$p < 0.05$ and **$p < 0.005$ as compared to control condition.

recruitment to nascent presynaptic terminals. Using the RB-CoPA synapse in zebrafish spinal cord as a model glutamatergic synapse (Figure 1, 2), we first showed a time delay between the recruitment of STV proteins and Synapsin to presynaptic terminals by IF labeling (Figure 3). We demonstrated using three independent methods that Synapsin is transported in discrete puncta independently of STVs and PTVs: by live 2-color imaging of Synapsin1 with STV and PTV markers (Figure 4), by live imaging of STVs or PTVs with post-imaging IF labeling of endogenous Synapsins (Figures 5 and 6), and through the specificity of Cdk5 regulation of Synapsin stabilization (Figure 7).

To date, the presynaptic terminal has not been described to assemble with a defined sequence of recruitment. Our experiments using time-lapse imaging with *post hoc* immunolabeling (Figures 5 and 6) and immunolabeling at different developmental times (Figure 3) argue for a defined sequence in presynaptic assembly. We present evidence that a primary step in synaptic assembly is the recruitment of STVs. PTVs are then added with about a ~30 minute delay. Subsequently, Synapsin transport packets, also with a ~30 minute delay, are recruited to the nascent terminal. Additionally, our studies suggest that a later step in assembly (> 2h) may be the aggregation of additional STVs (Figure 5D). Given the role of Synapsins in tethering synaptic vesicles at synapses (Fornasiero et al., 2010) and pause sites (Sabo et al., 2006), it is possible that the accumulation of synaptic vesicle components over two hours after initial STV recruitment is dependent on the prior accumulation of Synapsin transport packets at synapses.

Our results concerning the method of Synapsin transport were surprising for two reasons: (1) Synapsin is tightly associated with SVs at mature synapses (Huttner et al.,

1983), suggesting that Synapsin could be transported by STVs during synapse formation (Scott et al., 2011); (2) if Synapsin were not transported with STVs, it would be expected that this cytosolic protein might diffuse and then aggregate at synapses (Scott et al., 2011), much like PSD-95 (Barrow et al., 2009; Bresler et al., 2001). While it is important to note that our techniques may not detect the entire pool of available Synapsin, our studies do suggest that a certain proportion of Synapsin1 is associated either with a distinct vesicular transport organelle or with a complex of cytosolic proteins which may be transported by a discrete set of motor proteins (Figure 4E). Scott et al. (2011) suggest that Synapsin can traffic along axons either slowly as part of molecular motor-driven cytosolic protein aggregates, or quickly by associating with transport packets carrying the integral SV protein Synaptophysin. The slow cytosolic transport of Synapsin in cultured hippocampal neurons was diffuse and not clearly punctate, and was much slower than that which we have observed here (Scott et al., 2011). While it is unclear what proportion of Synapsin clusters are co-transported with Synaptophysin (Scott et al., 2011), it will be interesting to determine whether this is also a rare event (that we observed less than 10% of the time; Figure 4D) in hippocampal neurons, or whether this represents a difference in transport mechanisms between cultured hippocampal neurons and sensory neurons *in vivo*.

Previous studies of the transport of presynaptic components to new synapses have remained contradictory. Two reports suggest that all of the proteins necessary to form a presynaptic terminal, including STV proteins, active zone proteins, and Synapsins are co-transported (Ahmari et al., 2000; Tao-Cheng, 2007). On the other hand, immunoisolated PTVs containing only active zone proteins, but not VAMP2 or other SV proteins such as

Synaptotagmin and Synaptophysin, are transported to synapses (Shapira et al., 2003; Zhai et al., 2001). Recently, Bury and Sabo showed that a significant fraction of STVs and PTVs co-transport along axons of neurons in culture (Bury and Sabo, 2011). While we see that STV and PTV markers can co-transport in our system, we find that the majority of the time, STVs and PTVs traffic separately *in vivo* (Figure 4). Similarly to the study by Bury and Sabo (2011), we also found that STVs and PTVs co-pause at the same sites. Further, our data suggest that at certain times during transport, all three transport packets, STVs, PTVs and Synapsin transport packets, pause at common sites along the axon (Figure 4A-C). This would explain the colocalization of a wide variety of presynaptic proteins in post-imaging IF and immuno-EM studies (Ahmari et al., 2000; Tao-Cheng, 2007). In fact, interaction between all three transport packets, STVs, PTVs and Synapsin transport packets, at such reservoirs may regulate their pausing, as deletion of the Synapsins significantly decreases pause duration of STVs (Sabo et al., 2006). One would, thus, predict that a decrease in pausing of Synapsin transport packets (Figure 7) might result in a decrease in STV pausing. However, based on our data regarding the localization of Cdk5 activity (Figure 7I), we conclude that pausing of Synapsin transport packets is only compromised at synaptic sites when Cdk5 activity is reduced, and not at non-synaptic pause sites.

Transport properties of STVs and PTVs were indistinguishable in our experiments (Figure 4). This is in line with a similar study also performed in RB cells using Ncadherin and VAMP fusion proteins (Jontes et al., 2004). In that study, the authors examined the deposition of Ncad-GFP and VAMP-GFP puncta in RB axons in the wake of an extending growth cone and found that both were transported with similar kinetics (Jontes

et al., 2004). Since the postsynaptic component was not identified in these experiments, it is possible that these depositions were just paused, an occurrence that was frequently observed in our current study (Figures 5 and 6), and not stabilized at a synapse. This presynaptic precursor material may be deposited behind the advancing growth cone at predefined sites along the axon such as those described by Sabo et al. (Sabo et al., 2006). From these sites, STVs and PTVs could then be recruited to developing synapses, before these sites eventually also become synapses (Sabo et al., 2006).

In addition to regulating axonal transport of various cargoes, including neurofilament monomers (Cheung and Ip, 2007), Cdk5 has been implicated in regulating a number of aspects of synapse formation. Here, we now show that Cdk5 specifically regulates presynaptic recruitment of Synapsin transport packets. In nematodes, Cdk5 was shown to regulate presynaptic assembly (Park et al., 2011), but, in contrast to our data, Cdk5 appears to play a more comprehensive role in these invertebrates. Perhaps this difference suggests that regulation of the Synapsin transport packet by Cdk5 may be an evolutionarily conserved mechanism; and that subsequent millennia of evolution have brought additional layers of complexity in the assembly and in the regulation of the assembly of synapses in vertebrates. It is also possible that our manipulations did not entirely abrogate Cdk5 activity and that STV or PTV recruitment may require minimal Cdk5 activity. However, our data suggest, that STV recruitment might be negatively regulated by Cdk5, as Cdk5 overexpression or Cdk5 activation resulted in less Synaptotagmin puncta at CoPA cells (Figure 7J).

In trying to understand the underlying molecular mechanism of Synapsin1 recruitment, it is important to consider that Synapsin1 is highly phosphorylated

(Fornasiero et al., 2010). Cdk5 can phosphorylate two serine residues in mammalian Synapsin1 (S549, S551) (Matsubara et al., 1996) and one of these sites is conserved in zebrafish Synapsin1 (S512). Thus, it may be tempting to assume that direct phosphorylation of Synapsin by Cdk5 regulates its recruitment to synapses by dissociation from the carrier proteins. However, close examination of live imaging of Synapsin transport (Figure 4 and data not shown) suggests that Synapsin transport packets stop, rather than disassemble. Therefore, we propose that Cdk5 regulates Synapsin recruitment by phosphorylating one of its many other substrates, such as motor proteins or cargo adapters, for example CASK (Samuels et al., 2007).

Importantly, our data shines a spot-light on a potential local mechanism by which presynaptic transport packets may be stabilized at synapses. Activation of a cascade of kinases in the axon, triggered by upstream synaptogenic events, might regulate the sequential recruitment of individual presynaptic components at nascent synaptic sites. It will be critical to unravel these regulatory mechanisms governing synapse assembly to completely understand synapse formation and the pathologies that affect this process.

Experimental Procedures

Analysis of Zebrafish Synapsin Genes

To obtain transcripts for the coding sequences for zebrafish *synapsins*, predicted sequences were identified using the Ensemble Genome browser. 3 predicted *synapsin* gene transcripts were identified. For further details see Extended Experimental Procedures.

Zebrafish Husbandry

All zebrafish embryos, larvae and adults were raised and maintained at 28.5°C according to standard protocols (Westerfield, 2000). Lines used include AB/Tübingen, *neurogenin1:GFP* [*Tg(-3.1ngn1:GFP)sb2]*, *narrowminded* (*nrd*^{m805}), *macho* (*mao*^{tt261}), *s1102t:GAL4/UAS:Kaede* [*Et(-1.5hsp70l:Gal4-VP16)s1102t;Tg(UAS-E1b:Kaede)s1999t*]. For details on genotyping and injection see Extended Experimental Procedures.

Imaging

Live imaging was performed at room temperature on a spinning disk microscope (McBain Instruments, Simi Valley, Ca) using a Leica 63x oil objective (1.40NA). All live imaging data was acquired using Volocity software and a Hamamatsu EMCCD camera. All IF was imaged on an inverted Nikon TU-2000 microscope with an EZ-C1 confocal system (Nikon) with either a 40x objective (0.95 NA) or a 100x oil-immersion objective (1.45 NA). For further details on imaging techniques see Extended Experimental Procedures.

Immunofluorescence Labeling

Immunofluorescence (IF) labeling was performed by fixing embryos in 4% PFA for 1.5h. After rinsing in PBS with 0.1% Triton X-100 (PBST), embryos were blocked in block buffer: PBS with 1% BSA, 1% DMSO, 2% goat serum and 0.1% Triton X-100. Embryos were incubated in primary antibodies in block buffer overnight at 4°C, washed

3 times in PBST, and incubated with secondary antibodies for 5h at room temperature. For antibodies see Extended Experimental Procedures.

Analysis

Analysis of imaging data was performed on maximum intensity projections for all fixed images and live movies. Synaptic puncta were selected and counted using Image Pro Plus software as described previously (Washbourne et al., 2002). Stability maps were generated by identifying paused puncta in kymographs made in Image J (Figures 5,6; rsb.info.nih.gov/ij/; (Rasband, 1997-2011) . All graphs were prepared in Microsoft Excel, and statistics were analyzed using an unpaired 2-tailed Students t-test. For further details on image analysis refer to Extended Experimental Procedures.

Electron Microscopy

Zebrafish embryos at 25 and 28 hpf were anesthetized with 0.003% tricaine and then fixed and processed for EM essentially as described previously (Jontes et al., 2000). 70nm silver thin sections were placed on 200 mesh hexagonal copper grids and examined unstained in a JEOL 100 CX electron microscope at 80kV. Images were taken using a CCD digital camera system (XR-100 from AMT, Danvers, MA, USA). For the full EM protocol see Extended Experimental Procedures.

CHAPTER IV

CONCLUDING REMARKS

Synaptogenesis is a complex process involving the recruitment and stabilization of thousands of proteins at both pre- and postsynaptic contact sites. Our data provides insight into two key components of this process. First, we determined 4.1B-a was a necessary component of synapses, potentially stabilizing macromolecular complexes at sites of cell adhesion. These synapses were imperative for the proper formation of the touch response neuronal circuit, where knockdown of 4.1B-a caused altered kinetics of touch-evoked behaviors. Second, we determined the time course of proteins recruited to nascent synapses, with new insight into the recruitment of the protein synapsin. We found that synapsin was recruited to nascent synapses as a separate package, after STVs and PTVs had arrived. This recruitment was regulated by Cdk5, and thus provides the first evidence that kinases play a role during the early events of synaptogenesis. With this data, new questions have arisen in our understanding of how the nervous system works.

The Role of 4.1B During Synaptogenesis

4.1B is a scaffolding molecule involved in the stabilization of macromolecular complexes at sites of cell adhesion. 4.1B has been shown to enhance the recruitment of NMDA receptors to glutamatergic synapses in neuronal and nonneuronal cell culture assays, but the role of 4.1B at synapses *in vivo* has not been investigated (Hoy, 2009). Chapter II of this dissertation focused on the function of 4.1B at glutamatergic synapses in zebrafish. Zebrafish are well suited for studying the initial formation and subsequent

maturation of synapses because embryos are optically transparent, they have a small number of identified neurons within the spinal cord, and they exhibit simple behaviors at early developmental stages. Our studies show that loss of 4.1B in the nervous system caused a reduction in the number of synapses on primary motor neurons and affected touch-evoked responses. These results suggest 4.1B is necessary for the formation of synapses and circuit development, but the exact mechanisms remain unknown. To gain a better understanding of the role of 4.1B during the development of synapses, it will be necessary to study the interactions of 4.1B with respect to NMDA receptors in developing zebrafish embryos. NMDA receptors are expressed within the spinal cord at 26 hpf (Cox, 2005). If 4.1B can recruit and stabilize NMDA receptors at sites of cell adhesion, as seen *in vitro,* we will have laid the foundation for dissecting the molecular mechanisms that underlie synaptogenesis. We will be able to study protein recruitment and stabilization at nascent synapses; we can perform a more detailed analysis of the proteins that are necessary for proper synapse function; and we can perform electrophysiological studies to determine how loss of 4.1B leads to altered kinetics of touch-evoked responses. Taken together, we found 4.1B to be an important component of synapses that are necessary for the proper function of the touch response neuronal circuit.

The Role of Cdk5 During Synapsin Recruitment

Synapsin is a phosphoprotein important for regulating the reserve pool of synaptic vesicles at presynaptic terminals. It had long been assumed that synapsin was transported to newly formed contact sites with STVs because of the tight association between synapsin and synaptic vesicles (Huttner, 1983). Our data, however, shows that synapsin is

transported independently of other known transport packets and thus provides new insight into the initial formation of synaptic contacts (Chapter III). It will be necessary to identify if other presynaptic proteins are cotransported to nascent synapses with synapsin, and which motor protein is involved in transporting this packet. Our work also identified Cdk5 as a key regulator of synapsin recruitment to nascent synapses. This work provides the first evidence that kinases are involved in the recruitment of synaptic transport packets. It will be interesting to determine the signaling cascades that are involved in the recruitment of STVs and PTVs; this includes determining the kinases that may be involved in signaling synapse formation and transport packet recruitment, how the various transport packets are regulated, and how the transport packets stop and unload at nascent synapses. Taken together, these data provide insight into the initial formation of synaptic contacts, and it lays the foundation for future studies that will be imperative for studies of neurological disorders.

Our very existence as a human being is dependent on the proper formation and regulation of synaptic contacts within the central nervous system. Alterations in the functioning of the nervous system due to mutations within the vast number of proteins can lead to devastating diseases such as autism and schizophrenia. It will be necessary to continue to study the mechanisms that underlie synapse formation as this will be imperative for helping the millions of people who suffer from the various neurological disorders. The work described in this dissertation helps get us one step closer to understanding the extreme complexity of the brain, while opening the door to a wide array of new questions.

APPENDIX

SUPPLEMENTAL MATERIAL FOR CHAPTER III

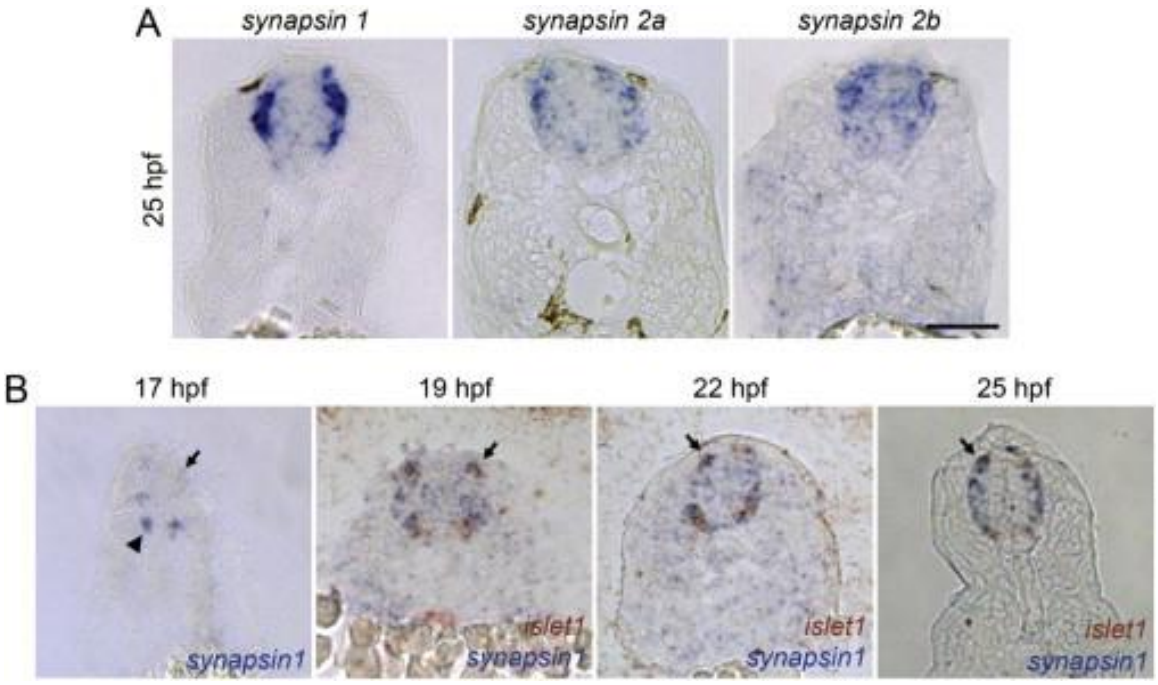

Figure S1. Zebrafish *synapsin* genes are expressed in RBs, related to Figure 3. (A) *In situ* hybridization (ISH) for zebrafish *synapsins1*, *2a*, and *2b* at 25 hpf in transverse sections. *synapsin1* showed the strongest expression of the three in RBs. Scale bar 50μm. (B) *synapsin1* ISH on 17, 19, 22, and 25 hpf transverse sections (2 color ISH with *islet-1* to label RBs and motor neurons in 19, 22, and 25 hpf images). *synapsin1* transcript was first seen at 17 hpf in motor neuron domain (arrowhead), but not in RBs (arrow). *synapsin1* and *islet1* were seen in RBs from 19 hpf on (arrows). Scale bar 50μm.

Figure S2 (next page). Validation of fluorescently-tagged fusion constructs, related to Figure 4. (A) Synapsin1-GFP in a RB neuron in the zebrafish spinal cord at 25 hpf. Left panel: Dorsal view of IF labeling of GFP overlaid with a brightfield image. The midline (ML) and extent of the spinal cord (SC) are indicated. Rostral is to the left. Right panel: enlargement of IF outlined in box showing Synapsin1-GFP. PA: peripheral arbor, CA: central axon. Scale bar, 10 μm. (B) Synapsin1-GFP was localized with a similar distribution as endogenous Synapsin 1/2 in RB axons in the zebrafish spinal cord. (C) Selected sequence of 6 frames, 30 seconds apart, from a 30 minute movie. Arrowheads highlight a moving punctum labeled with both Synapsin1-GFP and Synapsin1-mKate2. (D) A RB neuron expressing VAMP2-mKate2 at 25 hpf in a dorsal view. Left panel, IF for VAMP2-mKate2 overlayed on a bright field image. Right panel, magnification of myc IF labeling, showing the peripheral arbor (PA) and central axon (CA) of the RB. Scale bar, 10 μm. (E) IF labeling of SV2 was highly colocalized with VAMP2-mKate2 labeling. Scale bar 10μm. (F) IF labeling of STV marker Synaptotagmin2b is highly colocalized with VAMP2-mKate2. Scale bar 10μm. (G) IF for bassoon on Ncad-GFP transfected rat hippocampal neurons shows that the majority of Bassoon puncta colocalize with Ncad-GFP puncta. (H) IF for Synaptotagmin2b colocalized with only a small percentage of Ncad-GFP puncta. Scale bar 10μm.

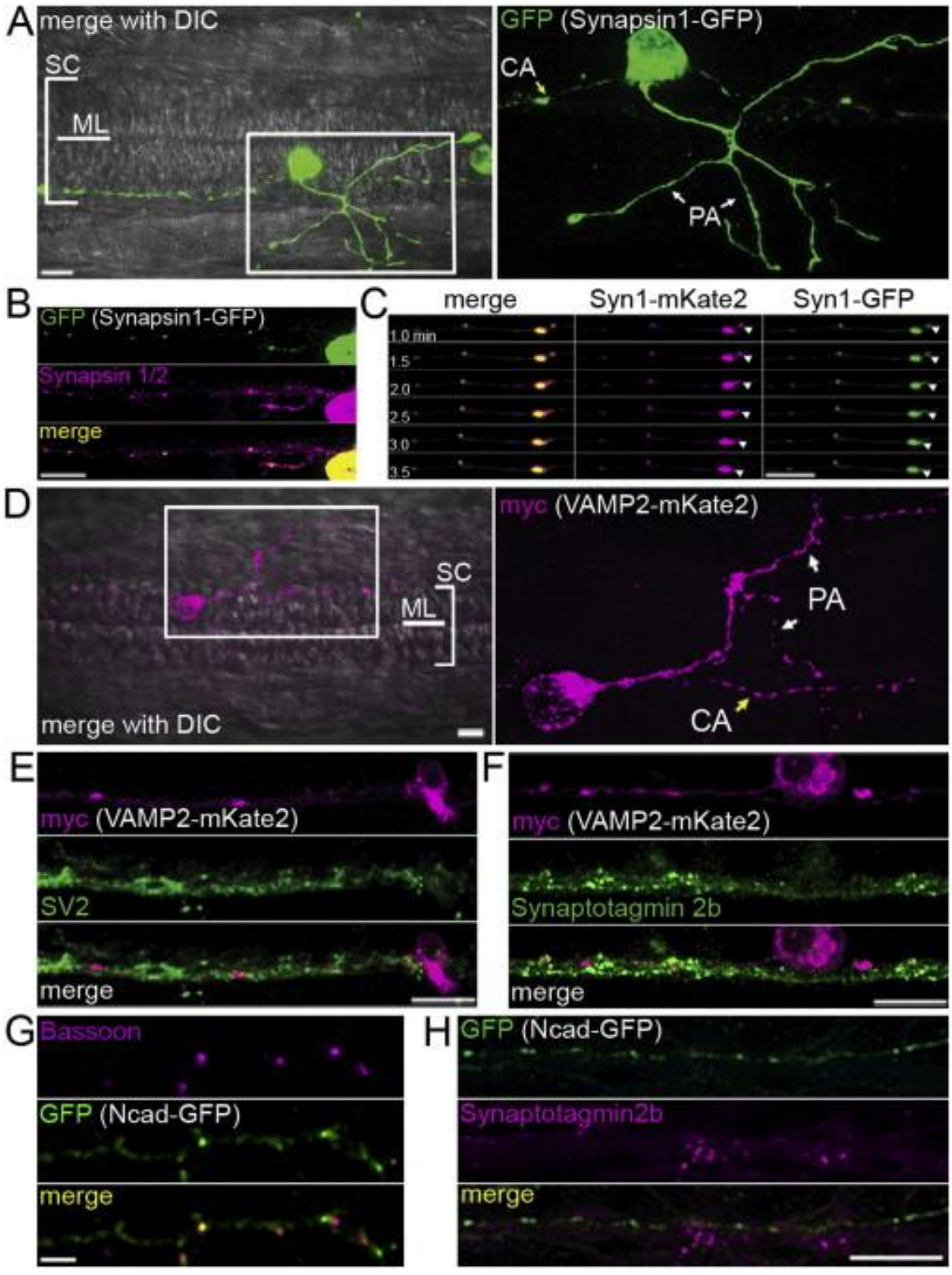
A
merge with DIC
SC
ML
GFP (Synapsin1-GFP)
CA
PA
B
GFP (Synapsin1-GFP)
Synapsin 1/2
merge
C
merge
Syn1-mKate2
Syn1-GFP
1.0 min
1.5
2.0
2.5
3.0
3.5
D
SC
ML
merge with DIC
myc (VAMP2-mKate2)
PA
CA
E
myc (VAMP2-mKate2)
SV2
merge
F
myc (VAMP2-mKate2)
Synaptotagmin 2b
merge
G
Bassoon
GFP (Ncad-GFP)
merge
H
GFP (Ncad-GFP)
Synaptotagmin2b
merge

Extended Results

MAGUK labeling specificity

MAGUK proteins localize to both axonal and somatodendritic compartments (Meyer et al., 2005), however, at this stage of development and under these labeling conditions, 100% of pan MAGUK puncta localized to the lateral face of CoPA cell bodies, with no labeling visible in the dlf (n = 10 embryos). In comparison, up to 35% of Synapsin1/2 puncta observed in the dlf were not colocalized with CoPA cells (n = 21 CoPA cells). Further analysis with multiple GFP transgenic zebrafish lines confirmed that CoPA interneurons are the only neurons in the dorsal spinal cord at 25 hpf that exhibit punctate MAGUK immunoreactivity. At 28 hpf commissural secondary ascending (CoSA) interneurons start to show pan MAGUK labeling, but with a significantly smaller number of puncta (data not shown; A. Tallafuss and P. Washbourne).

Extended Experimental Procedures

Analysis of zebrafish *synapsin* genes

To obtain transcripts for the coding sequences for zebrafish *synapsins*, predicted sequences were identified using the Ensemble Genome browser (www.ensembl.org/index.html). 3 predicted *synapsin* gene transcripts were identified. An alignment was made with ClustalW2 (www.ebi.ac.uk/Tools/msa/clustalw2/) using a Gonnet protein weight matrix and default alignment parameters (see below). Percent identity between mouse and zebrafish *synapsins* was calculated for the actin binding region using Jalview (www.jalview.org/help.html) (Waterhouse et al., 2009). To confirm the gene identities were correctly assigned, we examined zebrafish, human, mouse and

pufferfish chromosomes for syntenic regions surrounding the *synapsin* gene locations (teleost.cs.uoregon.edu/acos/synteny_db/) (Catchen et al., 2009). Based on these analyses, we conclude that zebrafish possess one ortholog of mammalian Synapsin1, two orthologs of the mammalian Synapsin2 gene and no ortholog of Synapsin3. We call the two *synapsin2* orthologs *synapsin2a* and *synapsin2b*, based on existing annotation in the zebrafish genome assembly (Zv9). Image clones of both *synapsin2a* and *2b* (Open Biosystems; *synapsin2a*: NM_001002597.1; *synapsin2b*: NM_001037576.1) were obtained to make *in situ* probes. A predicted coding sequence for *synapsin1* (NM_001126437) was used to design primers to amplify that sequence from 24hpf cDNA, made using the Superscript III first strand synthesis system for RT-PCR (Invitrogen, Carlsbad, CA). This PCR fragment was subcloned into the Zero Blunt TOPO cloning vector (Invitrogen).

DNA constructs

UAS:Synapsin1-GFP was constructed by inserting the *synapsin1* coding sequence into UAS:GFP by PCR using primers incorporating 5' EcoRI and 3' PstI restriction sites. UAS:GFP was generated by inserting a 10X UAS sequence, 1Eb minimal promoter, carp beta-actin transcriptional start, coding sequence for eGFP and a polyA site into a cloning vector. UAS:Synapsin1-mKate2 was made by inserting the *synapsin1* coding sequence into UAS:mKate2 (a derivative of the UAS:GFP vector made by substituting the eGFP coding sequence for the red fluorescent protein mKate2) by PCR, incorporating 5' EcoRI, 3' PstI and the myc epitope tag sequence. mKate2 was chosen for these experiments due to its high fluorescence quantum yield and photostability (Shcherbo et al., 2009). Control

experiments to determine that mKate2 did not adversely affect localization or trafficking of fusion proteins were performed by comparing the localization of mKate2 to GFP (data not shown).

Zebrafish VAMP2 coding sequence was identified using ensemble and cloned as described for *synapsin1* (NM_200005.1). UAS:VAMP2-myc-mKate2 (VAMP2-mKate2) was constructed by inserting the VAMP2 coding sequence into UAS:mKate2 as described above. All cloning steps were confirmed by sequencing.

Validation of fluorescently-tagged constructs

Our *in situ* hybridization experiments (Figure S1A) revealed that all three *synapsin* genes (*1, 2a*, and *2b*) were expressed in RB cells, with *synapsin1* showing the strongest expression. Thus, we chose to examine the trafficking of Synapsin1 in RB axons. Zebrafish Synapsin1 was expressed as a fusion with either the red fluorescent protein mKate2 or GFP in RB cells. We drove the expression of the fusion proteins by injecting DNA into fertilized zebrafish eggs from the et101.2 Gal4/VP16 line (Scott et al., 2007) which expresses Gal4/VP16 in RB cells. By titrating the concentration of the plasmid, embryos were obtained that expressed fusion proteins in only one or two RB neurons (Figure S2A). Synapsin1-GFP was targeted to both central and peripheral axons. Immunolabeling of Synapsin1-GFP expressing embryos with Synapsin 1/2 antibody showed 100% colocalization (100%, n = 3 embryos; Figure S2B), suggesting that fluorescently-tagged Synapsin1 behaves like the endogenous protein. We found that Synapsin1-GFP and Synapsin1-mKate2 both trafficked anterogradely and retrogradely in RB axons as puncta (Figure 1A,B and Figure S2C). The two tagged versions of Synapsin

were seen to move together all the time (Figure S2C) ensuring that the mKate2 and GFP tags did not differentially alter the transport of Synapsin1, and that we were able to detect cotransport with our imaging regimen.

Fluorescent fusion proteins of VAMP2 and Ncadherin (*Cadherin2,* Ncad-GFP) have been described previously (Jontes et al., 2000; Jontes et al., 2004). However, we further examined the specificity of these constructs for localization with STVs and PTVs, respectively. VAMP2-mKate2 and Ncad-GFP were targeted to both central and peripheral axons of RB cells (Figure S2D). Immunolabeling of VAMP2-mKate2 expressing embryos showed that VAMP2-mKate2 puncta colocalize with the SV proteins SV2 (95.2% ± 3.7%, n = 3) and Synaptotagmin (86.7% ± 3.9%, n = 3), suggesting that VAMP2-mKate2 is a component of STVs (Figure S2E). Since Bassoon and Piccolo antibodies were not immunoreactive in zebrafish embryos, we performed IF for the PTV marker Bassoon on rat hippocampal neurons expressing zebrafish Ncad-GFP. This analysis showed strong colocalization between Bassoon puncta and Ncad-GFP puncta (95.36% ±3.5; n = 5 neurons; Figure S2G). Only around 16% Ncad-GFP puncta colocalized with the SV protein Synaptotagmin (16.6% ±3.4, n = 3 embryos; Figure S2H) in RB axons, suggesting that it is present in a different transport organelle than SV proteins. Live imaging of the central axons showed that VAMP2-mKate2 and Ncad-GFP were transported in punctate structures both anterogradely and retrogradely in RB axons (Figure 4A-C). Our control experiments and comparisons with previous studies of STV and PTV trafficking in live zebrafish embryos and in mammalian cultures (Ahmari et al., 2000; Bury and Sabo, 2011; Jontes et al., 2004; Sabo et al., 2006) suggest that these markers are reliable markers for the visualization of STV and PTV transport in RB axons.

Zebrafish Husbandry

All zebrafish embryos, larvae and adults were raised and maintained at 28.5°C according to standard protocols (Westerfield, 2000). All procedures were performed in accordance with the University of Oregon Animal Care and Use Committee. Lines used include AB/Tübingen, *neurogenin1:GFP* (*Tg(-3.1ngn1:GFP)sb2*), *narrowminded* (*nrd*^{m805}; provided by Dr. Kristin Artinger, University of Colorado, Denver), *s1102t:GAL4/UAS:Kaede* [*Et(-1.5hsp70l:Gal4-VP16)s1102t;Tg(UAS-E1b:Kaede)s1999t*; provided by Dr. Herwig Baier, University of California, San Francisco]. *s1102t:GAL4* embryos were obtained by outcrossing *s1102t:GAL4/UAS:Kaede* to AB/Tübingen and PCR genotyping DNA obtained from fin clips using primers specific for the GAL4 cassette and the UAS:Kaede cassette. DNA, morpholine-modified oligonucleotides (MOs) and/or RNA were pressure injected into 1-2 cell zebrafish embryos using a MPPI-2 pressure injector (ASI, Eugene, OR). DNA constructs were injected into the yolk singly or in combination at concentrations of 20-30ng/µl each and embryos were screened for GFP or mKate2 expression the following day. A translation blocking MO to cdk5 (sequence:5'CCAGCTTCTCATACTTTTGCATGGT3'; Gene Tools, Philomath, OR) was injected at a concentration of 0.8mM. This concentration was determined to give a maximum effect on RB cell migration from the midline (40.2 ± 4.4% of RB cells lay on the midline versus 1.3 ± 0.4% of controls, $p < 0.001$, $n = 18$) with no negative effects on overall health and development of embryos, as previously described (Tanaka et al., 2012). Central axons localized to the dlf, despite midline localization of cell bodies (not shown). Rescue of MO-mediated knock-down was performed by co-injecting with *in vitro* transcribed mRNA encoding human CDK5-GFP at 10ng/µl (Dr. Li-Huei Tsai, MIT,

Cambridge, MA). Ectopic activation of Cdk5 was achieved by injecting mRNA encoding human p25C-GFP at 10ng/µl (Dr. Li-Huei Tsai, MIT, Cambridge, MA). Embryos used were of either sex and were staged according to Kimmel et al. (Kimmel et al., 1995).

Imaging

Embryos used for live imaging were dechorionated, then anesthetized in 0.003% tricaine in embryo medium (EM). Embryos were then mounted in 1.5% low melt agarose/EM. Dishes were flooded with EM plus 0.003% tricaine and the embryos were imaged at room temperature on a spinning disk microscope (McBain Instruments, Simi Valley, Ca) using a Leica 63x oil objective (1.40NA). For time lapse experiments with single fluorescent constructs, images were captured at 30 second intervals over 0.5 µm steps through the z depth traversed by the axon (from ~5-10 µm) over a 2 hour imaging period. For the kinase inhibitor experiments, images were captured over a 1 hour period. For two-color imaging, embryos were live imaged for 30 to 60 minutes with z-stacks acquired with 0.5 µm steps through the depth traversed by the axon at 30 – 60 second intervals. Stacks were generated by obtaining images for each wavelength sequentially at each z-plane. This was a slower acquisition method than capturing all z-planes for one channel followed by all z-planes for a second channel, but allowed us to be confident that any differences in movement of the two colors of puncta was due to differences in transport. All live imaging data was acquired using Volocity software and a Hamamatsu EMCCD camera. All IF was imaged on an inverted Nikon TU-2000 microscope with an EZ-C1 confocal system (Nikon) with either a 40x objective (0.95 NA) or a 100x oil-immersion objective (1.45 NA). Image stacks through the depth of the dlf (~10-15

microns) were acquired to capture synaptic puncta at all points of contact between RB axons and CoPAs unless otherwise noted. Images were acquired for each channel separately. All immunofluorescence images presented in the figures are flattened, maximum intensity projections of z-stacks except for the insets in Figure 3A, which show single z-planes.

Kinase Inhibitor Treatment

All kinase inhibitors were purchased from Sigma (Saint-Louis, MO). Stocks were prepared in DMSO according to manufacturer instructions. For incubations, stocks were diluted in EM with tricaine to the following concentrations, roscovitine 40μM, SB203580 100μM, FAK inhibitor 14 100μM, KN-62 20μM, KN-93 20μM. The inhibitor concentrations have been used in previously published studies for treatment of zebrafish embryos at this developmental time point. Final concentration of DMSO was 0.2% or less, and appropriate vehicle controls were utilized. For imaging experiments embryos were dechorionated at 23hpf and incubated in stated concentrations of a given kinase inhibitor for 1-3 hours prior to imaging.

Immunofluorescence Labeling

Immunofluorescence (IF) labeling was performed with the following primary antibodies and dilutions: mouse anti-panMAGUK (1:100 ; NeuroMab, Davis, CA), rabbit anti-Synapsin 1/2 (1:1000: Synaptic Systems, Goettingen, Germany), rabbit anti-Piccolo (1:300; Synaptic Systems), chicken anti-c-myc (1:125; Aves, Tigard, Oregon), chicken anti-GFP (; 1:500; Abcam, Cambridge, MA), mouse anti-con-1 (1:150; gift from Dr. John

Kuwada, University of Michigan, Ann Arbor), mouse anti-Synaptotagmin2b (znp-1; 1:750; Developmental Studies Hybridoma Bank, University of Iowa), SV2 (1:1000 dilution; Developmental Studies Hybridoma Bank, University of Iowa), and islet-1 (stock 39.4D, 1:200 dilution, Developmental Studies Hybridoma Bank, University of Iowa). Secondary antibodies used were: anti-Chicken Alexa 488, anti-chicken Alexa 546, anti-rabbit Alexa 546, anti-rabbit Alexa 633 (Molecular Probes) and anti-mouse Cy2, anti-mouse Cy3, (Jackson Immuno, West Grove, PA). For IF after live imaging, embryos were transferred from EM with 0.003% tricaine to fixative within 5 minutes of the completion of live imaging.

IF for endogenous Bassoon on cortical neurons was carried out as described in (Hoy et al., 2009) on 5 DIV neuron cultures. Anti-Bassoon (Enzo Life Sciences, Plymouth Meeting PA) was used at a 1:400 dilution.

Analysis

Analysis of imaging data was performed on maximum intensity projections for all fixed animals and live movies. Synaptic puncta were selected and counted using Image Pro Plus software (Figures 3,5-7 and S2; Media Cybernetics, Bethesda, MD) as described previously (Washbourne et al., 2002), but with one modification: background plus one standard deviation was subtracted from puncta fluorescence intensities prior to puncta selection. Background was calculated as the average intensity at points adjacent to the dlf. Puncta were counted as co-localized if they had significant overlap (>10%). In all cases where colocalization of puncta was identified, puncta were verified as being colocalized by examining the original z-stacks and determining whether puncta were in

the same z-plane. Stability maps were generated by identifying paused puncta in kymographs made in Image J (Figures 6 and 7; rsb.info.nih.gov/ij/) (Rasband, 1997-2011). The magnetic wand tool in Adobe Photoshop was used to trace the outline of each punctum, then a colored overlay was added to visually indicate the length of time that each punctum had been stable. Pausing was defined as movement of less than one punctum diameter between frames. Total fluorescence intensity (Figure 5C) was measured using Volocity software by summing the intensities at each pixel composing a punctum. Intensity data were normalized between images by subtracting a background value equal to the average background for a given image multiplied by the total number of pixels in a puncta. Velocities of puncta from live imaging experiments (Fig. 8) were calculated from the beginning to the end of a movement for puncta that moved unidirectionally over at least 2 μm and for at least 3 frames using Image Pro Plus software (Media Cybernetics). Prior to measuring puncta velocities, image stacks were aligned (to account for drift due to growth of the embryos during the imaging session) using the Stack Reg plug-in for Image J (bigwww.epfl.ch/thevenaz/stackreg/) (Thevenaz et al., 1998). Images were processed for presentation in Adobe Photoshop. Fluorescence panels were prepared by using the despeckle filter and adjusting the levels to allow for good contrast upon printing. All graphs were prepared in Microsoft Excel, and statistics were analyzed using an unpaired 2-tailed Students t-test.

In situ Hybridization

In situ hybridization (ISH) was carried out and RNA probes were made according to the methods described by (Pietri et al., 2008). Briefly, embryos were hybridized with

digoxygenin (DIG) and fluorescein labeled probes in 50% formamide hybridization buffer at 68°C overnight. Antibodies to DIG and fluorescein conjugated to alkaline phosphatase (Roche, Mannheim, Germany) were used and detected with NBT/BCIP or INT/BCIP. Sense and antisense probe templates were in vitro transcribed from PCR fragments of *synapsin1a*, *1b* or *2b* linked to a T7 or T3 promoter sequence. *synapsin1a* probes cover nucleotides (nt) 1467 to 1872 of the coding sequence (CDS; NM_001126437.2), nt 1480 to 1883 of CDS for *synapsin2a* (NM_001002597.1), and the 157 nt preceding the start codon plus the first 250 nt of the CDS for *synapsin2b* (NM_001037576.1). Probes were labeled with DIG and fluorescein according to manufacturer's protocol (Roche). Images were taken on a Zeiss Axioplan microscope using an Axiocam MRc5.

Electron Microscopy

Zebrafish embryos staged at 25 and 28 hpf were anesthetized using a few drops of tricaine solution. The medium was removed and replaced with primary fixative (2% paraformaldehyde and 2% glutaraldehyde in 0.1M cacodylate buffer pH 7.4). The dishes were immediately placed in a Ted Pella laboratory microwave oven (Ted Pella, Redding CA) equipped with a cold spot and water recirculator. They were pulsed at power level 1 (105w) for 1 minute on - 1 minute off -1 minute on then at power level 2(300w) for 20 seconds on - 20 seconds off - 20 seconds on three times, swirling the dishes in between steps. The fish sat in the fixative for an additional 30 minutes at room temperature. Following three washes in 0.1M cacodylate buffer, pH 7.4, the fish were placed in 2% osmium tetroxide in 0.1M cacodylate buffer and microwaved as in the primary fixation

step (above). The dishes were allowed to sit in the osmium fixative under the fume hood for an additional hour at room temperature.

The samples were washed with 0.1 M cacodylate buffer and then microwaved in 1.5% TCH (thiocarbohydrazide) in water for 1 minute on - 1 minute off - 1 minute on at power level 1. They were allowed to sit in the TCH solution for an additional 2 minutes before extensive washing with water. The fish were then treated with another round of osmium fixative for 1 minute on - 1 minute off - 1 minute on at power level 1 and allowed to sit at room temperature for 30 minutes. After washing well in dd water, the fish were dehydrated in the microwave using an ascending alcohol series. Propylene oxide (PPO) was used as a transition fluid for gradual infiltration in epoxy resin (overnight in 1:1 resin:PPO and overnight in 1:2 PPO:resin). The fish were embedded in coffin molds in fresh 100% Embed 812 resin hard formulation (Electron Microscopy Sciences, Warrington, PA) and hardened for 2 days at 60°C. After removing blocks from the molds, the fish were buzzed down to the selected area using a Leica EM trimmer (Leica Microsystems, Inc, Bannockburn, Il.) and sectioned using a Diatome Histo knife (Diatome, Warrington, PA). Semi-thin sections were stained with toluidine blue and examined by LM. Silver thin sections 70nm in thickness were placed on 200 mesh hexagonal copper grids and examined unstained in a JEOL 100 CX electron microscope at 80kV. Images were taken using a CCD digital camera system (XR-100 from AMT, Danvers, MA, USA).

REFERENCES CITED

Chapter I

Ahmari SE, Buchanan J, Smith SJ. 2000. Assembly of presynaptic active zones from cytoplasmic transport packets. Nat Neurosci 3:445-451.

Beattie CE. 2000. Control of motor axon guidance in the zebrafish embryo. Brain Res Bull 53:489-500.

Benfenati F, Valtorta F, Bahler M, Greengard P. 1989. Synapsin I, a neuron-specific phosphoprotein interacting with small synaptic vesicles and F-actin. Cell Biol Int Rep 13:1007-1021.

Bernhardt RR, Chitnis AB, Lindamer L, Kuwada JY. 1990. Identification of spinal neurons in the embryonic and larval zebrafish. J Comp Neurol 302:603-616.

Bonanomi D, Menegon A, Miccio A, Ferrari G, Corradi A, Kao HT, Benfenati F, Valtorta F. 2005. Phosphorylation of synapsin I by cAMP-dependent protein kinase controls synaptic vesicle dynamics in developing neurons. J Neurosci 25:7299-7308.

Carlin RK, Grab DJ, Cohen RS, Siekevitz P. 1980. Isolation and characterization of postsynaptic densities from various brain regions: enrichment of different types of postsynaptic densities. J Cell Biol 86:831-845.

Chia PH, Li P, Shen K. 2013. Cell biology in neuroscience: cellular and molecular mechanisms underlying presynapse formation. J Cell Biol 203:11-22.

Clarke JD, Hayes BP, Hunt SP, Roberts A. 1984. Sensory physiology, anatomy and immunohistochemistry of Rohon-Beard neurones in embryos of Xenopus laevis. J Physiol 348:511-525.

Cox JA, Kucenas S, Voigt MM. 2005. Molecular characterization and embryonic expression of the family of N-methyl-D-aspartate receptor subunit genes in the zebrafish. Dev Dyn 234:756-766.

Dent EW, Gupton SL, Gertler FB. 2011. The growth cone cytoskeleton in axon outgrowth and guidance. Cold Spring Harb Perspect Biol 3.

Drapeau P, Saint-Amant L, Buss RR, Chong M, McDearmid JR, Brustein E. 2002. Development of the locomotor network in zebrafish. Prog Neurobiol 68:85-111.

Drapeau P, Buss RR, Ali DW, Legendre P, Rotundo RL. 2001. Limits to the development of fast neuromuscular transmission in zebrafish. J Neurophysiol 86:2951-2956.

Easley-Neal C, Fierro J, Jr., Buchanan J, Washbourne P. 2013. Late recruitment of synapsin to nascent synapses is regulated by Cdk5. Cell Rep 3:1199-1212.

Eisen JS, Pike SH, Romancier B. 1990. An identified motoneuron with variable fates in embryonic zebrafish. J Neurosci 10:34-43.

Eisen JS, Myers PZ, Westerfield M. 1986. Pathway selection by growth cones of identified motoneurones in live zebra fish embryos. Nature 320:269-271.

Friedman HV, Bresler T, Garner CC, Ziv NE. 2000. Assembly of new individual excitatory synapses: time course and temporal order of synaptic molecule recruitment. Neuron 27:57-69.

Hagenmaier HE. 1973. The hatching process in fish embryos. 3. The structure, polysaccharide and protein cytochemistry of the chorion of the trout egg, Salmo gairdneri (Rich.). Acta Histochem 47:61-69.

Hale ME, Ritter DA, Fetcho JR. 2001. A confocal study of spinal interneurons in living larval zebrafish. J Comp Neurol 437:1-16.

Hoppmann V, Wu JJ, Soviknes AM, Helvik JV, Becker TS. 2008. Expression of the eight AMPA receptor subunit genes in the developing central nervous system and sensory organs of zebrafish. Dev Dyn 237:788-799.

Jontes JD, Buchanan J, Smith SJ. 2000. Growth cone and dendrite dynamics in zebrafish embryos: early events in synaptogenesis imaged in vivo. Nat Neurosci 3:231-237.

Kandel E, Schwartz J, Jessell T, Siegelbaum S, Hudspeth A. Principles of Neuroscience 5th Edition. New York; McGraw-Hill, Health professions division, 2012.

Kim DH, Hwang CN, Sun Y, Lee SH, Kim B, Nelson BJ. 2006. Mechanical analysis of chorion softening in prehatching stages of zebrafish embryos. IEEE Trans Nanobioscience 5:89-94.

Kim SH, Ryan TA. 2010. CDK5 serves as a major control point in neurotransmitter release. Neuron 67:797-809.

Knogler LD, Drapeau P. 2014. Sensory gating of an embryonic zebrafish interneuron during spontaneous motor behaviors. Front Neural Circuits 8:121.

Kuromi H, Kidokoro Y. 1998. Two distinct pools of synaptic vesicles in single presynaptic boutons in a temperature-sensitive Drosophila mutant, shibire. Neuron 20:917-925.

Kuwada JY, Bernhardt RR, Nguyen N. 1990. Development of spinal neurons and tracts in the zebrafish embryo. J Comp Neurol 302:617-628.

Lieschke GJ, Currie PD. 2007. Animal models of human disease: zebrafish swim into view. Nat Rev Genet 8:353-367.

McAllister AK. 2007. Dynamic aspects of CNS synapse formation. Annu Rev Neurosci 30:425-450.

Melancon E, Liu DW, Westerfield M, Eisen JS. 1997. Pathfinding by identified zebrafish motoneurons in the absence of muscle pioneers. J Neurosci 17:7796-7804.

Mendelson B. 1986. Development of reticulospinal neurons of the zebrafish. II. Early axonal outgrowth and cell body position. J Comp Neurol 251:172-184.

Metcalfe WK, Myers PZ, Trevarrow B, Bass MB, Kimmel CB. 1990. Primary neurons that express the L2/HNK-1 carbohydrate during early development in the zebrafish. Development 110:491-504.

Metcalfe WK, Kimmel CB, Schabtach E. 1985. Anatomy of the posterior lateral line system in young larvae of the zebrafish. J Comp Neurol 233:377-389.

Meyer MP, Trimmer JS, Gilthorpe JD, Smith SJ. 2005. Characterization of zebrafish PSD-95 gene family members. J Neurobiol 63:91-105.

Ogino K, Ramsden SL, Keib N, Schwarz G, Harvey RJ, Hirata H. 2011. Duplicated gephyrin genes showing distinct tissue distribution and alternative splicing patterns mediate molybdenum cofactor biosynthesis, glycine receptor clustering, and escape behavior in zebrafish. J Biol Chem 286:806-817.

Pietri T, Manalo E, Ryan J, Saint-Amant L, Washbourne P. 2009. Glutamate drives the touch response through a rostral loop in the spinal cord of zebrafish embryos. Dev Neurobiol 69:780-795.

Pike SH, Melancon EF, Eisen JS. 1992. Pathfinding by zebrafish motoneurons in the absence of normal pioneer axons. Development 114:825-831.

Postlethwait JH, Yan YL, Gates MA, Horne S, Amores A, Brownlie A, Donovan A, Egan ES, Force A, Gong Z, Goutel C, Fritz A, Kelsh R, Knapik E, Liao E, Paw B, Ransom D, Singer A, Thomson M, Abduljabbar TS, Yelick P, Beier D, Joly JS, Larhammar D, Rosa F, Westerfield M, Zon LI, Johnson SL, Talbot WS. 1998. Vertebrate genome evolution and the zebrafish gene map. Nat Genet 18:345-349.

Reyes R, Haendel M, Grant D, Melancon E, Eisen JS. 2004. Slow degeneration of zebrafish Rohon-Beard neurons during programmed cell death. Dev Dyn 229:30-41.

Roberts A, Sillar KT. 1990. Characterization and Function of Spinal Excitatory Interneurons with Commissural Projections in Xenopus laevis embryos. Eur J Neurosci 2:1051-1062.

Saint-Amant L, Drapeau P. 2001. Synchronization of an embryonic network of identified spinal interneurons solely by electrical coupling. Neuron 31:1035-1046.

Shapira M, Zhai RG, Dresbach T, Bresler T, Torres VI, Gundelfinger ED, Ziv NE, Garner CC. 2003. Unitary assembly of presynaptic active zones from Piccolo-Bassoon transport vesicles. Neuron 38:237-252.

Shen, K., & Cowan, C. W. 2010. Guidance Molecules in Synapse Formation and Plasticity. Cold Spring Harb Perspect Biol 2.

Sheng M, Kim E. 2011. The postsynaptic organization of synapses. Cold Spring Harb Perspect Biol 3.

Sudhof TC. 2013. A molecular machine for neurotransmitter release: synaptotagmin and beyond. Nat Med 19:1227-1231.

Takamori S, Holt M, Stenius K, Lemke EA, Gronborg M, Riedel D, Urlaub H, Schenck S, Brugger B, Ringler P, Muller SA, Rammner B, Grater F, Hub JS, De Groot BL, Mieskes G, Moriyama Y, Klingauf J, Grubmuller H, Heuser J, Wieland F, Jahn R. 2006. Molecular anatomy of a trafficking organelle. Cell 127:831-846.

Waites CL, Craig AM, Garner CC. 2005. Mechanisms of vertebrate synaptogenesis. Annu Rev Neurosci 28:251-274.

Washbourne P, Dityatev A, Scheiffele P, Biederer T, Weiner JA, Christopherson KS, El-Husseini A. 2004. Cell adhesion molecules in synapse formation. J Neurosci 24:9244-9249.

Washbourne P, Liu XB, Jones EG, McAllister AK. 2004. Cycling of NMDA receptors during trafficking in neurons before synapse formation. J Neurosci 24:8253-8264.

Washbourne P, Bennett JE, McAllister AK. 2002. Rapid recruitment of NMDA receptor transport packets to nascent synapses. Nat Neurosci 5:751-759.

Westerfield M, McMurray JV, Eisen JS. 1986. Identified motoneurons and their innervation of axial muscles in the zebrafish. J Neurosci 6:2267-2277.

Wilson SW, Ross LS, Parrett T, Easter SS, Jr. 1990. The development of a simple scaffold of axon tracts in the brain of the embryonic zebrafish, Brachydanio rerio. Development 108:121-145.

Vautrin J. 2009. SV2 frustrating exocytosis at the semi-diffusor synapse. Synapse 63:319-338.

Zhai RG, Vardinon-Friedman H, Cases-Langhoff C, Becker B, Gundelfinger ED, Ziv NE, Garner CC. 2001. Assembling the presynaptic active zone: a characterization of an active one precursor vesicle. Neuron 29:131-143.

Chapter II

Ali DW, Buss RR, Drapeau P. 2000. Properties of miniature glutamatergic EPSCs in neurons of the locomotor regions of the developing zebrafish. J Neurophysiol 83:181-191.

Bailey SM, Murnane JP. 2006. Telomeres, chromosome instability and cancer. Nucleic Acids Res 34:2408-2417.

Baines AJ. 2006. A FERM-adjacent (FA) region defines a subset of the 4.1 superfamily and is a potential regulator of FERM domain function. BMC Genomics 7:85.

Baines AJ. 2010. Evolution of the spectrin-based membrane skeleton. Transfus Clin Biol 17:95-103.

Baines AJ, Lu HC, Bennett PM. 2013. The Protein 4.1 family: hub proteins in animals for organizing membrane proteins. Biochim Biophys Acta 1838:605-619.

Biederer T, Sara Y, Mozhayeva M, Atasoy D, Liu X, Kavalali ET, Sudhof TC. 2002. SynCAM, a synaptic adhesion molecule that drives synapse assembly. Science 297:1525-1531.

Boeckers TM, Bockmann J, Kreutz MR, Gundelfinger ED. 2002. ProSAP/Shank proteins - a family of higher order organizing molecules of the postsynaptic density with an emerging role in human neurological disease. J Neurochem 81:903-910.

Bonanomi D, Pfaff SL. 2010. Motor axon pathfinding. Cold Spring Harb Perspect Biol 2:a001735.

Bonanomi D, Menegon A, Miccio A, Ferrari G, Corradi A, Kao HT, Benfenati F, Valtorta F. 2005. Phosphorylation of synapsin I by cAMP-dependent protein kinase controls synaptic vesicle dynamics in developing neurons. J Neurosci 25:7299-7308.

Brosamle C, Halpern ME. 2002. Characterization of myelination in the developing zebrafish. Glia 39:47-57.

Burkin DJ, Wallace GQ, Nicol KJ, Kaufman DJ, Kaufman SJ. 2001. Enhanced expression of the alpha 7 beta 1 integrin reduces muscular dystrophy and restores viability in dystrophic mice. J Cell Biol 152:1207-1218.

Busam RD, Thorsell AG, Flores A, Hammarstrom M, Persson C, Obrink B, Hallberg BM. 2011. Structural basis of tumor suppressor in lung cancer 1 (TSLC1) binding to differentially expressed in adenocarcinoma of the lung (DAL-1/4.1B). J Biol Chem 286:4511-4516.

Buss RR, Drapeau P. 2000. Physiological properties of zebrafish embryonic red and white muscle fibers during early development. J Neurophysiol 84:1545-1557.

Campbell DB, Sutcliffe JS, Ebert PJ, Militerni R, Bravaccio C, Trillo S, Elia M, Schneider C, Melmed R, Sacco R, Persico AM, Levitt P. 2006. A genetic variant that disrupts MET transcription is associated with autism. Proc Natl Acad Sci U S A 103:16834-16839.

Campbell KP, Kahl SD. 1989. Association of dystrophin and an integral membrane glycoprotein. Nature 338:259-262.

Catchen JM, Conery JS, Postlethwait JH. 2009. Automated identification of conserved synteny after whole-genome duplication. Genome Res 19:1497-1505.

Chang WP, Sudhof TC. 2009. SV2 renders primed synaptic vesicles competent for Ca2+ -induced exocytosis. J Neurosci 29:883-897.

Chen L, Hughes RA, Baines AJ, Conboy J, Mohandas N, An X. 2011. Protein 4.1R regulates cell adhesion, spreading, migration and motility of mouse keratinocytes by modulating surface expression of beta1 integrin. J Cell Sci 124:2478-2487.

Cifuentes-Diaz C, Chareyre F, Garcia M, Devaux J, Carnaud M, Levasseur G, Niwa-Kawakita M, Harroch S, Girault JA, Giovannini M, Goutebroze L. 2011. Protein 4.1B contributes to the organization of peripheral myelinated axons. PLoS One 6:e25043.

Coleman SK, Cai C, Mottershead DG, Haapalahti JP, Keinanen K. 2003. Surface expression of GluR-D AMPA receptor is dependent on an interaction between its C-terminal domain and a 4.1 protein. J Neurosci 23:798-806.

Colman H, Lichtman JW. 1993. Interactions between nerve and muscle: synapse elimination at the developing neuromuscular junction. Dev Biol 156:1-10.

Conboy JG, Chasis JA, Winardi R, Tchernia G, Kan YW, Mohandas N. 1993. An isoform-specific mutation in the protein 4.1 gene results in hereditary elliptocytosis and complete deficiency of protein 4.1 in erythrocytes but not in nonerythroid cells. J Clin Invest 91:77-82.

Constantin B. 2014. Dystrophin complex functions as a scaffold for signalling proteins. Biochim Biophys Acta 1838:635-642.

Cox JA, Kucenas S, Voigt MM. 2005. Molecular characterization and embryonic expression of the family of N-methyl-D-aspartate receptor subunit genes in the zebrafish. Dev Dyn 234:756-766.

De Bleecker JL, Engel AG. 1994. Expression of cell adhesion molecules in inflammatory myopathies and Duchenne dystrophy. J Neuropathol Exp Neurol 53:369-376.

Delhommeau F, Dalla Venezia N, Moriniere M, Collin H, Maillet P, Guerfali I, Leclerc P, Fardeau M, Delaunay J, Baklouti F. 2005. Protein 4.1R expression in normal and dystrophic skeletal muscle. C R Biol 328:43-56.

Dereeper A, Guignon V, Blanc G, Audic S, Buffet S, Chevenet F, Dufayard JF, Guindon S, Lefort V, Lescot M, Claverie JM, Gascuel O. 2008. Phylogeny.fr: robust phylogenetic analysis for the non-specialist. Nucleic Acids Res 36:W465-469.

Discher DE, Winardi R, Schischmanoff PO, Parra M, Conboy JG, Mohandas N. 1995. Mechanochemistry of protein 4.1's spectrin-actin-binding domain: ternary complex interactions, membrane binding, network integration, structural strengthening. J Cell Biol 130:897-907.

Drapeau P, Saint-Amant L, Buss RR, Chong M, McDearmid JR, Brustein E. 2002. Development of the locomotor network in zebrafish. Prog Neurobiol 68:85-111.

Einheber S, Meng X, Rubin M, Lam I, Mohandas N, An X, Shrager P, Kissil J, Maurel P, Salzer JL. 2013. The 4.1B cytoskeletal protein regulates the domain organization and sheath thickness of myelinated axons. Glia 61:240-253.

Eisen JS, Myers PZ, Westerfield M. 1986. Pathway selection by growth cones of identified motoneurones in live zebra fish embryos. Nature 320:269-271.

Eisen JS, Pike SH. 1991. The spt-1 mutation alters segmental arrangement and axonal development of identified neurons in the spinal cord of the embryonic zebrafish. Neuron 6:767-776.

Ervasti JM. 2007. Dystrophin, its interactions with other proteins, and implications for muscular dystrophy. Biochim Biophys Acta 1772:108-117.

Faivre-Sarrailh C, Devaux JJ. 2013. Neuro-glial interactions at the nodes of Ranvier: implication in health and diseases. Front Cell Neurosci 7:196.

Fehon RG, Dawson IA, Artavanis-Tsakonas S. 1994. A Drosophila homologue of membrane-skeleton protein 4.1 is associated with septate junctions and is encoded by the coracle gene. Development 120:545-557.

Fernandez-Chacon R, Konigstorfer A, Gerber SH, Garcia J, Matos MF, Stevens CF, Brose N, Rizo J, Rosenmund C, Sudhof TC. 2001. Synaptotagmin I functions as a calcium regulator of release probability. Nature 410:41-49.

Friedman HV, Bresler T, Garner CC, Ziv NE. 2000. Assembly of new individual excitatory synapses: time course and temporal order of synaptic molecule recruitment. Neuron 27:57-69.

Fujita E, Urase K, Soyama A, Kouroku Y, Momoi T. 2005. Distribution of RA175/TSLC1/SynCAM, a member of the immunoglobulin superfamily, in the developing nervous system. Brain Res Dev Brain Res 154:199-209.

Gascard P, Parra MK, Zhao Z, Calinisan VR, Nunomura W, Rivkees SA, Mohandas N, Conboy JG. 2004. Putative tumor suppressor protein 4.1B is differentially expressed in kidney and brain via alternative promoters and 5' alternative splicing. Biochim Biophys Acta 1680:71-82.

Gimm JA, An X, Nunomura W, Mohandas N. 2002. Functional characterization of spectrin-actin-binding domains in 4.1 family of proteins. Biochemistry 41:7275-7282.

Goody MF, Kelly MW, Reynolds CJ, Khalil A, Crawford BD, Henry CA. 2012. NAD+ biosynthesis ameliorates a zebrafish model of muscular dystrophy. PLoS Biol 10:e1001409.

Gutmann DH, Donahoe J, Perry A, Lemke N, Gorse K, Kittiniyom K, Rempel SA, Gutierrez JA, Newsham IF. 2000. Loss of DAL-1, a protein 4.1-related tumor suppressor, is an important early event in the pathogenesis of meningiomas. Hum Mol Genet 9:1495-1500.

Hodges BL, Hayashi YK, Nonaka I, Wang W, Arahata K, Kaufman SJ. 1997. Altered expression of the alpha7beta1 integrin in human and murine muscular dystrophies. J Cell Sci 110 (Pt 22):2873-2881.

Horresh I, Bar V, Kissil JL, Peles E. 2010. Organization of myelinated axons by Caspr and Caspr2 requires the cytoskeletal adapter protein 4.1B. J Neurosci 30:2480-2489.

Hoy JL, Constable JR, Vicini S, Fu Z, Washbourne P. 2009. SynCAM1 recruits NMDA receptors via protein 4.1B. Mol Cell Neurosci 42:466-483.

Ippolito DM, Eroglu C. 2010. Quantifying synapses: an immunocytochemistry-based assay to quantify synapse number. J Vis Exp.

Jung Y, McCarty JH. 2012. Band 4.1 proteins regulate integrin-dependent cell spreading. Biochem Biophys Res Commun 426:578-584.

Kimmel CB, Ballard WW, Kimmel SR, Ullmann B, Schilling TF. 1995. Stages of embryonic development of the zebrafish. Dev Dyn 203:253-310.

Kimmel CB, Kane DA, Walker C, Warga RM, Rothman MB. 1989. A mutation that changes cell movement and cell fate in the zebrafish embryo. Nature 337:358-362.

Kneussel M, Betz H. 2000. Receptors, gephyrin and gephyrin-associated proteins: novel insights into the assembly of inhibitory postsynaptic membrane specializations. J Physiol 525 Pt 1:1-9.

Kontrogianni-Konstantopoulos A, Huang SC, Benz EJ, Jr. 2000. A nonerythroid isoform of protein 4.1R interacts with components of the contractile apparatus in skeletal myofibers. Mol Biol Cell 11:3805-3817.

Kutzing MK, Langhammer CG, Luo V, Lakdawala H, Firestein BL. 2010. Automated Sholl analysis of digitized neuronal morphology at multiple scales. J Vis Exp.

Lewis J, Chevallier A, Kieny M, Wolpert L. 1981. Muscle nerve branches do not develop in chick wings devoid of muscle. J Embryol Exp Morphol 64:211-232.

Li WC, Soffe SR, Roberts A. 2003. The spinal interneurons and properties of glutamatergic synapses in a primitive vertebrate cutaneous flexion reflex. J Neurosci 23:9068-9077.

McCarty JH, Cook AA, Hynes RO. 2005. An interaction between {alpha}v{beta}8 integrin and Band 4.1B via a highly conserved region of the Band 4.1 C-terminal domain. Proc Natl Acad Sci U S A 102:13479-13483.

Meyer MP, Trimmer JS, Gilthorpe JD, Smith SJ. 2005. Characterization of zebrafish PSD-95 gene family members. J Neurobiol 63:91-105.

Micheva KD, Busse B, Weiler NC, O'Rourke N, Smith SJ. 2010. Single-synapse analysis of a diverse synapse population: proteomic imaging methods and markers. Neuron 68:639-653.

Montgomery JM, Zamorano PL, Garner CC. 2004. MAGUKs in synapse assembly and function: an emerging view. Cell Mol Life Sci 61:911-929.

Nunes F, Shen Y, Niida Y, Beauchamp R, Stemmer-Rachamimov AO, Ramesh V, Gusella J, MacCollin M. 2005. Inactivation patterns of NF2 and DAL-1/4.1B (EPB41L3) in sporadic meningioma. Cancer Genet Cytogenet 162:135-139.

Opazo P, Choquet D. 2011. A three-step model for the synaptic recruitment of AMPA receptors. Mol Cell Neurosci 46:1-8.

Parra M, Gascard P, Walensky LD, Gimm JA, Blackshaw S, Chan N, Takakuwa Y, Berger T, Lee G, Chasis JA, Snyder SH, Mohandas N, Conboy JG. 2000. Molecular and functional characterization of protein 4.1B, a novel member of the protein 4.1 family with high level, focal expression in brain. J Biol Chem 275:3247-3255.

Pereda AE. 2014. Electrical synapses and their functional interactions with chemical synapses. Nat Rev Neurosci 15:250-263.

Peters LL, Weier HU, Walensky LD, Snyder SH, Parra M, Mohandas N, Conboy JG. 1998. Four paralogous protein 4.1 genes map to distinct chromosomes in mouse and human. Genomics 54:348-350.

Pietri T, Easley-Neal C, Wilson C, Washbourne P. 2008. Six cadm/SynCAM genes are expressed in the nervous system of developing zebrafish. Dev Dyn 237:233-246.

Pietri T, Manalo E, Ryan J, Saint-Amant L, Washbourne P. 2009. Glutamate drives the touch response through a rostral loop in the spinal cord of zebrafish embryos. Dev Neurobiol 69:780-795.

Postlethwait J, Ruotti V, Carvan MJ, Tonellato PJ. 2004. Automated analysis of conserved syntenies for the zebrafish genome. Methods Cell Biol 77:255-271.

Purcell AE, Jeon OH, Zimmerman AW, Blue ME, Pevsner J. 2001. Postmortem brain abnormalities of the glutamate neurotransmitter system in autism. Neurology 57:1618-1628.

Pyle RA, Schivell AE, Hidaka H, Bajjalieh SM. 2000. Phosphorylation of synaptic vesicle protein 2 modulates binding to synaptotagmin. J Biol Chem 275:17195-17200.

Rajaram V, Gutmann DH, Prasad SK, Mansur DB, Perry A. 2005. Alterations of protein 4.1 family members in ependymomas: a study of 84 cases. Mod Pathol 18:991-997.

Sabo SL, Gomes RA, McAllister AK. 2006. Formation of presynaptic terminals at predefined sites along axons. J Neurosci 26:10813-10825.

Sabo SL, McAllister AK. 2003. Mobility and cycling of synaptic protein-containing vesicles in axonal growth cone filopodia. Nat Neurosci 6:1264-1269.

Saint-Amant L, Drapeau P. 1998. Time course of the development of motor behaviors in the zebrafish embryo. J Neurobiol 37:622-632.

Saint-Amant L, Drapeau P. 2000. Motoneuron activity patterns related to the earliest behavior of the zebrafish embryo. J Neurosci 20:3964-3972.

Saint-Amant L, Drapeau P. 2001. Synchronization of an embryonic network of identified spinal interneurons solely by electrical coupling. Neuron 31:1035-1046.

Sakurai-Yageta M, Masuda M, Tsuboi Y, Ito A, Murakami Y. 2009. Tumor suppressor CADM1 is involved in epithelial cell structure. Biochem Biophys Res Commun 390:977-982.

Schivell AE, Mochida S, Kensel-Hammes P, Custer KL, Bajjalieh SM. 2005. SV2A and SV2C contain a unique synaptotagmin-binding site. Mol Cell Neurosci 29:56-64.

Scott C, Keating L, Bellamy M, Baines AJ. 2001. Protein 4.1 in forebrain postsynaptic density preparations: enrichment of 4.1 gene products and detection of 4.1R binding proteins. Eur J Biochem 268:1084-1094.

Scott C, Phillips GW, Baines AJ. 2001. Properties of the C-terminal domain of 4.1 proteins. Eur J Biochem 268:3709-3717.

Seeburg PH, Burnashev N, Kohr G, Kuner T, Sprengel R, Monyer H. 1995. The NMDA receptor channel: molecular design of a coincidence detector. Recent Prog Horm Res 50:19-34.

Seredick SD, Van Ryswyk L, Hutchinson SA, Eisen JS. 2012. Zebrafish Mnx proteins specify one motoneuron subtype and suppress acquisition of interneuron characteristics. Neural Dev 7:35.

Shen L, Liang F, Walensky LD, Huganir RL. 2000. Regulation of AMPA receptor GluR1 subunit surface expression by a 4. 1N-linked actin cytoskeletal association. J Neurosci 20:7932-7940.

Shi ZT, Afzal V, Coller B, Patel D, Chasis JA, Parra M, Lee G, Paszty C, Stevens M, Walensky L, Peters LL, Mohandas N, Rubin E, Conboy JG. 1999. Protein 4.1R-deficient mice are viable but have erythroid membrane skeleton abnormalities. J Clin Invest 103:331-340.

Singh PK, Gutmann DH, Fuller CE, Newsham IF, Perry A. 2002. Differential involvement of protein 4.1 family members DAL-1 and NF2 in intracranial and intraspinal ependymomas. Mod Pathol 15:526-531.

Subramaniam S. 1998. The Biology Workbench--a seamless database and analysis environment for the biologist. Proteins 32:1-2.

Tan JS, Mohandas N, Conboy JG. 2005. Evolutionarily conserved coupling of transcription and alternative splicing in the EPB41 (protein 4.1R) and EPB41L3 (protein 4.1B) genes. Genomics 86:701-707.

Tosney KW. 1987. Proximal tissues and patterned neurite outgrowth at the lumbosacral level of the chick embryo: deletion of the dermamyotome. Dev Biol 122:540-558.

Tosney KW, Hageman MS. 1989. Different subsets of axonal guidance cues are essential for sensory neurite outgrowth to cutaneous and muscle targets in the dorsal ramus of the embryonic chick. J Exp Zool 251:232-244.

Vachon PH, Xu H, Liu L, Loechel F, Hayashi Y, Arahata K, Reed JC, Wewer UM, Engvall E. 1997. Integrins (alpha7beta1) in muscle function and survival. Disrupted expression in merosin-deficient congenital muscular dystrophy. J Clin Invest 100:1870-1881.

Valor LM, Grant SG. 2007. Integrating synapse proteomics with transcriptional regulation. Behav Genet 37:18-30.

Walensky LD, Shi ZT, Blackshaw S, DeVries AC, Demas GE, Gascard P, Nelson RJ, Conboy JG, Rubin EM, Snyder SH, Mohandas N. 1998. Neurobehavioral deficits in mice lacking the erythrocyte membrane cytoskeletal protein 4.1. Curr Biol 8:1269-1272.

Wang J, Song J, An C, Dong W, Zhang J, Yin C, Hale J, Baines AJ, Mohandas N, An X. 2014. A 130-kDa protein 4.1B regulates cell adhesion, spreading, and migration of mouse embryo fibroblasts by influencing actin cytoskeleton organization. J Biol Chem 289:5925-5937.

Wang L, Wang Y, Li Z, Gao Z, Zhang S. 2013. Functional characterization of protein 4.1 homolog in amphioxus: defining a cryptic spectrin-actin-binding site. Sci Rep 3:2873.

Wang Z, Zhang J, Ye M, Zhu M, Zhang B, Roy M, Liu J, An X. 2014. Tumor suppressor role of protein 4.1B/DAL-1. Cell Mol Life Sci.

Welten MC, de Haan SB, van den Boogert N, Noordermeer JN, Lamers GE, Spaink HP, Meijer AH, Verbeek FJ. 2006. ZebraFISH: fluorescent in situ hybridization protocol and three-dimensional imaging of gene expression patterns. Zebrafish 3:465-476.

Westerfield M, McMurray JV, Eisen JS. 1986. Identified motoneurons and their innervation of axial muscles in the zebrafish. J Neurosci 6:2267-2277.

Wilhelm BG, Mandad S, Truckenbrodt S, Krohnert K, Schafer C, Rammner B, Koo SJ, Classen GA, Krauss M, Haucke V, Urlaub H, Rizzoli SO. 2014. Composition of isolated synaptic boutons reveals the amounts of vesicle trafficking proteins. Science 344:1023-1028.

Williams JA, Holder N. 2000. Cell turnover in neuromasts of zebrafish larvae. Hear Res 143:171-181.

Wozny C, Breustedt J, Wolk F, Varoqueaux F, Boretius S, Zivkovic AR, Neeb A, Frahm J, Schmitz D, Brose N, Ivanovic A. 2009. The function of glutamatergic synapses is not perturbed by severe knockdown of 4.1N and 4.1G expression. J Cell Sci 122:735-744.

Yageta M, Kuramochi M, Masuda M, Fukami T, Fukuhara H, Maruyama T, Shibuya M, Murakami Y. 2002. Direct association of TSLC1 and DAL-1, two distinct tumor suppressor proteins in lung cancer. Cancer Res 62:5129-5133.

Zelenchuk TA, Bruses JL. 2011. In vivo labeling of zebrafish motor neurons using an mnx1 enhancer and Gal4/UAS. Genesis 49:546-554.

Zhang X, Li W, Kang Y, Zhang J, Yuan H. 2013. SynCAM, a novel putative tumor suppressor, suppresses growth and invasiveness of glioblastoma. Mol Biol Rep 40:5469-5475.

Zhiling Y, Fujita E, Tanabe Y, Yamagata T, Momoi T, Momoi MY. 2008. Mutations in the gene encoding CADM1 are associated with autism spectrum disorder. Biochem Biophys Res Commun 377:926-929.

Chapter III

Ahmari, S.E., and Smith, S.J. (2002). Knowing a nascent synapse when you see it. Neuron 34, 333–336.

Ahmari, S.E., Buchanan, J., and Smith, S.J. (2000). Assembly of presynaptic active zones from cytoplasmic transport packets. Nat. Neurosci. 3, 445–451.

Ando, K., Uemura, K., Kuzuya, A., Maesako, M., Asada-Utsugi, M., Kubota, M., Aoyagi, N., Yoshioka, K., Okawa, K., Inoue, H., et al. (2011). N-cadherin regulates p38 MAPK signaling via association with JNK-associated leucine zipper protein: implications for neurodegeneration in Alzheimer disease. J. Biol. Chem. 286, 7619–7628.

Barrow, S.L., Constable, J.R., Clark, E., El-Sabeawy, F., McAllister, A.K., and Washbourne, P. (2009). Neuroligin1: a cell adhesion molecule that recruits PSD-95 and NMDA receptors by distinct mechanisms during synaptogenesis. Neural Dev. 4, 17.

Bernhardt, R.R., Chitnis, A.B., Lindamer, L., and Kuwada, J.Y. (1990). Identification of spinal neurons in the embryonic and larval zebrafish. J. Comp. Neurol. 302, 603–616.

Bonanomi, D., Menegon, A., Miccio, A., Ferrari, G., Corradi, A., Kao, H.T., Benfenati, F., and Valtorta, F. (2005). Phosphorylation of synapsin I by cAMP-dependent protein kinase controls synaptic vesicle dynamics in developing neurons. J. Neurosci. 25, 7299–7308.

Bozdagi, O., Valcin, M., Poskanzer, K., Tanaka, H., and Benson, D.L. (2004). Temporally distinct demands for classic cadherins in synapse formation and maturation. Mol. Cell. Neurosci. 27, 509–521.

Bresler, T., Ramati, Y., Zamorano, P.L., Zhai, R., Garner, C.C., and Ziv, N.E. (2001). The dynamics of SAP90/PSD-95 recruitment to new synaptic junctions. Mol. Cell. Neurosci. 18, 149–167.

Bury, L.A., and Sabo, S.L. (2011). Coordinated trafficking of synaptic vesicle and active zone proteins prior to synapse formation. Neural Dev. 6, 24.

Catchen, J.M., Conery, J.S., and Postlethwait, J.H. (2009). Automated identification of conserved synteny after whole-genome duplication. Genome Res. 19, 1497–1505.

Cheung, Z.H., and Ip, N.Y. (2007). The roles of cyclin-dependent kinase 5 in dendrite and synapse development. Biotechnol. J. 2, 949–957.

Douglass, A.D., Kraves, S., Deisseroth, K., Schier, A.F., and Engert, F. (2008). Escape behavior elicited by single, channelrhodopsin-2-evoked spikes in zebrafish somatosensory neurons. Curr. Biol. 18, 1133–1137.

Downes, G.B., and Granato, M. (2006). Supraspinal input is dispensable to generate glycine-mediated locomotive behaviors in the zebrafish embryo. J. Neurobiol. 66, 437–451.

Eisen, J.S., and Pike, S.H. (1991). The spt-1 mutation alters segmental arrangement and axonal development of identified neurons in the spinal cord of the embryonic zebrafish. Neuron 6, 767–776.

Fabry, B., Klemm, A.H., Kienle, S., Schäffer, T.E., and Goldmann, W.H. (2011). Focal adhesion kinase stabilizes the cytoskeleton. Biophys. J. 101, 2131– 2138.

Fornasiero, E.F., Bonanomi, D., Benfenati, F., and Valtorta, F. (2010). The role of synapsins in neuronal development. Cell. Mol. Life Sci. 67, 1383–1396.

Gleason, M.R., Higashijima, S., Dallman, J., Liu, K., Mandel, G., and Fetcho, J.R. (2003). Translocation of CaM kinase II to synaptic sites in vivo. Nat. Neurosci. 6, 217–218.

Hernandez-Lagunas, L., Choi, I.F., Kaji, T., Simpson, P., Hershey, C., Zhou, Y., Zon, L., Mercola, M., and Artinger, K.B. (2005). Zebrafish narrowminded disrupts the transcription factor prdm1 and is required for neural crest and sensory neuron specification. Dev. Biol. 278, 347–357.

Hoy, J.L., Constable, J.R., Vicini, S., Fu, Z., and Washbourne, P. (2009). SynCAM1 recruits NMDA receptors via protein 4.1B. Mol. Cell. Neurosci. 42, 466–483.

Huttner, W.B., Schiebler, W., Greengard, P., and De Camilli, P. (1983). Synapsin I (protein I), a nerve terminal-specific phosphoprotein III. Its association with synaptic vesicles studied in a highly purified synaptic vesicle preparation. J. Cell Biol. 96, 1374–1388.

Jontes, J.D., Buchanan, J., and Smith, S.J. (2000). Growth cone and dendrite dynamics in zebrafish embryos: early events in synaptogenesis imaged in vivo. Nat. Neurosci. 3, 231–237.

Jontes, J.D., Emond, M.R., and Smith, S.J. (2004). In vivo trafficking and targeting of N-cadherin to nascent presynaptic terminals. J. Neurosci. 24, 9027–9034.

Kanungo, J., Li, B.S., Goswami, M., Zheng, Y.L., Ramchandran, R., and Pant, H.C. (2007). Cloning and characterization of zebrafish (Danio rerio) cyclindependent kinase 5. Neurosci. Lett. 412, 233–238.

Kanungo, J., Zheng, Y.L., Mishra, B., and Pant, H.C. (2009). Zebrafish Rohon-Beard neuron development: cdk5 in the midst. Neurochem. Res. 34, 1129–1137.

Kim, S.H., and Ryan, T.A. (2010). CDK5 serves as a major control point in neurotransmitter release. Neuron 67, 797–809.

Kimmel, C.B., Ballard, W.W., Kimmel, S.R., Ullmann, B., and Schilling, T.F. (1995). Stages of embryonic development of the zebrafish. Dev. Dyn. 203, 253–310.

Knockaert, M., Greengard, P., and Meijer, L. (2002). Pharmacological inhibitors of cyclin-dependent kinases. Trends Pharmacol. Sci. 23, 417–425.

Kraszewski, K., Mundigl, O., Daniell, L., Verderio, C., Matteoli, M., and De Camilli, P. (1995). Synaptic vesicle dynamics in living cultured hippocampal neurons visualized with CY3-conjugated antibodies directed against the lumenal domain of synaptotagmin. J. Neurosci. 15, 4328–4342.

Lazarevic, V., Schöne, C., Heine, M., Gundelfinger, E.D., and Fejtova, A. (2011). Extensive remodeling of the presynaptic cytomatrix upon homeostatic adaptation to network activity silencing. J. Neurosci. 31, 10189–10200.

Matsubara, M., Kusubata, M., Ishiguro, K., Uchida, T., Titani, K., and Taniguchi, H. (1996). Site-specific phosphorylation of synapsin I by mitogen-activated protein kinase and Cdk5 and its effects on physiological functions. J. Biol. Chem. 271, 21108–21113.

Meyer, M.P., Trimmer, J.S., Gilthorpe, J.D., and Smith, S.J. (2005). Characterization of zebrafish PSD-95 gene family members. J. Neurobiol. 63, 91–105.

Micheva, K.D., Busse, B., Weiler, N.C., O'Rourke, N., and Smith, S.J. (2010). Single-synapse analysis of a diverse synapse population: proteomic imaging methods and markers. Neuron 68, 639–653.

Park, M., Watanabe, S., Poon, V.Y., Ou, C.Y., Jorgensen, E.M., and Shen, K. (2011). CYY-1/cyclin Y and CDK-5 differentially regulate synapse elimination and formation for rewiring neural circuits. Neuron 70, 742–757.

Pietri, T., Manalo, E., Ryan, J., Saint-Amant, L., and Washbourne, P. (2009). Glutamate drives the touch response through a rostral loop in the spinal cord of zebrafish embryos. Dev. Neurobiol. 69, 780–795.

Pietri, T., Easley-Neal, C., Wilson, C., and Washbourne, P. (2008). Six cadm/SynCAM genes are expressed in the nervous system of developing zebrafish. Dev. Dyn. 237, 233–246.

Pineda, R.H., Heiser, R.A., and Ribera, A.B. (2005). Developmental, molecular, and genetic dissection of INa in vivo in embryonic zebrafish sensory neurons. J. Neurophysiol. 93, 3582–3593.

Rasband, W.S. (1997–2011). ImageJ (Bethesda, MD: U.S. National Institutes of Health).

Ribera, A.B., and Nüsslein-Volhard, C. (1998). Zebrafish touch-insensitive mutants reveal an essential role for the developmental regulation of sodium current. J. Neurosci. 18, 9181–9191.

Sabo, S.L., Gomes, R.A., and McAllister, A.K. (2006). Formation of presynaptic terminals at predefined sites along axons. J. Neurosci. 26, 10813–10825.

Saint-Amant, L., and Drapeau, P. (1998). Time course of the development of motor behaviors in the zebrafish embryo. J. Neurobiol. 37, 622–632.

Samuels, B.A., Hsueh, Y.P., Shu, T., Liang, H., Tseng, H.C., Hong, C.J., Su, S.C., Volker, J., Neve, R.L., Yue, D.T., and Tsai, L.H. (2007). Cdk5 promotes synaptogenesis by regulating the subcellular distribution of the MAGUK family member CASK. Neuron 56, 823–837.

Scott, D.A., Das, U., Tang, Y., and Roy, S. (2011). Mechanistic logic underlying the axonal transport of cytosolic proteins. Neuron 70, 441–454.

Scott, E.K., Mason, L., Arrenberg, A.B., Ziv, L., Gosse, N.J., Xiao, T., Chi, N.C., Asakawa, K., Kawakami, K., and Baier, H. (2007). Targeting neural circuitry in zebrafish using GAL4 enhancer trapping. Nat. Methods 4, 323–326.

Shapira, M., Zhai, R.G., Dresbach, T., Bresler, T., Torres, V.I., Gundelfinger, E.D., Ziv, N.E., and Garner, C.C. (2003). Unitary assembly of presynaptic active zones from Piccolo-Bassoon transport vesicles. Neuron 38, 237–252.

Shcherbo, D., Souslova, E.A., Goedhart, J., Chepurnykh, T.V., Gaintzeva, A., Shemiakina, I.I., Gadella, T.W., Lukyanov, S., and Chudakov, D.M. (2009). Practical and reliable FRET/FLIM pair of fluorescent proteins. BMC Biotechnol. 9, 24.

Takamori, S., Holt, M., Stenius, K., Lemke, E.A., Grønborg, M., Riedel, D., Urlaub, H., Schenck, S., Brügger, B., Ringler, P., et al. (2006). Molecular anatomy of a trafficking organelle. Cell 127, 831–846.

Tanaka, H., Morimura, R., and Ohshima, T. (2012). Dpysl2 (CRMP2) and Dpysl3 (CRMP4) phosphorylation by Cdk5 and DYRK2 is required for proper positioning of Rohon-Beard neurons and neural crest cells during neurulation in zebrafish. Dev. Biol. 370, 223–236.

Tao-Cheng, J.H. (2007). Ultrastructural localization of active zone and synaptic vesicle proteins in a preassembled multi-vesicle transport aggregate. Neuroscience 150, 575–584.

Thévenaz, P., Ruttimann, U.E., and Unser, M. (1998). A pyramid approach to subpixel registration based on intensity. IEEE Trans. Image Process. 7, 27–41.

Valor, L.M., and Grant, S.G. (2007). Integrating synapse proteomics with transcriptional regulation. Behav. Genet. 37, 18–30.

Washbourne, P., Bennett, J.E., and McAllister, A.K. (2002). Rapid recruitment of NMDA receptor transport packets to nascent synapses. Nat. Neurosci. 5, 751–759.

Waterhouse, A.M., Procter, J.B., Martin, D.M., Clamp, M., and Barton, G.J. (2009). Jalview Version 2—a multiple sequence alignment editor and analysis workbench. Bioinformatics 25, 1189–1191.

Westerfield, M. (2000). The Zebrafish Book, Fourth Edition (Eugene, OR: Institute for Neuroscience, University of Oregon).

Zhai, R.G., Vardinon-Friedman, H., Cases-Langhoff, C., Becker, B., Gundelfinger, E.D., Ziv, N.E., and Garner, C.C. (2001). Assembling the presynaptic active zone: a characterization of an active one precursor vesicle. Neuron 29, 131–143.

Zoghbi, H.Y. (2003). Postnatal neurodevelopmental disorders: meeting at the synapse? Science 302, 826–830.

Chapter IV

Cox JA, Kucenas S, Voigt MM. 2005. Molecular characterization and embryonic expression of the family of N-methyl-D-aspartate receptor subunit genes in the zebrafish. Dev Dyn 234:756-766.

Hoy JL, Constable JR, Vicini S, Fu Z, Washbourne P. 2009. SynCAM1 recruits NMDA receptors via protein 4.1B. Mol Cell Neurosci 42:466-483.

Huttner WB, Schiebler W, Greengard P, De Camilli P. 1983. Synapsin I (protein I), a nerve terminal-specific phosphoprotein. III. Its association with synaptic vesicles studied in a highly purified synaptic vesicle preparation. J Cell Biol 96:1374-1388.

Pietri T, Easley-Neal C, Wilson C, Washbourne P. 2008. Six cadm/SynCAM genes are expressed in the nervous system of developing zebrafish. Dev Dyn 237:233-246.

Wozny C, Breustedt J, Wolk F, Varoqueaux F, Boretius S, Zivkovic AR, Neeb A, Frahm J, Schmitz D, Brose N, Ivanovic A. 2009. The function of glutamatergic synapses is not perturbed by severe knockdown of 4.1N and 4.1G expression. J Cell Sci 122:735-744.